THE UNIVERSITY
of EDINBURGH

Investigating the clonality and formation of memory populations of non-conventional NKp46+ CD3+ T-cells

Yu Wang

MSc by Research

The University of Edinburgh

2016

Declaration

I declare that the work presented in this thesis is my own original work, except where specified, and it does not include work forming part of a thesis presented successfully for a degree in this or another university.

Yu Wang

Edinburgh 2016

Abstract

NKp46+ CD3+ T cells have been defined as a novel non-conventional T lymphocyte subset of cattle that express both NK cell and T cell receptors. It has been hypothesized that NKp46+ CD3+ cells may form a niche bridging the innate and adaptive immune response and there is now evidence they may play a role in the responses against *Theileria parva* and *Mycobacteria*. Thus, NKp46+ CD3+ cells may offer a novel population to target in vaccination strategies. In bovine, recent studies have shown that NKp46+ CD3+ cells can recognize and respond to autologous *Theileria parva* infected cells (TpM) and that NKp46+ CD3+ cell lines can be generated and maintained *in vitro*. Functional analysis has indicated that both NKp46 receptor and CD3 (i.e. TCR) cross-linking can lead to cell activation, however, the function of the T cell receptor is still not clear. The aim of this study is to analyze the TCR repertoire of TpM-stimulated NKp46+CD3+ populations to look for evidence of TCR selection that would indicate a role for TCR in mediating recognition of TpM. To address this aim, we use high resolution NGS TRB sequence analysis to compare the TCR repertoires observed in TpM-stimulated and non-specific stimulated NKp46+CD3+ populations derived from naïve and *T. parva*-immune animals. TpM specific-stimulated NKp46+CD3+ cell lines were successfully generated from naive and *T. parva* immunized cattle, but generation and maintenance of NKp46+CD3+ cell lines through use of non-specific stimulant was unsuccessful. The results of this study provide evidence of clonal selection in the *T. parva*-specific response of NKp46+ CD3+ T-cells and in 2 naïve animals highly overlapping TRB repertoires. From the current data it is confirmed that NKp46+CD3+ cells express a highly diverse TRB repertoire with no obvious and consistent overt bias for usage of particular TRBV or TRBJ genes.

Lay summary

Conventionally, the immune system can be divided into innate and adaptive components. T lymphocytes play an important role in adaptive immunity, whilst natural killer (NK) cells are classified as a part of the innate immunity. T cells are defined by expression of the T cell receptor (TCR) and the associated CD3 molecule. NKp46 is a natural killer receptor expressed by NK cells and was considered to be a marker specific for this population. A novel lymphocyte subset—NKp46+ CD3+ cells - has been recently described in cattle and over livestock species, which co-expresses NKp46 and CD3 and exhibits features of both NK cells and T cells. Previous studies have demonstrated that NKp46+ CD3+ cells play a role in the responses against *Theileria parva* and tuberculosis, therefore this cell subset may be a target for novel vaccines. Moreover, these studies proved that NKp46+ CD3+ cells could be stimulated by both NKp46 receptor and CD3 signalling pathways (i.e. TCR). However, the role of the TCR in mediating recognition of target cells by NKp46+CD3+ cells is still not clear. The aim of this project is to investigate the TRB repertoire of NKp46+ CD3+ cells that have been stimulated with autologous *T. parva*-infected cells to look for evidence of clonal selection and/or biased TCR usage that could indicate a role for TCR mediated selection and so suggest a role for TCR in NKp46+ CD3+ cells recognition of this pathogen.

Acknowledgements

My sincerely thanks must firstly be given to Dr Timothy Connelley for his patient guidance, enthusiastic encouragement, and critical scientific support during this research work. Discussing with him about this project always gives me new idea and inspires me how to think like a scientist, which will greatly benefit my future career. I would like to thank Professor Bernadette Dutia for providing me the precious chance to undertake this project and I really appreciate all the discussions and encouragement from her.

A special thank need to go to my best friend and teacher, Laura Agundez Muriel, she taught me not only laboratory techniques but also a positive attitude toward life. I must give my acknowledgements to Mr Deepali Vasoya, who's been providing all the bioinformatics support for the project.

Table of Contents

List of Figures

List of Tables

Abbreviations

BSA	Bovine serum albumin
bp	base pair
^{o}C	degrees Celsius
C	constant gene segment
CD	cluster of differentiation
cDNA	complementary deoxyribonucleic acid
CDR3	complementary determining region three
CO_2	carbon dioxide
CTL	cytotoxic T lymphocyte
D	Diversity gene segment
DNA	deoxyribonucleic acid
dNTP	mixture of dATP, dCTP, dGTP, and Dttp
dTTP	2'-deoxythymidine triphosphate
DMSO	Dimethylsulphoxide
EDTA	Ethylene-diamine-tetra-acetic acid
FACS	fluorescent-activated cell sorting
FCS	foetal calf serum
g	grams
hr	hours
IFN	interferon
Ig	immunoglobulin
IL	interleukin
IMGT	Immunogenetics Database
J	Joining segment
L	litre
mA	mili-amps
mAb	mono-clonal antibody
mM	mili-molar
MHC	Major-histocompatability complex
MHCI	Major-histocompatability complex class I
min	minute

ug	micro-grams
ml	milli-litres
ul	micro-litres
mRNA	messenger ribonucleic acid
NK	Natural-killer
PBMC	peripheral blood mono-nuclear cells
PBS	Phosphate Buffered Saline
PCR	polymerase chain reaction
pMHC	peptide-Major-histocompatability complex composite ligand
RBS	red blood cells
RNase	ribonuclease
rpm	revolutions per minute
RSS	recombination signal sequence
RT	reverse transcriptase
TAE	Tris-acetate/EDTA electrophoresis buffer
TAP	transporter associated with Antigen Processing
TCR	T-cell receptor
TRB	T-cell receptor β chain
TRBC	T-cell receptor beta chain constant gene segment
TRBD	T-cell receptor beta chain diversity gene segment
TRBJ	T-cell receptor beta chain joining gene segment
TRBV	T-cell receptor beta chain variable gene segment
Tdt	Terminal deoxynucleotidy1 transferase
Tp	*Theileria parva*
TpM	*Theileria parva* (Muguga)-infected lymphocyte
V	Variable gene segment
Vα	T-cell receptor alpha chain variable gene segment
Vβ	T-cell receptor beta chain variable gene segment

Chapter 1. Introduction

1.1 T cells

The immune system provides organisms with defence against invasion by a wide variety of pathogens. Conventionally, the immune system can be classified into innate and adaptive components. Adaptive immunity is mediated by two lymphocyte subsets—T-cells and B—cells. B-cells produce immunoglobulin (Ig) that provides humoral immunity, whereas T-cells are involved with provision of cell-mediated immunity. In contrast to innate immunity, the adaptive immune system is characterised by 1) the requirement for initial priming, 2) recognition of antigen via a somatically rearranged heterodimeric antigen-specific receptor (TCR or Ig) and 3) formation following primary antigen exposure of long-term protective immunological memory. However, recent studies have shown that components of the innate system also appear to have the capacity to form 'memory' (Netea 2013).

T cells can be divided into two lineages based on expression of either an αβ or γδ T cell receptor (TCR). Generally, αβ T-cells can further be subdivided into two populations co-expressing either the CD4 or CD8 co-receptor. CD8+ T cells are also known as CTL (cytotoxic T-cell lymphocytes) and can have the capacity to lyse target cells as well as produce cytokines such as interferon-γ (IFNG) and tumour necrosis factor-α (TNFA). CD4+ T cells are also referred to as Helper T cells (Th cells) and frequently are involved in facilitating the functions of other immune cells – for example antibody production by B-cells, activation and proliferation of CTL-cells and assisting phagocytes to destroy ingested microbes by releasing T-cell cytokines. There are at least four different Th cell subsets that are defined by the expression of different 'master regulator' transcription factors: Th1 (T-bet/STAT4), Th2 (GATA-3/STAT5), Th17 (Rorγt/STAT3) and induced T-regulatory cells (Foxp3/STAT5), each of which has distinct effector functions in regulating the immune response. Th1 cells are essential for macrophage activation, cell-mediated immunity and phagocyte-dependent protective responses by secreting cytokines (Saraiva et al. 2009); Th2 cells have a role in eosinophil activation and inhibition of several macrophage functions (Paul & Seder 1994); T_H17 cells participate in neutrophil activation through production of IL-17a, IL-17f and IL-22 (Harrington et al. 2005) and iTreg cells (also known as suppressor T cells) function in down-regulating induction and proliferation of effector T cells (Takahashi et al. 1998).

1.2 The αβ T cell receptor

The αβ T cell receptor (TCR) is a heterodimeric, somatically rearranged, clonotypicallly distributed receptor, which in conventional T-cells is responsible for recognizing peptide fragments presented within the context of host MHC molecules and thus dictates epitope-specificity. Each protein chain of the TCR is composed of two extracellular domains: Variable (V) region and Constant (C) region, and is expressed on the cell surface of the T-cell in conjunction with the cluster of differentiation 3 (CD3) complex (Figure 1.1). The structure of TCR is crucial for understanding the function and formation of TCR.

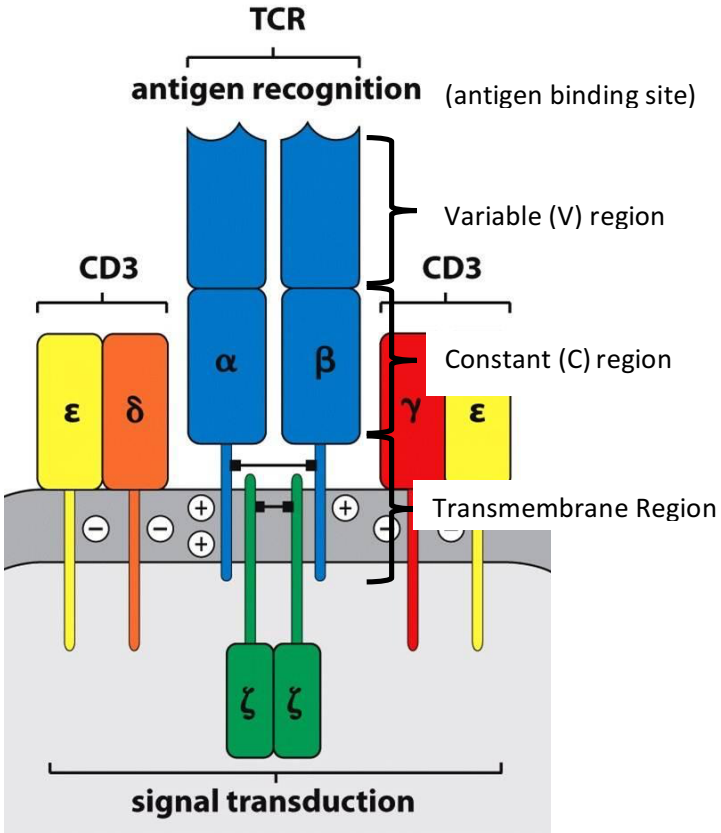

Figure 1.1 Structure of the T cell receptor. The T cell receptor heterodimer is composed of two glycoprotein chains, α and β chain (blue). Each chain consists of two domains, variable (V) region and constant (C) region. The CD3 molecules (CD3γ , CD3δ, and CD3ε) in yellow and orange, and ζ-chain accessory molecules in green together constitute the TCR complex.

1.2.1 Somatic recombination of αβ TCR

To enable recognition of the vast array of different peptide antigens, conventional T-cells express a hugely diverse αβ TCR repertoire that is generated by V(D)J recombination during the early stage of T lymphocyte maturation in the thymus. This recombination involves the assembly of individual V (variable), D (diversity-β chain only), J (joining), and C (constant) gene segments in α and β chains (Tonegawa 1983) (Figure 1.2). Recombination signal sequences (RSS) flanking the 3' end of V, the 5' end of J, and both 5' and 3' ends of the D gene segments, are recognised by a hetero-multimer encoded by recombination activating genes 1 and 2 (RAG1, RAG2) which initiates somatic rearrangement. The RSS is composed of heptamer and nonamer motifs separated by a spacer of either 12bp (12-RSS) or 23bp (23-RSS) length, the V genes are flanked by 23-RSS, the J genes by a 12-RSS and the D genes are flanked by a 5'end 12-RSS and 3' 23-RSS (Hesse et al., 1989). The requirement for recombination to occur between 12-RSS and 23-RSS genes (the 12/23 rule) ensures ordered rearrangement, with the molecular mechanisms upon which this dependent having recently been established (Ru et al. 2015). More than75% of αβ TCR diversity is produced by this so called 'combinatorial diversity' (i.e. different V(D)J permutations), which is then further amplified by the activity of exonuclease and terminal deoxynucleotide transferase (TdT) which respectively remove and insert bases to the 5' end of V, the 5' and 3' end of D and the 3' end of J gene segments – termed 'junctional diversity' (Gauss and Lieber 1996).

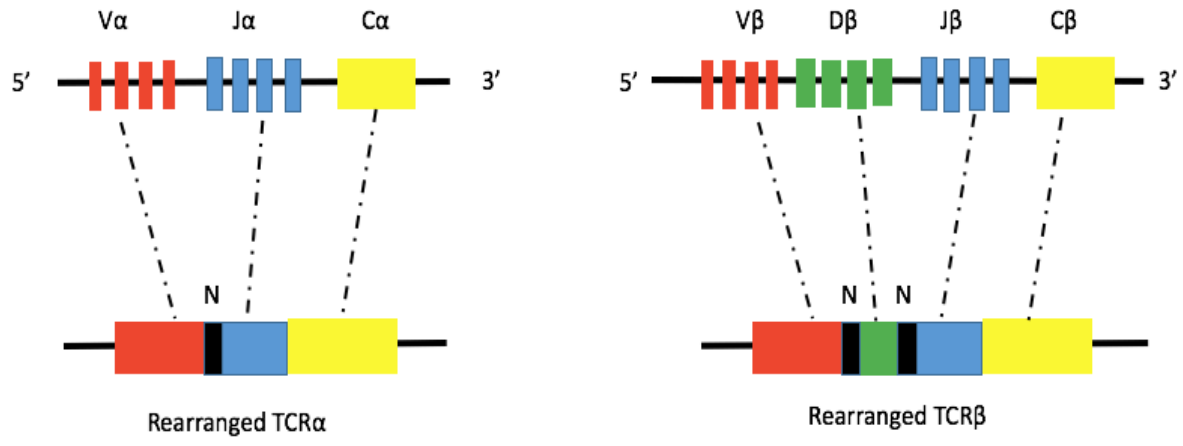

Figure 1.2 Schematic illustration of somatic recombination of TCRα and TCRβ genes. The αβ TCR consist of three different gene segments: variable (V)—red, diversity (D)—green, and joining (J)—blue gene segments. αβ TCR are generated by somatic recombination of V and J gene segments for the TCRα chain and V, D and J gene segments for the TCRβ chain. Rearranged gene segments are then splicned with constant (C) region (yellow) to form the functional αβTCR. During somatic recombination, non-germline (N) regions (black) are generated due to nucleotide additions and deletions (Turner et al. 2006).

In each of the rearranged αβ TCR genes there are 6 loops called the Complementarity Determining Regions (CDRs). These form the membrane-distal surface of the TCR and directly interact with the peptide-MHC ligand. Three CDRs are derived from the α chain (CDRα1, CDRα2 and CDRα3) and 3 from the β chain (CDRβ1, CDRβ2 and CDRβ3) (Garboczi et al. 1996; Garcia et al. 1996). The CDR3s are encoded by the V(D)J junction, which as this is non-germline encoded is hypervariable and consequently the most polymorphic of the CDRs. The CDR1 and 2s are encoded within the V gene germline sequence and so their diversity is determined by the genome repertoire.

1.2.2 TCR loci in human and mouse

The gene segments encoding the TCR are located in 3 genomic loci – TRA/D (which includes the TCRα and TCRδ gene segments), TRB (TCRβ) and TRG (TCRγ). Sequencing of these loci has permitted comparative descriptions of the genomic repertoires in a number of species (Rowen et al. 1996) and subsequent comparative analyses. The TRA/D loci in humans and mice are located on chromosome 14q11.2 and 14c2 respectively. The human TRA/D locus contains 54 TRAV genes belonging to 41 Vα subgroups (V gene subgroups are defined by members sharing >75% nucleotide sequence identity), 3 TRDV, 3 TRDJ, 3 TRDD, 61 TRAJ, and single TRAC and TRDC genes. The mouse TRA/D locus has 100 TRAV genes which are distributed across 23 Vα subgroups, 6 TRDV, 2 TRDJ, 2 TRDD, 61 TRAJ, and single TRAC and TRDC genes (Table 1.1). The TRG loci are located on chromosome 7p14 in human and chromosome 13 in mice, and consist of 14 TRGV and 5 TRGJ genes, and 7 TRGV and 4 TRGJ genes respectively. The TRB locus includes 64-67 V (classified into 32 subgroups), 2 D and 14 J gene segments in human, and 35 V (classified into 31 subgroups), 2 D and 14 J gene segments in mouse (Table 1.1) and are located on chromosome 7q34 and chromosome 6A-C, respectively (Barker et al. 1984; Caccia et al. 1984). The structure of the TRB loci in human and mouse are very similar (Figure 1.3), with the majority of the V genes located at the 5' end and 2 tandemly arranged DJC clusters (comprising a single TRBD gene, 6-7 TRBJ genes and a single TRBC gene) with a single TRBV gene with an inverted transcriptional orientation located at the 3'end of the loci (Glusman et al. 2001).

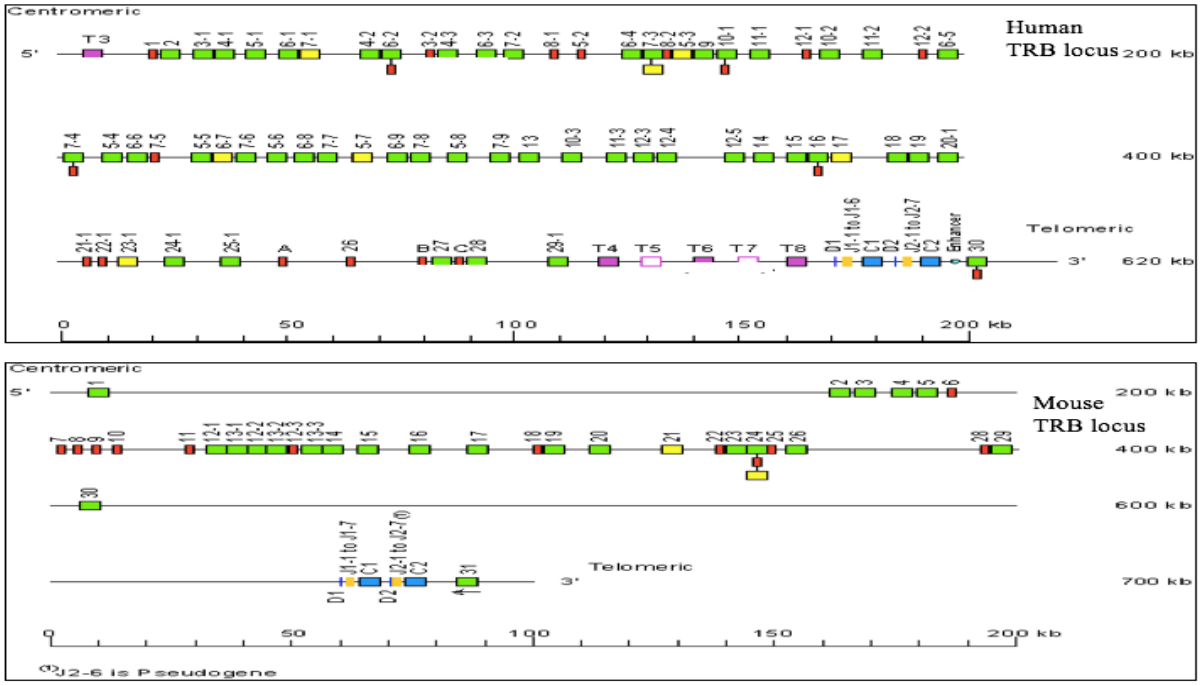

Figure 1.3 Schematic representation of the human and mouse TRB loci (IMGT database). TRBV genes are classified as functional , ORF , pseudogene , and other TCRβgenes: Dβ genes—purple vertical line, Jβ gene cluster , Cβ gene , non-TCRβgene: Trypsinogen . The human (upper) and mouse loci are shown from the 5' end to 3' end.

1.2.3 TCR loci in cattle

Compared to humans and mice, the cattle TRA/D and TRB loci are characterised by a massive expansion of Vα and Vβ genes (Connelley et al. 2009; Connelley et al. 2014) the cattle TRA/D locus is located on chromosome 10 and contains 371 TRAV/TRDV genes (distributed into 42 subgroups), 62 TRAJ, 3 TRDJ, 6 TRDD, and single TRAC and TRDC genes, whilst the TRB locus is located on chromosome 4 and includes 134 V genes belonging to 24 subgroups (Table 1.1). Notably in both loci this expansion has predominantly occurred through the duplication of 'gene cassettes' which contain multiple V genes and have led to the massive expansion of some of the V gene subgroups; in the TRB locus around 68% of genes belong to TRBV6, 9 or 21 subgroups. This massive duplication, with over-representation of certain V gene subgroups has obvious implications of the diversity and bias in the expressed TCR repertoire. The schematic representation of the cattle TRB loci shown in Figure 1.4 represents the duplication events observed which, in addition to the expansion of the V gene repertoire has also generated a third DJC cluster.

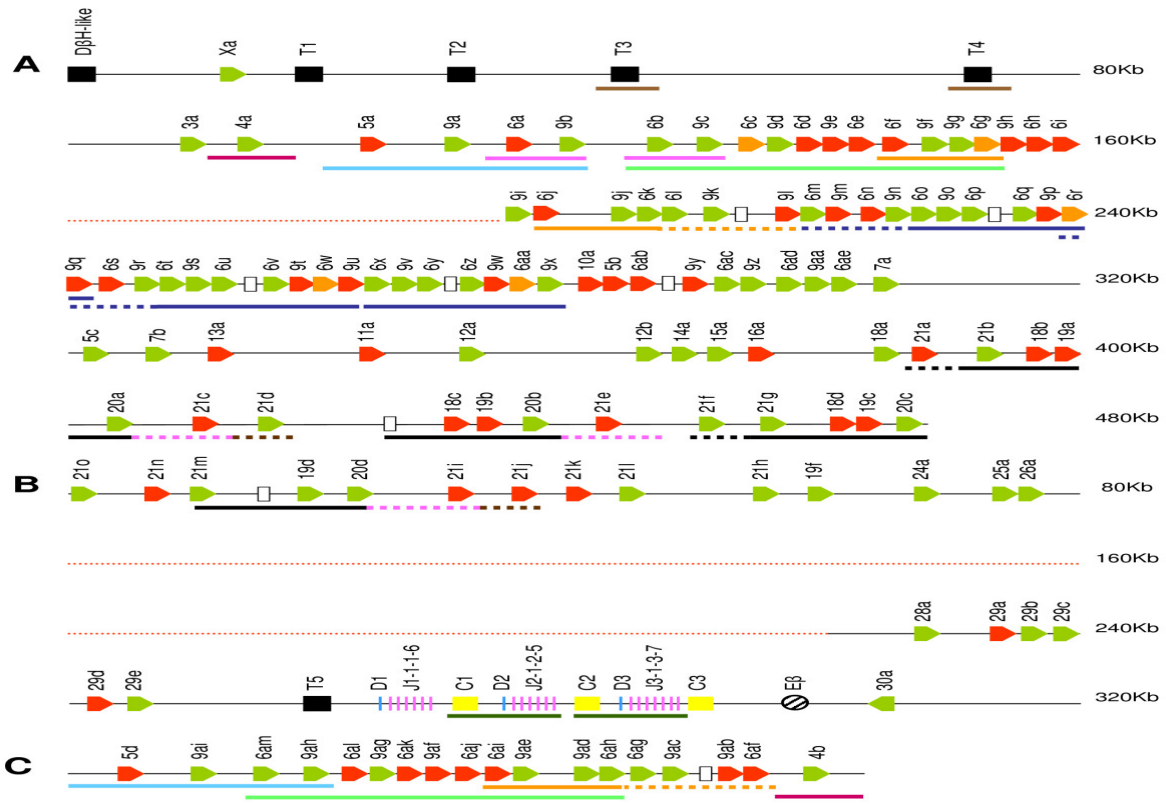

Figure 1.4 Genomic organisation of genes in the bovine TRB locus (Connelley et al. 2009). Undetermined sequence in red dotted lines; TRBV functional genes—green; TRBV non-functional genes—orange; pseudogenes genes— red; TRBD genes—blue vertical lines; TRBJ genes—pink vertical lines. TRBC genes—yellow boxes; bovine TRB enhancer (Eβ)—black diagonal shading; non TRB genes—black box. Regions of duplicated DNA are indicated by the colour-coordinated boxes located beneath the scheme of gene location. Broken lines indicate regions of DNA that are not present in all copies of the duplicated region.

		αβ TCR diversity						
		TCRA				TCRB		
		V	J	C		V	D	J	C
Humans	Total	54 (41)	61	1		64-67 (32)	2	14	2
	Functional	45(34)	50	1		36 (23)	2	10	2
Mice	Total	100 (23)	61	1		35 (31)	2	14	3
	Functional	71 (19)	49	1		21 (19)	2	3	2
Bovine	Total	>300	62	1		134 (24)	3	21	3
	Functional	215 (38)	52	1		79 (19)	3	16	3

Table 1.1 Summary of the number of αβ TCR gene segments in human, mice and bovine. Number in parenthesis shows the number of subgroups. Human and murine repertoire data obtained from the website http://www.imgt.org/IMGTrepertoire/. Bovine genome repertoire data obtained from [Connelley et al. 2009; Connelley et al. 2014].

1.2.4 Diversity of the αβTCR repertoire

Theoretically, V(D)J recombination has the capacity to produce a potential repertoire of 1×10^{15} αβ TCRs. However, this repertoire could not be fully expressed in any individual and the influence of negative and positive selection during thymic development has been shown to place severe constraints on the TCR repertoire (reducing the pre-selection repertoire by ~100 fold) that can be expressed within any individual (Correia-Neves et al. 2001). Attempts to directly estimate TCR diversity have suggested the expressed repertoire in mice and humans are much lower – approximately 2×10^{6} and 2.5×10^{7} unique TCRs respectively (Arstila et al. 1999; Casrouge et al. 2000). NGS sequencing has also been applied to measure TCR diversity (Warren et al. 2011). Although in this study a total of 1,061,522 sequences were recorded from an individual, repetitive sampling from that individual showed limited overlap indicating that despite this intensive analysis the full TCR repertoire had not be captured (Warren et al. 2011).

The highly diverse TCR repertoire in conventional T-cells confers the ability to recognize a broad range of antigenic epitopes and so combat the wide range of pathogens to which individuals can be exposed. The highest TCR diversity is present in the naïve compartment; following antigen exposure TCR diversity is narrowed as antigen-driven selection leads to expansion of specific TCR clonotypes (Rudd et al. 2011).

1.2.5 αβ TCR interaction with peptide-MHC complex

The ligands for conventional CD8+ and CD4+ T-cells are peptide-MHC-I complexes (pMHC-I) peptide-MHCII complexes (pMHCII) respectively. Crystallographic studies have enabled the structure of the TCR/pMHC binding to be determined (Kass et al. 2014). In general, αβ TCRs bind to the pMHC in a conserved diagonal orientation (Figure 1.5), although there is considerable variation in the binding angle which can vary by up to $\pm45^{o}$ (Rudolph et al. 2006; Teng et al. 1998). As a consequence of the binding orientation the hypervariable CDR3s of the α and β chains have the most intimate association with antigen peptide component of the peptide-MHC (pMHC) complex while the CDR1 and CDR2 are predominantly involved in the interaction with the MHC helices (Figure 1.5). Thus, the most variable parts of the TCR dominate the binding of the most variable part of the pMHC ligand,

whilst the more conserved CDR1 and CDR2 dominate the binding to the more conserved MHC.

Studies using alanine-screening mutagenesis show that different TCRs binding to the same pMHC ligand are reliant on different amino acid residues of the presenting peptide (Manning et al. 1998; Borg et al. 2005). This data demonstrates that the contribution of CDR loops to the binding energy of the TCR-pMHC ligation varies between individual TCR/pMHC complexes.

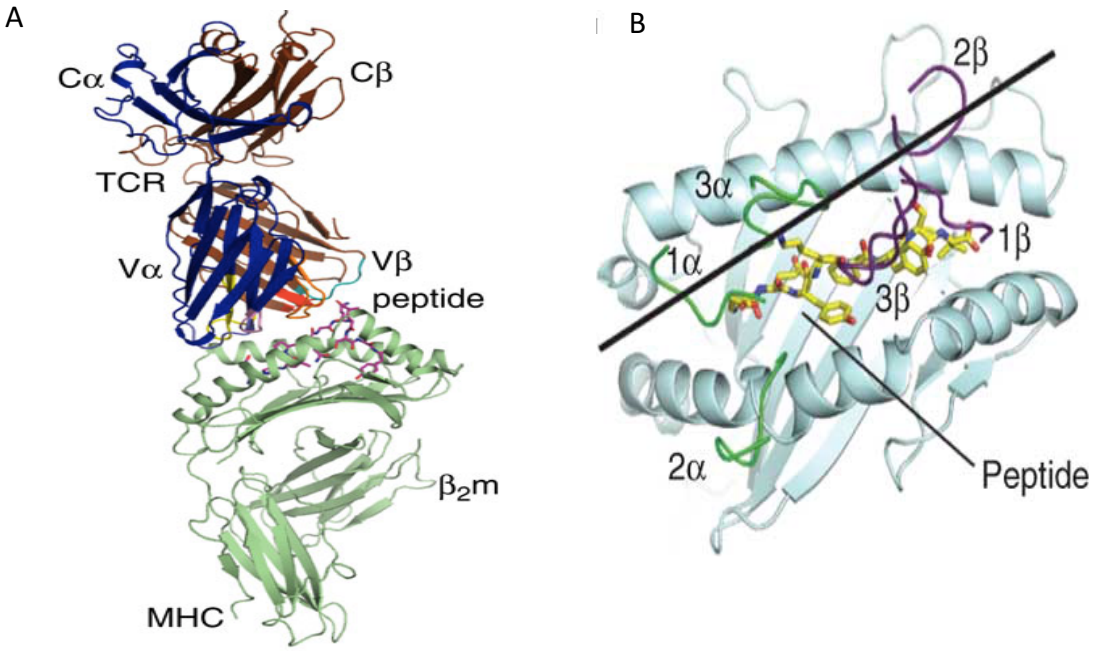

Figure 1.5 αβTCR interaction with pMHC ligands. (A) Lateral review of TCR/pMHC complex. αβ TCR on top (α chain in blue, β chain in brown), pMHC on bottom. Peptide in pink (Patel et al. 2013). (B) "Diagonal" docking mode of the CDR loops of a conventional TCR. CDR1α, CDR2α, and CDR3α -green, CDR1β, CDR2β, and CDR3β—purple, peptide—yellow (Godfrey et al. 2010).

1.3 Non-conventional T cells

Besides the majority conventional αβ T cells, there are many other αβ T cell subsets possessing distinct features, which include CD1-restricted T cells and MR1-restricted mucosal associated invariant T cells (MAIT cells). These cells are often termed 'non-conventional' T cells and are characterised by recognizing non-polymorphic antigen-presenting molecules rather than peptide-MHC complexes. The common feature of unconventional T cells is co-expression of a T cell receptor and natural killer (NK) cell receptors on the cell surface and possession of both innate and adaptive immune cell characteristics.

1.3.1 CD1-restricted T cells

CD1 (cluster of differentiation 1) is a family of non-polymorphic class I MHC related antigen-presenting molecules, which are expressed on various types of cells, including monocytes, macrophages and dendritic cells (DCs). In humans and other mammals, CD1 molecules have been classified into four types and two groups: group 1 (CD1a, CD1b and CD1c) and group 2 (CD1d) (Calabi et al. 1989). Mice and rats have CD1d only. Evidence now strongly indicates that each CD1 type has a distinct function and specificity for particular lipid antigens (Kasmar et al. 2009; Van Rhijn et al. 2015). The group 1 CD1 molecules have been characterized most extensively in humans and have been demonstrated to present microbial lipid antigens and certain self-lipids to a diverse group of T cells (Felio et al. 2009). The group 2 CD1 molecule-CD1d is able to activate natural killer T cells by presenting lipid antigens (Girardi and Zajonc 2012).

1.3.1.1 Group 1 CD1-restricted T cells

Different from MHC molecules, the group 1 CD1 molecules are highly expressed on the cell surface of CD4+ CD8+ cortical thymocytes and APCs (Brigl and Brenner 2004). CD1c is the most extensively expressed group 1 CD1 molecule, which can be found on B cells, monocyte-derived DCs, and Langerhans cells (Sugita et al. 2000). Meanwhile, CD1a and CD1b molecules are limited to expression on skin resident DCs and myeloid-derived dendritic cells, respectively (Wollenberg et al. 1996; Olivier et al. 2013). However, the expression of group 1 CD1 can also be regulated by various cytokines and different infections. For example, GM-CSF and IL-4 can increase the expression of group 1 CD1 by

promoting DCs differentiation, and infection with *Mycobacterium leprae* and *Borrelia burgdorferi* also can cause high levels of group 1 CD1 expression (Kasinrerk et al. 1993; Sieling et al. 1999; Yakimchuk et al. 2011) .

The group 1 CD1-restricted T cells have been implicated to play crucial roles in a variety of autoimmune and infectious diseases by producing multiple cytokines such as IFN-α, IFN-γ, IL-17, and IL-22. CD1a molecules can bind to the mycobacterial lipopeptide didehydroxymycobactin (DDM) (Moody et al. 2004), and the DDM-specific CD1a-restricted T cells can produce different levels of IL-2 in response to different DDM antigens (Young et al. 2009). The CD1c molecule has a unique antigen-binding mode and like CD1a also presents lipopeptide antigens to T cells. Phoshomycokeide (PM) is the only know antigen presented by CD1c molecule and can active CD1c-restricted T cells (Moody et al. 2000). The CD1b molecule has the biggest antigen-binding groove of the group 1 CD1 members and binds the most diverse array of lipid species, including glucose monomycolate (GMM), mycolic acid, phosphatidylinositol mannosides (PIMs), glycerol monomycolate, sulfoglycolipids and lipoarabinomannans (LAM) (Siddiqui et al. 2015).

Group 1 CD1-restricted T cells are known to have diverse TCRs, but CD1b-restricted T cells were recently described to express highly conserved TCRs composed of a TRAV1-2V segment rearranged with TRAJ9, and with limited CDR3α diversity (Van Rhijn et al. 2013).

1.3.1.2 CD1d-restricted natural killer T cell

The 'natural killer' T cells (NKT cells) are regarded as a bridge between the innate and adaptive responses and combine features of T cells and NK cells. These cells were referred to as 'natural killer' T cells in early studies. However, after decades of research, it is clear that the function of these cells is not only based on NK receptor expression, but depends more on the specificity of these cells for lipid antigens presented by CD1d (Bendelac et al. 2007). Based on the utilization of TCR-α and β genes, the CD1d restricted NKT cells can be divided into two types: type I NKT cells and type II NKT cells.

1.3.1.2.1 Type I NKT cells

Type I NKT cells are also known as invariant NKT (iNKT) cells and express a semi-invariant TCR α-chain (Vα14-Jα18 in mouse, Vα24-Jα18 in human) paired with a limited but not invariant TCR β-chain (Vβ7, Vβ8 and Vβ2 in mice, Vβ11 in human) (Godfrey et al. 2004; Rossjohn et al. 2012). In the mouse, the type I NKT cells represent up to 50% of T cells in liver and bone marrow and 0.5-1% of T cells in the thymus, blood and peripheral lymph nodes (Godfrey Poulton et al. 2001). In contrast, iNKT cells are less frequent in human (around 0.1% of T cells in peripheral blood) (Chan et al. 2013). In human and mice, the majority of type I NKT cells either express CD4 or are double negative (DN) for the CD4 and CD8 receptor (Bendelac et al. 2007).

iNKT cells are activated by foreign lipids derived from microbes, tumours, and allergens, as well as self-lipids. In the mouse, the iNKT cells are known as an important component for responding to various bacteria, viruses and parasites, and abundant evidence indicates that iNKT cells also play the same role in pathogen infection in humans. The marina sponge-derived glycolipid α-galactosylceramide (α-GalCer) is the earliest discovered CD1d presented lipid antigen (Kawano et al. 1997), and later many other α-linked bacterial sources of the glycolipid antigens have been reported, such as *Sphingomonas* species-derived α-glycuronosylceramides, α-galactosyldiacylglycerol from *Borrelia burgdorferi*, α-glucosyldiacylglycerol from *Streptococcus pneumonia* and phosphatidylinositol tetramannoside , and a weak iNKT-cell antigen originally extracted from *Mycobacteria spp* (Godfrey et al. 2015). In addition, two potent self-antigens of iNKT cells have been discovered: isoglobotrihexosylceramide (iGb3) and α-glucosylceramide (α-GlcCer) (Zhou et al. 2004; Brennan et al. 2011). Upon TCR recognition of the CD1d glycolipid complex, iNKT cells are capable of a rapid response and release of various chemokines and cytokines to influence the Th1 and Th2 immune response (such as IFN-γ and IL-4) (Fujii et al. 2002). Type I NKT cells are also able to regulate the function of antigen-presenting cells, macrophages, and B cells.

In a previous study, a conserved, tilted and parallel docking mode of iNKT TCR-CD1d glycolipid complex was determined from the crystal structures (Patel et al. 2011), which indicates the iNKT TCRs recognise the lipid CD1d in a homologous fashion, despite the various glycolipid antigens and diverse TCRβ chain. This crystal structure also demonstrated

that a single α-GalCer/CD1d complex interacts with different mouse iNKT TCRs sharing the same α chain and adopt a similar docking topology (Figure 1.6). Accordingly, the conserved manner of iNKT TCRs docking onto CD1d is mainly dependent on the invariant α-chain of iNKT cells. Thus, the iNKT TCRs contact CD1d predominantly with the α-chain and recognise lipid antigen only through the CDR3α loop, suggesting that the α chain is responsible for the majority of the epitope specificity whilst the β-chain diversity modulates this.

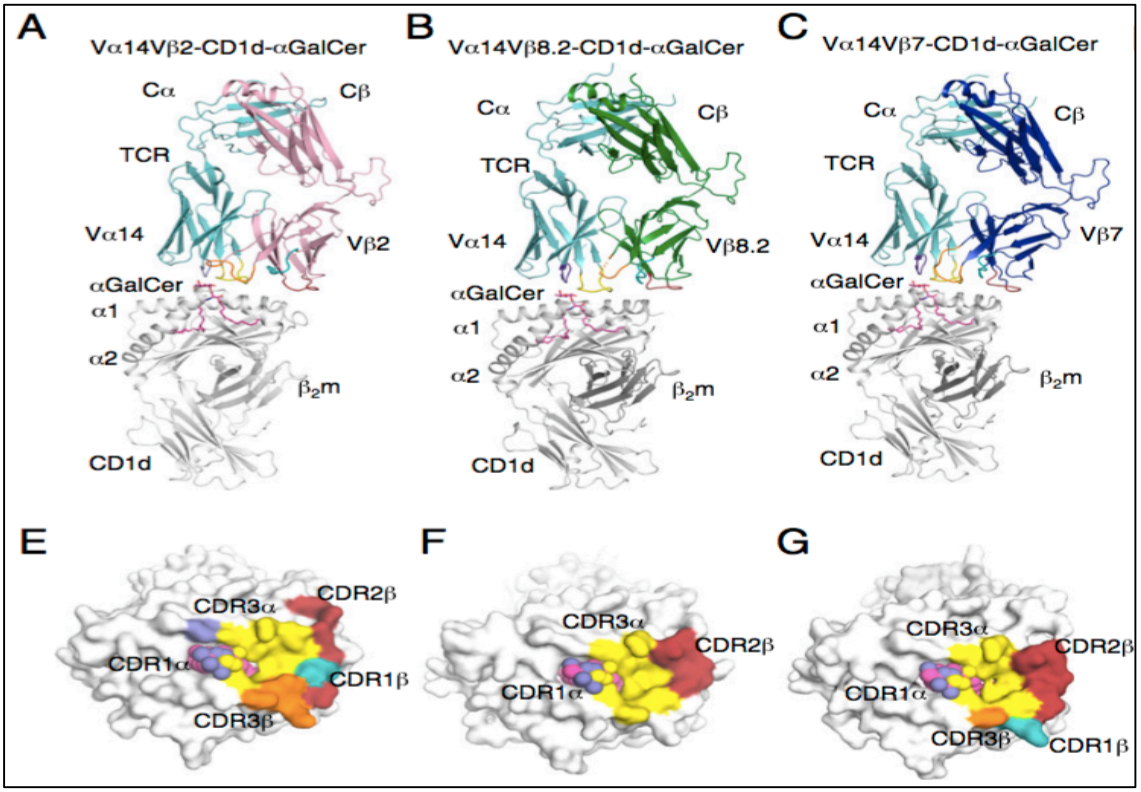

Figure 1.6 Structure of mouse NKT TCRs in complex with mouse CD1d-αGalCer (Patel et al. 2011). (A) Vα14Vβ2 NKT TCR-CD1d-α-GalCer. α-GalCer-Magenta; CD1d heterodimer-gray; Vα14-cyan; Vβ2-pink; CDR1α-purple; CDR3α-yellow; CDR1β-teal; CDR2β-ruby; CDR3β-orange. (B) Vα14Vβ8.2 NKT TCR-CD1d-α-GalCer. Vβ8.2. α-GalCer-Green; CD1d, Vα14, and CDR loops color coding as in A. (C) Vα14Vβ7 NKT TCR-CD1d-α-GalCer. Vβ7; α-GalCer-Dark blue; CD1d, Vα14, and CDR loops color coding as in A. (E) Footprint of Vα14Vβ2 on the surface of CD1d-α-GalCer. α-GalCer is shown in spheres. (F) Footprint of Vα14Vβ8.2 on the surface of CD1d-α-GalCer. (G) Footprint of Vα14Vβ7 on the surface of CD1d-α-GalCer. E to G color coding is the same as in A.

1.3.1.2.2 Type II NKT cells

The type II NKT cells express a diverse TCR repertoire and so are also known as diverse NKT (dNKT) cells. Different from type I NKT cells, type II NKT cells recognise different CD1d-associated ligands and cannot respond to α-linked glycolipids, such as α-GalCer. A widely studied antigen of type II NKT cells is sulfatide (Jahng et al. 2004), a sulphated form of β-galactosylceramide (β –GalCer).

In recent studies, some distinct functions of type II NKT cells have been demonstrated by comparing mice lacking type I NKT cells (Jα18-deficient mice) with mice lacking type I and II NKT cells (CD1d-deficient mice) (Terabe et al. 2005; Ambrosino et al. 2007). Type II NKT cells play an important immune-regulatory role in infection, autoimmune disease and tumour immune surveillance - producing both pro-inflammatory cytokines (such as IFN-γ, TNF-α and IL-17) and anti-inflammatory cytokines (such as IL-4 and IL-10) (Fuss et al. 2014).

The binding mode of type II NKT TCRs combines features of both MHC-restricted T cells and iNKT cells. Like MHC-TCR interactions, both α chain and β chain contact the CD1d molecule with a diagonal orientation. However, similar to iNKT cells which recognise the epitope solely with α chain, the type II NKT TCRs recognise antigen exclusively with one chain but in this case the β chain (Girardi et al. 2012). The crystal structure and docking orientation of a type II NKT TCR on CD1d-LSF complex is shown in Figure 1.7.

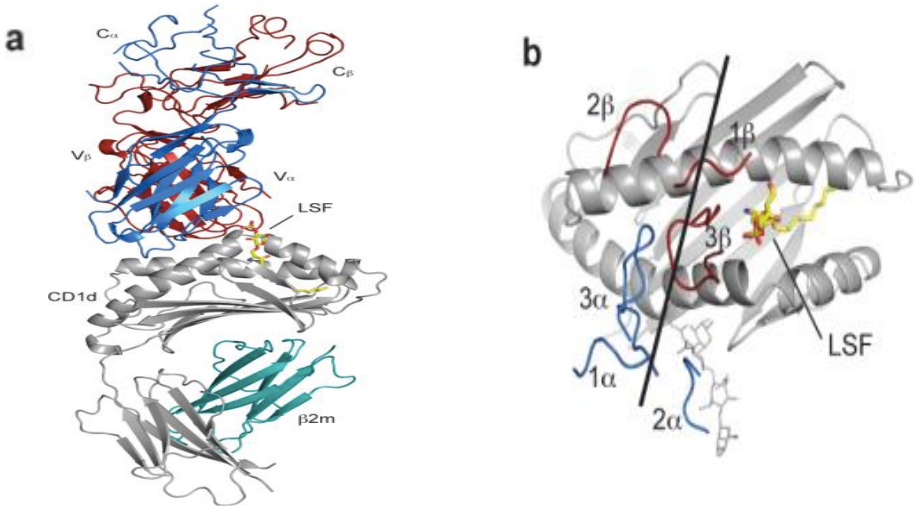

Figure 1.7 Crystal structure and docking orientation of a type II NKT TCR on the CD1d-LSF complex (Girardi et al. 2012). (a) Crystal structure of the mouse CD1d–LSF–Hy19.3 TCR complex. CD1d in gray; β2-microglobulin (β2m) in aqua; TCR α-chain in blue; TCR β-chain in dark red; LSF in yellow. (b) TCR footprint and binding orientation of the mouse CD1d–LSF–Hy19.3 TCR complex. TCR α-chain- cyan; TCR β-chain-red.

1.3.2 Mucosal associated invariant T cells (MAIT cells)

Mucosal-associated invariant T (MAIT) cells are a highly conserved αβ T cell subset, found in most mammalian species. MAIT cells are characterised by two features 1) they process the evolutionarily conserved semi-invariant TCR α chain, which is composed of Vα7.2-Jα33 (TRAV1-2—TRAJ33) in human and Vα19-Jα33 (TRAV1-TRAJ33) in mice, that is associated with Vβ6 (TRBV19) and Vβ8 (TRBV13) in mice, and Vβ 2 (TRBV20) and Vβ13 (TRBV6) in humans (Ussher et al. 2014) and 2). These cells can be activated by ligands presented by the MHC related-1 molecule MR1 (Treiner et al. 2003). In humans, the MAIT cells express an effector memory phenotype, expressing the CD161 receptor (Dusseaux et al. 2011), so it has been hypothesised that they may generate effector or memory cells. Upon activation, the MAIT cells are able to participate in antibacterial immune responses, against pathogens such as *Mycobacterium tuberculosis, Salmonella typhimurium,* and *Escherichia coil*, by expressing proinflammatory cytokines (such as IFN-γ, IFN-α and IL-17) and acting as cytolytic effector cells (Le Bourhis et al. 2010).

In previous studies, a conserved docking mode was observed in MAIT TCRs binding the epitope-MR1 complex. Similar to conventional T cells which interact with pMHC, both α and β chains contact with MR1 molecule and CDR3s loops (CDR3α and CDR3 β) are responsible for recognizing their variable ligands. The studies also suggest that the docking footprint does not vary with MR1-presented ligands. The crystal structure and footprint of MAIT cell TCR interaction with MRI is shown in Figure 1.8.

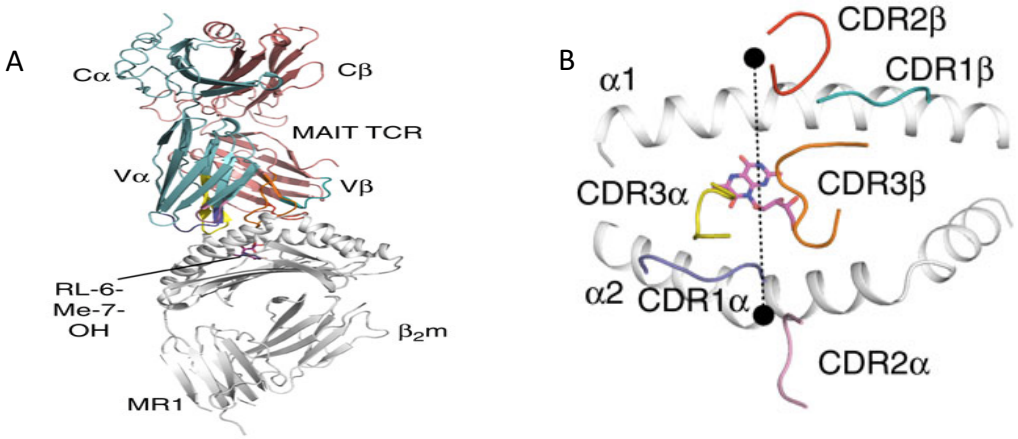

Figure 1.8 The crystal structure and footprint of MAIT cells interact with MR1 (Patel et al. 2013). (A) MAIT TCR in complex with MR1–RL-6-Me-7-OH. MAIT TCR α-chain—cyan; MAIT TCR β-chain—salmon; CDR1α—purple; CDR2α—pink; CDR3α—yellow; CDR1β—teal; CDR2β—red; CDR3β—orange; RL-6-Me-7-OH—magenta; and MR1—grey. (B) MAIT TCR–MR1–RL-6-Me-7-OH complex, CDR loops color coding as in A.

1.4 Bovine NKp46+ CD3+ T-cells

The NKp46 (NCR1. CD335) is an activating receptor belonging to the natural cytotoxicity receptors (NCRs) (Lanier et al. 2005) whose expression is generally considered to be restricted to natural killer (NK) cells (Sivori et al. 1997). Thus, the CD3-NKp46+ phenotype has been used to identify and characterise NK cells in various mammalian species (Walzer et al. 2007). Triggering the NKp46 receptor on NK cells leads to the induction of cytokines such as IFN-γ and to cytolytic activity (Sivori et al. 1997).

In human and mouse, the expression of NKp46 has been identified only on aberrantly activated T cells (Meresse et al. 2006; Narni-mancinelli et al. 2011; Tomasello et al. 2012). However, in recent studies, the expression of NKp46 has been observed on a minor fraction of T cells in various species, and the NKp46+ CD3+ T-cells have been defined as a novel non-conventional T cell subset.

In cattle, the expression of NKp46 has been found on both αβ and γδ T cells, and there is now evidence that NKp46+ CD3+ T cells may play a role in the responses against *Theileria parva* and *Mycobacterium tuberculosis*, and it has been hypothesised that they may form a niche bridging the innate and adaptive immune response (Connelley, Longhi, et al. 2014). Thus, NKp46+CD3+ cells may offer a novel population to target in vaccination strategies. Bovine NKp46+CD3+ cells have been shown to recognize and respond to autologous TpM and the NKp46+CD3+ cell lines can be generated and maintained *in vitro* by co-culture with autologous *T. parva*-infected cells (Connelley et al. 2014). Functional analysis has demonstrated that cross-linking of both the NKp46 receptor and the CD3 complexes (i.e. TCR) can lead to cell activation, however, the function of TCR in mediating recognition of target cells is still not clear.

1.5 Analysis of TCR repertoire

Analysis of the TCR repertoire has been used to address a wide variety of biological questions, such as analysis of the diversity of antigen-specific responses, examining the clonality of T cell responses, and tracking clonally expanded T-cell populations (reviewd in Rufer, 2005).In previous studies, a number of molecular tools have been used to analysis TCRs. Due to the potentially huge diversity of TCR repertoire, the capacity of analysis technologies to provide sufficient resolution of the repertoire has been the major challenge. Due to the more stringent allelic exclusion of the TRB chain rearrangement analysis (resulting in T-cells generally expressing only a single functional TRB chain but more frequently expressing two TRA chains) and the more prominent role CDR3B has in interaction with the peptide epitopes of pMHC complexes, many techniques have focused on analysis of the TRB chain. Vβ subfamily-specific monoclonal antibodies (Cose et al. 1995; Trautmann et al. 2005) and semi-quantitative RT-PCR (Lehner et al. 1995) have been commonly used to identify preferential Vβ gene expression but they can not delineate the CDR3β sequence and clonality of T-cell responses. Another two widely used methods are spectratyping (immunoscope) and heteroduplex analysis (Bousso et al. 1998; Bernardin et al. 2004) which both can provide some information on the CDR3 length distribution in addition to TRBV subgroup usage but provide limited data of the sequence of the TCRβ-chains. Sub-cloning and Sanger sequencing of individual TRB provides more complete information on the expressed TRB chains but due to the high costs and laborious effort required has generally only been used on a limited number of clones and so provides low resolution data of complex repertoires.

Recently, high throughput next generation sequencing (NGS) technologies have been applied to analyzing TCR repertoires. Compared with previous molecular tools, NGS offers opportunities to perform unbiased, quantitative, time-efficient and cost-effective analysis of diverse TCR repertoire (Bolotin et al. 2012). The NGS platforms used include Illumina sequencing, Roche 454 sequencing, Ion torrent and SOLiD sequencing, among these techniques the Illumia sequencing offers the highest number of sequencing reads per run. For preparing the library of NGS, the most common strategy is using the switching mechanism at the 5'-terminus of the RNA transcript (SMART) and 5’ rapid amplification of cDNA ends (RACE) technologies. SMART uses reverse transcriptases to switch templates in cDNA synthesis process to insert a primer annealing site at the 5’end of the TCR chain transcripts.

RACE using primers specific to the TRC genes (3') and the inserted primer (5') then permits unbiased PCR amplification of the TCR chains (Quigley et al. 2011). To analysis the NGS data, establish specialized bioinformatic pipelines are essential to compensate and correct for errors of sequencing/PCR, identify and quantify the expressed TCR chains. Currently, the pipelines are available for human and mouse TCR data (Bolotin et al. 2013), however recent work in the Morrison group at Roslin have adapted these pipelines to analysis of bovine TRB and TRG data (Connelley – personal communication).

1.6 Aims and objectives of the project

Currently, the ability of bovine NKp46+ CD3+ T cells to respond to *T. parva*-infected cells (TpM) has been demonstrated. Furthermore, functional analysis also indicates cell activation can be initiated by either NKp46 or CD3 signaling pathways (i.e. TCR), but whether the TCRs actually are required for recognition of autologous TpM has yet to be determined. The aim of this study is to examine the TCR repertoire of NKp46+ CD3+ T-cells responding to *T. parva* to better understand the clonality of this response and determine if there is evidence of conserved/semi-conserved TCR usage that could indicate TCR mediated selection and so suggest a role for TCR in NKp46+ CD3+ cells recognition of this pathogen.

The aim of this study is to **analyze the TCR repertoire of TpM-stimulated NKp46+CD3+ populations to look for evidence of TCR selection that would indicate a role for TCR in mediating recognition of TpM**. To enable this to be done the aim is to use high resolution NGS TRB sequence analysis to compare the TCR repertoires observed in TpM-stimulated and non-specific stimulated NKp46+CD3+ populations derived from naïve and T. parva-immune animals. So far, TpM specific-stimulated NKp46+CD3+ cell lines have been generated successfully from naive and *T. parva* immunized cattle and generation and maintenance of NKp46+CD3+ cell lines through use of non-specific stimulant hasn't been demonstrated. Thus to achieve the aim of the study the objectives are:

i) Optimize generation of TpM specific-stimulated cell lines from *T. parva* immunized cattle.
ii) Attempt to generate non-specific antigen stimulated NKp46+ CD3+ cell lines *in vitro.*
iii) Apply NGS technology to characterize the TCR β chain (TCRB) repertoire of NKp46+ CD3+ cells responding to non-specific stimulant and *T. parva* to identify the TCR usage.

Chapter 2. Isolation and expansion of bovine NKp46+ CD3+ T cell lines

2.1 Introduction

In a recent study, bovine NKp46+ CD3+ T cells were isolated from naïve cattle, and *in vitro* cell lines generated and maintained by repeated stimulation with irradiated autologous *Theileria parva* infected cells (TpM). Experiments as part of that study confirmed that the *in vitro* NKp46+ CD3+ cell lines originated from the *in vivo* NKp46+ CD3+ cell population (Connelley, Longhi, et al. 2014). Functional analysis indicated that the NKp46+ CD3+ T cells could recognize and respond to TpM (e.g. by cytotoxicity), and cross-linking of CD3 (i.e. stimulation of the TCR signaling pathway) led to cell activation (Connelley, Longhi, et al. 2014). However, the function of the TCR in mediating NKp46+CD3+ T cells recognition of TpM has still not been determined.

During antigen-specific T-cell responses clonotypes bearing TCR capable of binding the antigen undergo proliferation, leading to an over-representation of expression of those TCR in the responding populations. The objective of this chapter is to generate parallel *in vitro* NKp46+CD3+ cell lines from animals by i) co-culture with autologous TpM and ii) using non-specific stimulants, to provide material for subsequent TCR analysis. Comparison of the TCR repertoire of these lines in the subsequent chapter will then be used to determine if TpM co-culture (and therefore antigen-specific stimulation) generates cell lines with TCR repertoires with defined features that would suggest NKp46+CD3+ cells are using TCR to recognize autologous TpM.

The population of NKp46+CD3+ cells in the PBMC is small (0.1-1.7%) but it has been noted that following immunisation against *T. parva* the population shows a small but consistent expansion in size (Connelley – personal communication), suggesting they may have the capacity to form a memory population. Therefore, in this chapter initial experiments started using PBMC from animals that had been previously immunised against *T. parva*. Although attempts to generate NKp46+CD3+ cell lines by co-culture with autologous TpM were successful for all animals, it was not possible to generate and maintain NKp46+CD3+ cell lines using non-specific stimulation. Notably, and against expectations, NKp46+CD3+ cell lines appeared to be easier to generate from naïve than from immune animals.

2.2 Material and methods

2.2.1 Experimental animals

A total of 6 Friesian-Holstein cattle (302977, 202990, 202997, 702988, 106180, and 106222) obtained from the University of Edinburgh Farm were used in this study. Four animals (302977, 202990, 202997, and 702988) had been immunized with the Muguga stock of *T. parva* by the infection and treatment as described previously (Radley et al. 1975). Two animals (106180 and 106222) hadn't been immunized against *T. parva* and were regarded as naïve animals. The MHC phenotypes of these animals had been partially determined using a panel of class I MHC-specific monoclonal antibodies as part of other ongoing studies (Ellis et al. 1999); 302977, 202990, 202997 carried the A10 MHCI haplotype whilst 106180 and 106222 carried the A14 MHCI haplotype.

2.2.2 Cellular techniques

2.2.2.1 Conditions for cell culture

All the cells were cultivated in complete culture media: RPMI1640 (Gibco, Paisley, UK) supplemented with 10% heat-inactivated Fetal Calf Serum (FCS) (Gibco, Paisley, UK), 50 µM 2-mercaptoethanol, penicillin, streptomycin and glutamine solution (100x solution -Gibco, Paisley, UK). Cells were incubated in humid atmosphere at 37°C and 5% CO2 in air.

2.2.2.2 Isolation of peripheral blood mononuclear cells (PBMC)

Blood was obtained by jugular venupuncture and collected into citrate-phosphate-dextrose (CPD) anticoagulant. Peripheral blood mononuclear cells (PBMC) were isolated by density gradient centrifugation over Ficoll-Paque Plus solution (GE Healthcare Life Sciences). Aliquots of 30ml of blood was carefully overlaid onto 20ml of Ficoll-Paque Plus in pre-labelled 50ml Falco tube and centrifuged at 2500rpm for 30 minutes with no brakes at room temperature. The PBMC layer was harvested and washed 3 times in PBS containing 2mM EDTA and then counted (using trypan blue solution haemocytometer). If the PBMC pellet appeared to contain high numbers of red blood cells (RBCs) then RBC lysis was performed as an additional step (prior to the final wash in PBS/EDTA) by resuspending the pellet in 5ml RBC lysis buffer (50ml 0.175M TRIS, pH 7.4 added to 450ml 0.16M Ammonium Chloride) pre-heated to 37^{o}C, and then incubating at 37^{o}C for 1 minutes.

2.2.2.3 Isolation of NKp46+ cells using pan mouse IgG Dynabeads

The PBMC pellets were re-suspended into PBS+2mM EDTA+0.5% BSA to give final concentration of 5×10^7 cells/ml and incubated with 3ug/ml anti-ovine NKp46 mAb EC1.1 (Connelley et al. 2011) for 30 minutes at 4°C. Ten microliters of the immunomagnetic anti-mouse Ig beads (Dynabeads pan mouse IgG, Life Technologies, Paisley, U.K.) were prepared for every 1ml of cells (5×10^7) by washing and re-suspending in PBS+2mM EDTA+ 0.5% BSA (in brief beads were placed in the magnet for 2 minutes, the fluid removed, washed once with 1ml of PBS+ 2mM EDTA+ 0.5% BSA) before being replaced in the magnet, supernatant removed and the re-suspended in PBS+ 2mM EDTA+ 0.5% BSA). PBMC were washed in 50ml PBS+2mM EDTA at 1300rpm for 10 minutes for two washes, then incubated with the prepared Dynabeads for 30 minutes at 4°C on a rotator. After this incubation the cells were placed in a magnet, washed three times, and positively selected cells were collected. Cells were plated at 5×10^5 cells/ml in complete tissue culture media with 100U/ml recombinant human (rh) IL-2 (Chiron, Emeryville, CA) added at 100u/ml, in a 24 well plate overnight in 37°C incubator to allow the beads to dissociate from the cells. On the following day, cells were harvested placed in the magnet for 2 minutes and the NKp46+ cells collect and counted.

2.2.2.4. Isolation of NKp46+ CD3+ cells using flow cytometry sorting

NKp46+ CD3+ population were isolated from NKp46+ cells by flow cytometry sorting. The NKp46+ cells were stained with primary antibodies: AKS6 (murine IgG2b anti-bovine NKp46) and MM1A (murine IgG1 anti-bovine CD3) mAbs (each at 1ug/ml), then incubated at 4°C for 15-20 minutes. Cells were then washed 3 times in PBS + 0.5%BSA before being stained with Alexa Fluor 488-conjugated anti-murine IgG2b and Alexa Fluor 647-conjugated anti-murine IgG1 Abs (Molecular Probes, Paisley, UK), both at 1ug/ml. Flow cytometry sorting was performed using a FACSAria III (BD Biosciences, Oxford, U.K.).

2.2.2.5. Culture of Theileria parva infected cells (TpM)

Infected *Theileria parva* cell lines for the six animals were previously established using well established techniques (Connelley—personal communication). TpM are maintained in culture (expanded into culture flasks and kept in a humidified atmosphere of 5% CO_2 at 37°C) by replacing ½ or ¾ of the cell suspension with complete culture media every 2 days. Their

growth was frequently monitored by microscopic observation (clumps of cells and absence of dead cells).

2.2.2.6 Generation of IL-2 non-specific NKp46+ CD3+ cell lines

NKp46+ cells were plated at 2× 10^5 cells/ml and cultured with 100U/ml rhIL-2 in 96 round bottomed well plates (200ul/well). After 7 days of culture at 37°C in 5% CO_2 in a humidified atmosphere, cells were counted and assessed for purity by flow cytometry, and NKp46+CD3+ cells purified by flow cytometric sorting. The purified NKp46+ CD3+ cells were re-stimulated with 100 U/ml of rhIL-2 and cultured under the conditions described above. The cell number and purity were counted and analyzed every 7 days before re-stimulation with IL-2.

2.2.2.7 Generation of Concavalin A (Con A) non-specific NKp46+CD3+ cell lines

Following optimisation of generation of Con A non-specific stimulated NKp46+CD3+ cell lines, flow cytometry sorting of NKp46+ CD3+ cells was performed two days after Dynabead sorting (NKp46+ cells were plated at 2× 10^5 cells/ml and co-cultured with 100 U/ml of rhIL-2 in 96-well round-bottom plates for 2 days). After flow cytometry sorting, purified NKp46+ CD3+ cells were stimulated with Con A (2.5ug/ml, Amersham biosciences, Uppsala, Sweden) and 100 U/ml of rhIL2 in 96-well round-bottom plates for 7 days under the same conditions. The cells were counted, re-stimulated and the purity were assessed every 7 days.

2.2.2.8 Generation of TpM-specific NKp46+ CD3+ cell lines

Purified NKp46+ CD3+ cells were co-cultured with irradiated autologous TpM cells at 2× 10^5 cells/ml (4:1 ratio) in 96-well round-bottom plates under the conditions described above, supplemented with 100 U/ml of rhIL2. Every 7 days the cell lines were assessed by flow cytometry, counted and re-stimulated cells with irradiated TpM. If required, cell lines were subjected to additional purification by flow cytometry.

2.2.2.9 Flow cytometry analysis

Cells were re-suspended at <$2x10^7$cells/ml and 50µl aliquots were incubated for 30 min at 4°C with 50µl of primary antibody: AKS6 (murine IgG2b anti-bovine NKp46) and MM1A (murine IgG1 anti-bovine CD3); both at a final concentration of 1ug/ml in PBS/0.5% BSA/0.2% sodium azide. Cells were washed 3 times in FACS buffer (PBS+0.5%BSA+Na azide) and then incubated for 30 min at 4°C with 50µl secondary antibody: Alexa Fluor 488-conjugated anti-murine IgG2b and Alexa Fluor 647-conjugated anti-murine IgG1 Abs; both at 2ug/ml. Following another 3 washes in FACs buffer, analysis was completed on a FACSCalibur (BD Biosciences, Oxford, UK) flow cytometer. Cells were initially gated on FSC/SSC parameters to identify viable cells and $5x10^4$ viable cell events were collected. Analysis was performed using FloJo software (Ashland, Oregon, USA).

2.3 Results

2.3.1 Optimisation of NKp46+ cell line generation

Analysis of the frequency of NKp46+ CD3+ cells in PBMC using two-colour flow cytometry showed the percentage of the cells to be very low (varying from 0.14-0.26%) in both naïve and *T. parva* immunized animals (Table 2.1). Due to the low frequency of NKp46+ CD3+ cells and the absence of a single marker that could be used for cell sorting, it was decided to maintain the previous method of isolating the cells from *ex vivo* PBMC – i.e. sorting NKp46+ cells using Dynabeads (the frequency of NKp46+ cells in PBMC varied from 1.33-2.55%) followed by flow cytometric sorting of NKp46+ CD3+ cells after a short period of *in vitro* culture. Evaluation of NKp46+ isolation using the previously used parameters showed a recovery rate of 43-93% of the NKp46+ cells in the PBMC population with a purity of NKp46+ cells of 83-87%. An attempt to increase the recovery rate by doubling the Dynabead bead to cell ratio doubled the number of cells recovered (from 1.84×10^6 to 3.36×10^6) but the purity of NKp46+ cells dramatically reduced (from 83% to 52%), suggesting that the additional cells were largely NKp46- contaminants (data not shown).

	T.parva immunized animals				Naïve animals	
Animal	202997	202990	302977	702988	106222	106180
PBMC	9×10^8	1.36×10^9	1×10^9	9×10^8	2×10^9	2×10^9
NKp46+ CD3+ cells in total PBMC	0.18%	0.26%	0.16%	0.14%	0.22%	0.17%
NKp46+ cells in total PBMC	2.55%	2.42%	1.40%	1.76%	1.87%	1.33%
EXPECTED NKp46+ cell number	2.295×10^7	3.29×10^7	1.4×10^7	1.58×10^7	3.74×10^7	2.66×10^7
ACTUAL NKp46+ cell number from Dynabeads sorting	1.0×10^7 57% cell lost	2.8×10^7 15% cell lost	1.3×10^7 8% cell lost	1.23×10^7 23% cell lost	2.8×10^7 26% cell lost	1.4×10^7 47% cell lost
Recovery rate of Dynabeads sorting	43%	85%	93%	77%	74%	53%
Purification of NKp46+ cells	NKp46+ cell: 83%-87%; NKp46+ CD3+ cells: 2%-4%; NKp46-CD3+ cells <3%; NKp46-CD3- cells: 6%-12%					

Table 1.1 Cell number of PBMC and the frequency of i) NKp46+ CD3+ cells and ii) NKp46+ cells of PBMC. Recovery rate of Dynabeads sorting; number and purification of NKp46+ cells.

During some attempts at NKp46+ isolation clumping of the cells was observed, leading to dramatically reduced numbers of cells recovered. This clumping appeared to occur after the washing to remove the NKp46+ antibody. To address this issue the effects of adding BSA or performing all stages of the cell isolation at 4^{o}C was examined. The latter appeared to effectively avoid the cell clumping issue (data not shown). Consequently, it was decided to use the initial sorting protocol but perform all stages at 4^{o}C.

2.3.2 Generation of NKp46+ CD3+ cell-lines by non-specific stimulation

2.3.2.1 Interleukin 2 (IL-2) stimulation for non-specific NKp46+ CD3+ cell line generation

To address the study objective of comparing the TCR repertoire between non-specific stimulated and TpM specific-stimulated NKp46+ CD3+ cell lines, it was necessary to determine if NKp46+ CD3+ cells could be maintained *in vitro* using non-specific stimulants. Interleukin 2 (IL-2) is a potent T cell growth factor and has been shown to stimulate bovine NK cell proliferation *in vitro* (Liao et al. 2011). We hypothesised that IL-2 could be effective as a non-specific stimulant of NKp46+ CD3+ cells *in vitro*.

To evaluate the effect of IL-2 alone as a stimulant of NKp46+ CD3+ cells, NKp46+ cells were isolated from 2 animals (702988 and 302977) and parallel cultures generated with ¼ of the NKp46+ cells cultured with autologous irradiated TpM and IL-2 (as described above) and ¾ with IL-2 only. After 7 days in culture, a significant decline in total cell numbers was observed in all cultures, especially in non-specific stimulated cell lines (Table 2.2). Notably, the number of NKp46+ CD3+ cells in the non-specifically stimulated cultures also declined whereas in the TpM stimulated cultures there was an increase in NKp46+ CD3+ cell number (Table 2.2). After 7 days NKp46+ CD3+ cells were isolated from each culture by flow cytometry to a purity of >95% and re-stimulated using similar conditions. After a further 7 days of culture the frequency to NKp46+ CD3+ cells in the culture from animal 702988 was 91.3% (Figure 2.1) and the cell number had approximately doubled (Table 2.2), however the frequency of NKp46+ CD3+ cells in the culture from 302977 stimulated with TpM and IL-2 was only 5.5% (probably due to contamination with highly proliferative *T. parva*-specific CD8+ T-cells – data not shown) despite an expansion following the second stimulation. In contrast, the cultures stimulated with IL-2 alone both continued to decline in number and the frequency of NKp46+CD3+ became negligible (0.32-0.38%), with NKp46-CD3+ T-cells

apparently the dominant population (Figure 2.1). Consequently, it was concluded that non-specific stimulation with IL-2 was not sufficient to maintain NKp46+ CD3+ cell lines *in vitro.*

	Animal			
	702988		302977	
	TpM+ IL-2	Only with IL-2	TpM+ IL-2	Only with IL-2
NKp46+ cells from Dynabeads sorting	3.0×10^6	9.0×10^6	3.25×10^6	9.75×10^6
count cells 7 days after Dynabeds sorting	1.52×10^6 2-fold decrease	7.25×10^5 12-fold decrease	1.27×10^6 2.5-fold decrease	3.82×10^5 25.5-fold decrease
Frequency of NKp46+CD3+ in NKp46+ cells after 7 days' culture	1.32-fold increase (2.13-2.82%)	1.97-fold decrease (2.13-1.08%)	1.17-fold increase (3.25-3.82%)	3.92-fold decrease (3.25-0.82%)
NKp46+ CD3+ cells sorted by flow cytometry	3.56×10^4	5.048×10^3	3.64×10^4	3.92×10^3
Total cell number after 7 days FACs sorting	7.10×10^4 1.99-fold increase	3.9×10^3 1.29-fold decrease	6.84×10^4 1.87-fold increase	1.92×103 2-fold increase
FACs analysis results	**Figure 2.1**			

Table 2.2 Cell number results of animal 702988 and 302977 co-cultured with TpM+IL-2 and only with IL-2

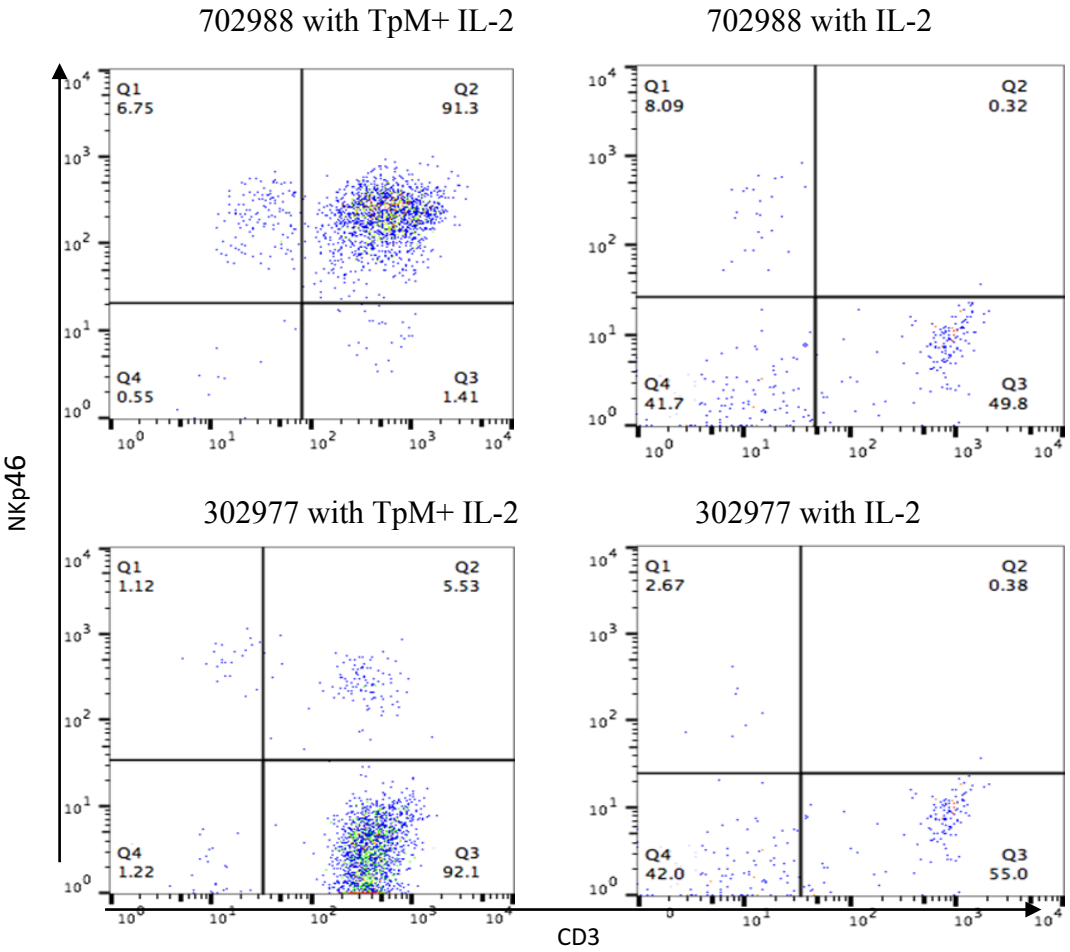

Figure 2.1. FACs analysis results of 7 days after flow cytometry sorting (7 days after second stimulation). The NKp46+ CD3+ cell lines of animal 702988 and 302977 were stimulated with either IL-2 or TpM+ IL-2.

2.3.2.2. Concanavalin A (Con A) stimulated non-specific NKp46+ CD3+ cell line generation

Concanavalin A (Con A) has the capacity to trigger T cell activation, proliferation, and differentiation. Con A was hypothesised as another potential non-specific stimulant of NKp46+ CD3+ cells and the ability to use this was therefore examined.

Isolated NKp46+ cells were stimulated *in vitro* in parallel cultures with either i) IL-2, ii) IL-2 + TpM or iii) IL-2 + Con A to examine the effect of Con A as a non-specific stimulant for NKp46+ CD3+ cells. After 7 days in culture, the total cell number decreased by more than 2-fold in both IL-2 and Con A+ IL-2 stimulated cell lines, but a dramatic increase (3-fold) was observed in the TpM stimulated cell line (Table 2.3). Flow cytometry analyses were performed after 7 days of cell culture to look at the phenotype of the cell lines. The results indicated that Con A promoted the proliferation of NKp46-CD3+ (i.e. T cell phenotype) cells (Figure 2.2), suggesting that NKp46-CD3+ cells need to be removed by flow cytometry sorting before addition of Con A. In the original protocol, cells were left for 7 days after Dynabead sorting to (i) ensure the removal of the Dynabeads from the cell surface and (ii) to allow recovery of NKp46 marker expression on the cell surface. In order to determine if it was necessary to leave the cells 7 days for recovery, FACs analysis was performed 2 days after Dynabead sorting; cells were stained with i) secondary antibody only (to verify that the NKp46 monoclonal antibody used during the primary sort was no longer present) and ii) with sequential primary and secondary antibodies (to ensure that NKp46 was expressed at the cell surface at this time point). The results showed that the cells were not effectively stained with the secondary antibody (Figure 2.3) only but were effectively stained with primary/secondary antibody combination (Figure 2.3); this indicated that by 2 days post-Dynabead sorting the cells could be re-stained for a secondary flow cytometric sort to remove NKp46-CD3+ cells and this was adopted as the new protocol.

Using this new protocol NKp46+CD3+ cells following the second, flow cytometric sort were equally divided into two aliquots and parallel cultures with either i) TpM+ IL-2 or ii) Con A+ IL-2 were established. FACs analysis performed after 7 further days of culture, indicated that the frequency of NKp46+ CD3+ cells in Con A stimulated cell line was only 0.37% and that the frequency of NKp46- CD3+ cells reached up to 96.7% (Figure 2.4). These results suggest that ConA was sufficiently biasing the proliferation of conventional T-cells over NKp46+CD3+ T-cells to not be useful as a non-specific stimulant in this project. For the

remainder of the study, cells were FACs sorted 2 days after Dynabeads stimulation as this gave a greater degree of purity.

Animal 202997	With TpM + IL-2	Only with IL-2	With Con A+ IL-2
Dynabeads sorting	1/4	1/2	¼
Total NKp46+ cells: 1.0×10^7	2.5×10^6	5×10^6	2.5×10^6
Total cell number after 7 days of culture	7.5×10^6 3-fold increase	7.0×10^5 7.14-fold decrease	1.2×10^6 2-fold decrease

Table 2.3 Cell number results of animal 202997 NKp46+ cell lines co-cultured with i) TpM+ IL-2, ii) only with IL-2 and iii) Con A+ IL-2

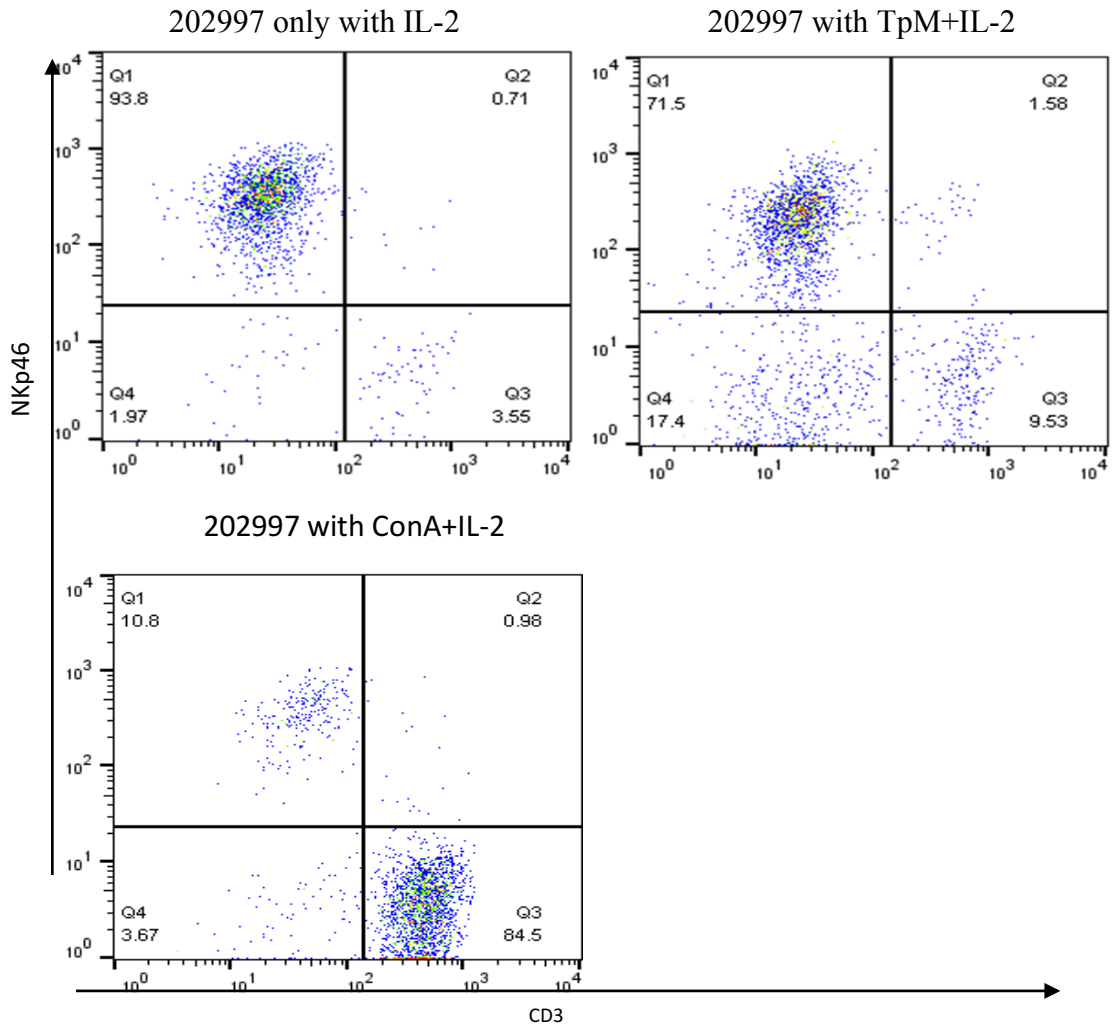

Figure 2.2. FACs analysis results of 7 days after Dynabeads sorting. The NKp46+ cell lines of animal 202997 were co-cultured with i) only IL-2, ii) TpM+ IL-2 and iii) ConA+IL-2.

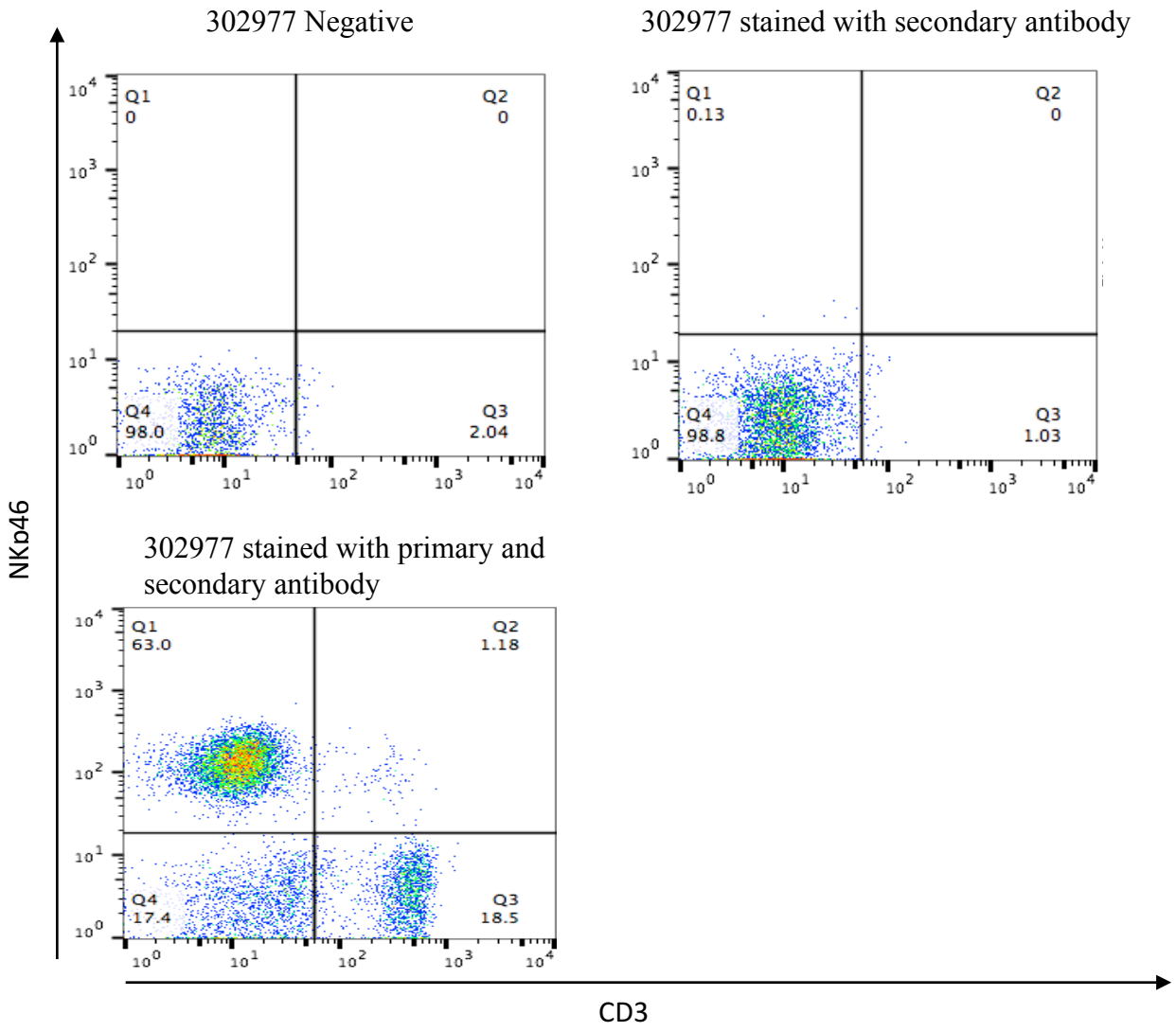

Figure 2.3 FACs analysis results of NKp46+ cells after two days of Dynabeads sorting. The cells were stained with i) negative buffer, ii) only second antibody, and iii) primary and secondary antibody.

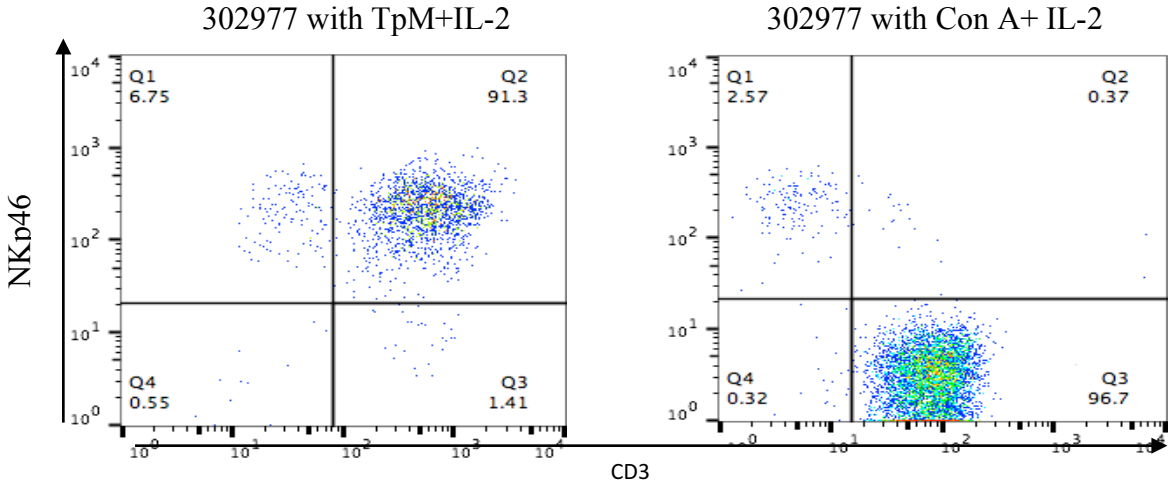

Figure 2.4. FACs analysis results of 7 days after flow cytometry sorting. The 302977 NKp46+ CD3+ cell lines were co-cultured either with TpM+ IL-2 or ConA+ IL-2.

2.3.3 Generation of TpM-specific stimulation NKp46+ CD3+ cell lines from T. parva immunized animals

Compared with the non-specific stimulated cell lines, *in vitro* generation of TpM-stimulated cell lines was much easier. In total, three TpM stimulated cell lines were generated from immunized animals (animal 302977, 202990 and 202997). The fold change in total cell number of the cultures (Figure 2.10, Table 2.4, Table 2.5, and Table 2.6) and the frequency of NKp46+ CD3+ cells (Figure 2.11) were determined 7 days after each stimulation with autologous TpM, and the corresponding fold-change in NKp46+CD3+ cell number was calculated (Figure 2.12). In all cell lines, the total cell number increased throughout the whole culture period (Figure 2.10), while the frequency of NKp46+ CD3+ cells decreased substantially after FACs sorting (first stimulation) but then steadily increased in the subsequent stimulations (Figure 2.11). For animal 302977 and 202990, a total of 1.6×10^6 and 2.0×10^5 cells were collected in the final cell lines (after 5^{th} and 3^{rd} stimulation respectively) and the frequency of NKp46+ CD3+ cells was 96.7% and 90.8% respectively (Figure 2.5 and Figure 2.6). For animal 202997, 3.0×10^5 cells were harvested for TCR analysis following the fourth TpM stimulation; at this point the frequency of NKp46+ CD3+ cells was relatively low (66.0%) with the predominant contaminating population being NKp46+ CD3- cells (33.6% - Figure 2.7). However, as NKp46+ CD3- cells do not express rearranged TCR chains segments this contamination was considered acceptable as it should not interfere with the subsequent TCR repertoire analysis.

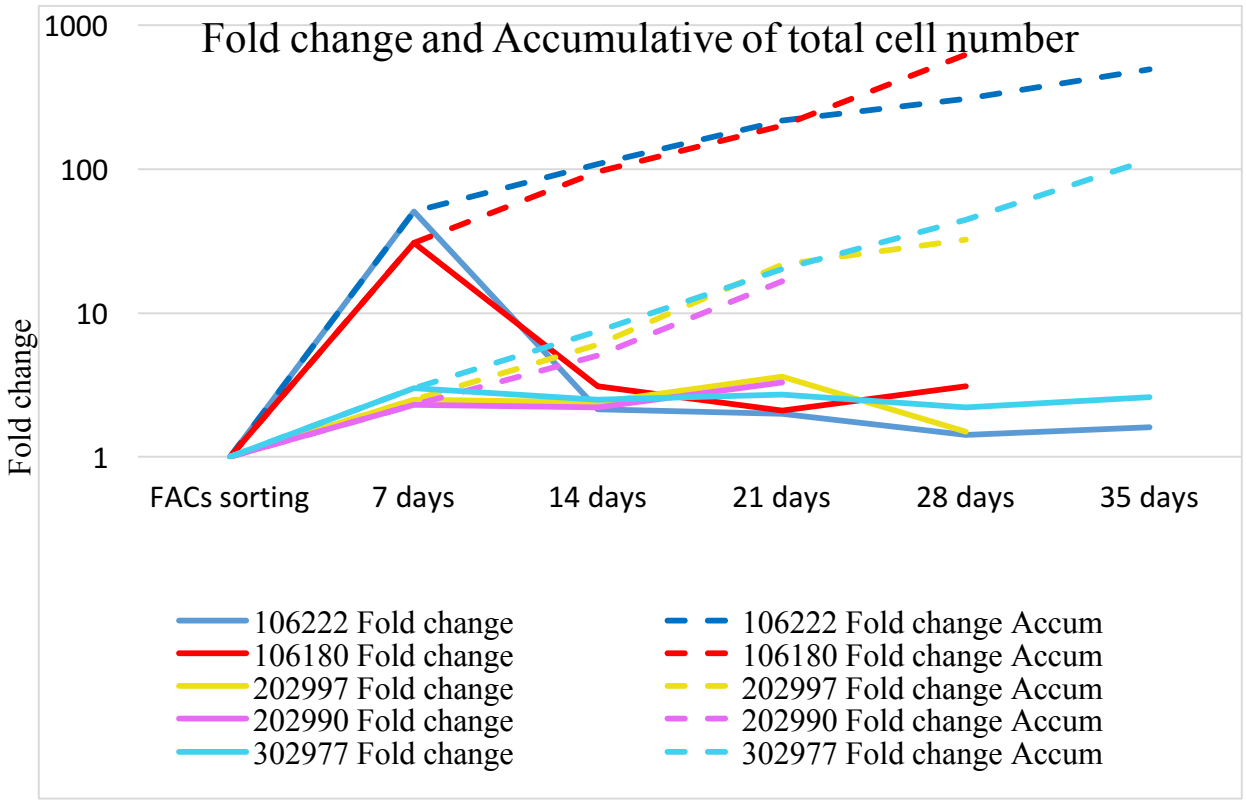

Figure 2.10 Fold change (compared to previous week) and Fold change accumulative (compared to number of cells at the beginning of the culture period) of total cell number for TpM specific-stimulated cell lines during repeated TpM stimulation.

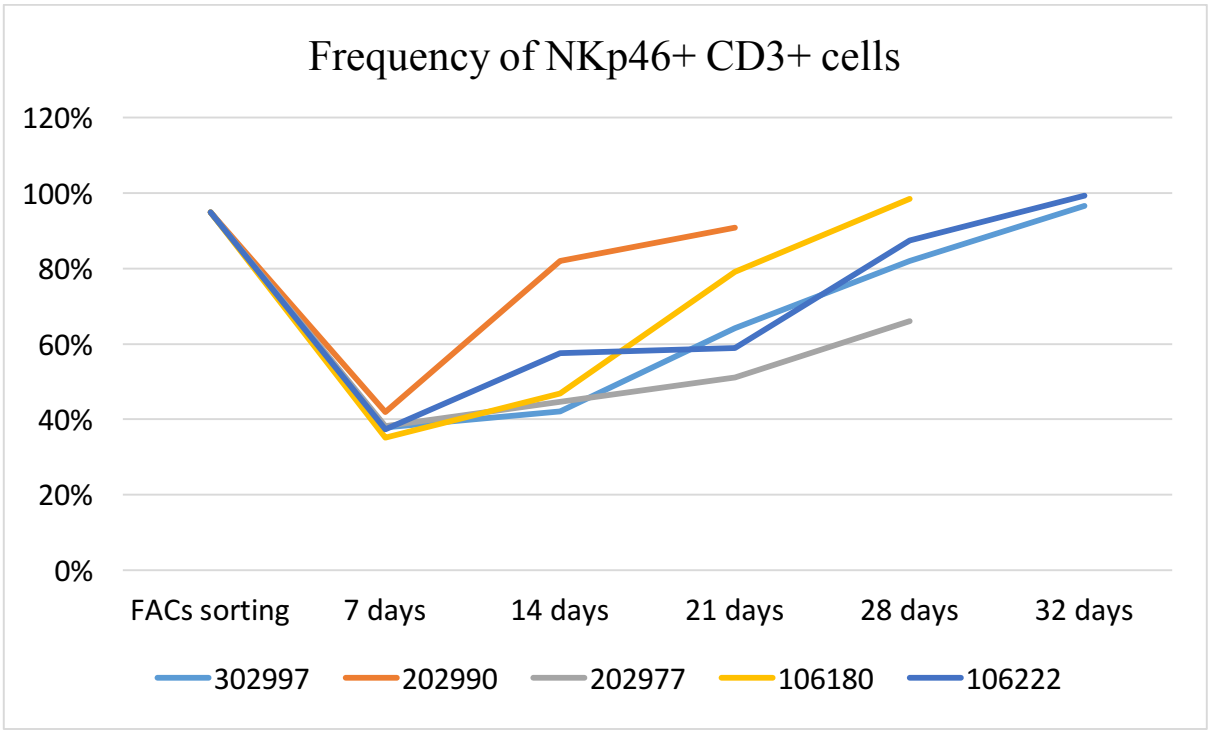

Figure 2.11 Frequency of NKp46+ CD3+ cells in all TpM specific stimulated cell lines during repeated stimulation

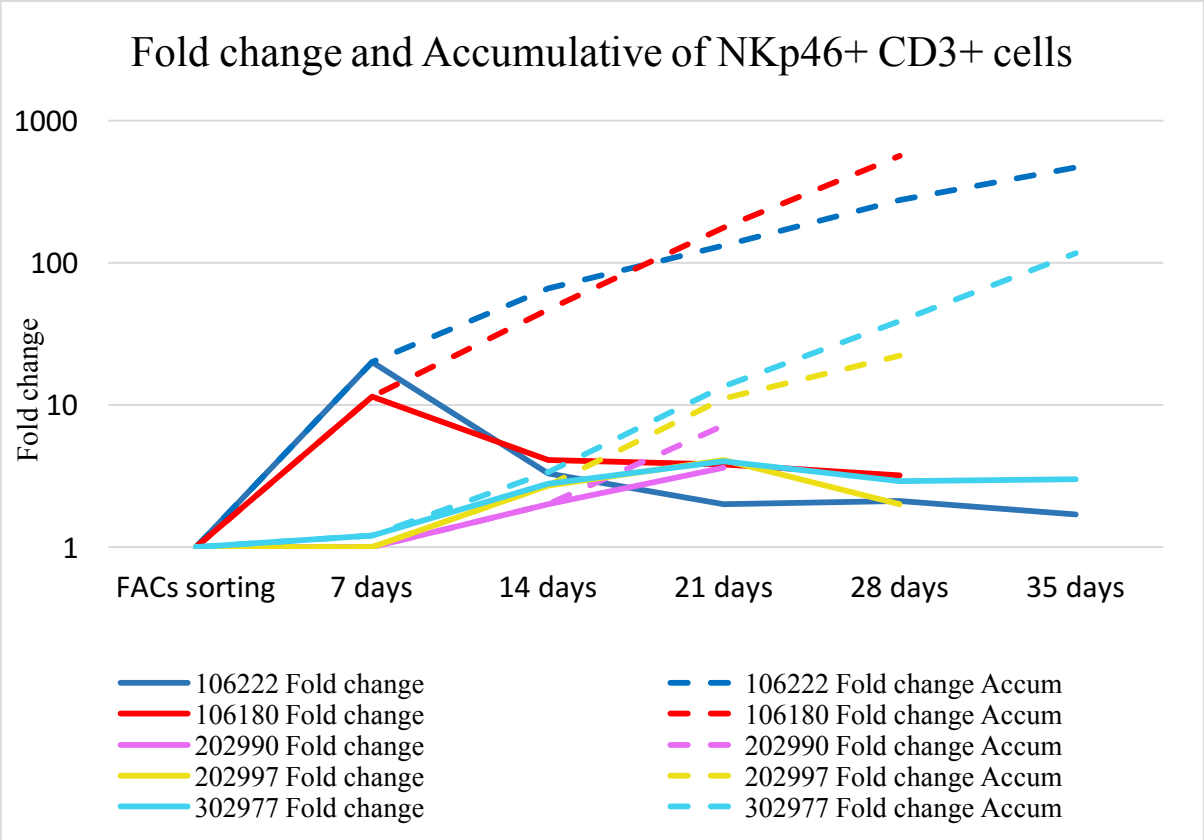

Figure 1.12. Fold change (compared to previous week) and Fold change accumulative of NKp46+ CD3+ cells (compared to beginning number of cells) for TpM specific stimulated cell lines during repeated TpM stimulation.

302977						
Procedure	Cell Type	Total cells number	Fold change of total cell number	Frequency of NKp46+ CD3+ cells	Number of NKp46+ CD3+ cells	Fold change of NKp46+ CD3+ cells
Flow cytometry sorting	NKp46+ CD3+ cells	1.3×10^4		95%	1.2×10^4	
7 days after first TpM stimulation	NKp46+ CD3+ cells	4.0×10^4	3.0-fold increase	37.8%	1.5×10^4	1.2-fold increase
7 days after second TpM stimulation	NKp46+ CD3+ cells	1.0×10^5	2.5-fold increase	42.1%	4.2×10^4	2.8-fold increase
7 days after Third TpM stimulation	NKp46+ CD3+ cells	2.7×10^5	2.7-fold increase	64.2%	1.7×10^5	4.0-fold increase
7 days after Fourth TpM stimulation	NKp46+ CD3+ cells	6.1×10^5	2.2-fold increase	82.0%	5.0×10^5	2.9-fold increase
Final NKp46+ CD3+ cell number	NKp46+ CD3+ cells	1.6×10^6	2.6-fold increase	96.7%	1.5×10^6	3.0-fold increase

Table 2.4 The cell number of total cells and NKp46+ CD3+ cells and fold change of total cells and NKp46+ CD3+ cells of animal 302977

202990						
Procedure	Cell Type	Total Cells number	Fold change of total cell number	Frequency of NKp46+ CD3+ cells	Number of NKp46+ CD3+ cells	Fold change of NKp46+ CD3+ cells
Flow cytometry sorting	NKp46+ CD3+ cells	8.4×10^4		95%	7.9×10^4	
7 days after first TpM stimulation	NKp46+ CD3+ cells	2.0×10^5	2.3-fold increase	42%	8.4×10^4	1.0-fold increase
Re-purification	NKp46+ CD3+ cells	2.64×10^4		95%	2.5×10^4	
7 days after second TpM stimulation	NKp46+ CD3+ cells	6.0×10^4	2.2-fold increase	82%	4.9×10^4	2.0-fold increase
Final NKp46+ CD3+ cell number	NKp46+ CD3+ cells	2.0×10^5	3.3-fold increase	90.8%	1.8×10^5	3.6-fold increase

Table 2.5 The cell number of total cells and NKp46+ CD3+ cells and fold change of total cells and NKp46+ CD3+ cells of animal 202990.

202997						
Procedure	Cell Type	Total cells number	Fold change of total cell number	Frequency of NKp4+CD3+ cells	Number of NKp46+ CD3+ cells	Fold change of NKp46+CD3+ cells
Flow cytometry sorting	NKp46+ CD3+ cells	9.0×10^3		95%	8.5×10^3	
7 days after first TpM stimulation	NKp46+ CD3+ cells	2.3×10^4	2.5-fold increase	38.2%	8.7×10^3	1.0-fold increase
7 days after second TpM stimulation	NKp46+ CD3+ cells	5.5×10^4	2.4-fold increase	44.6%	2.4×10^4	2.7-fold increase
7 days after Third TpM stimulation	NKp46+ CD3+ cells	2.0×10^5	3.6-fold increase	51.1%	1.0×10^5	4.1-fold increase
Final NKp46+ CD3+ cell number	NKp46+ CD3+ cells	3.0×10^5	1.5-fold increase	66.0%	2.0×10^5	2.0-fold increase

Table 2.6 The cell number of total cells and NKp46+ CD3+ cells and fold change of total cells and NKp46+ CD3+ cells of animal 202997.

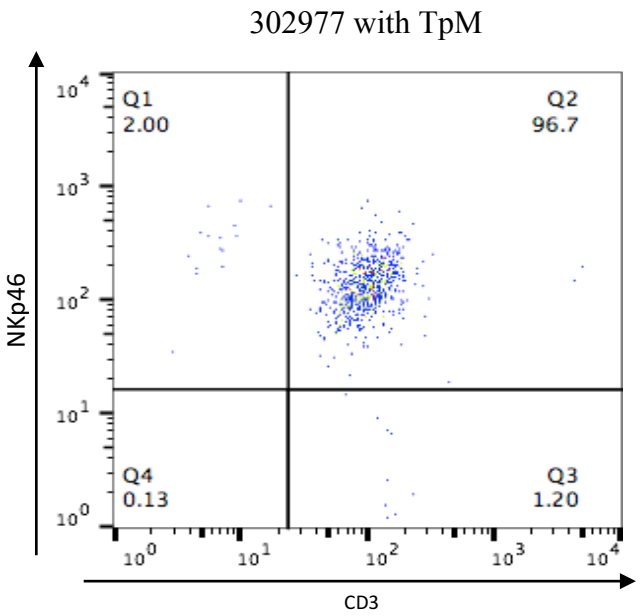

Figure 2.5. FACs analysis result of the final cell line (7 days after 5th stimulation) for animal 302977

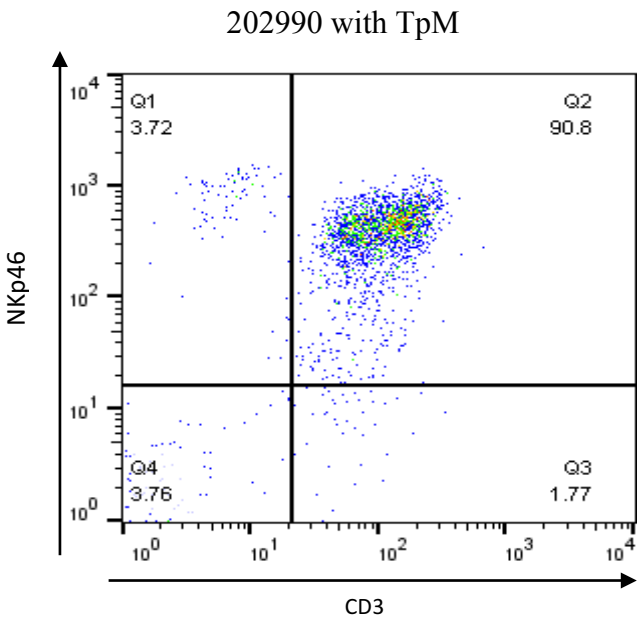

Figure 2.6. FACs analysis result of the final cell line (7 days after 3rd stimulation) for animal 202990

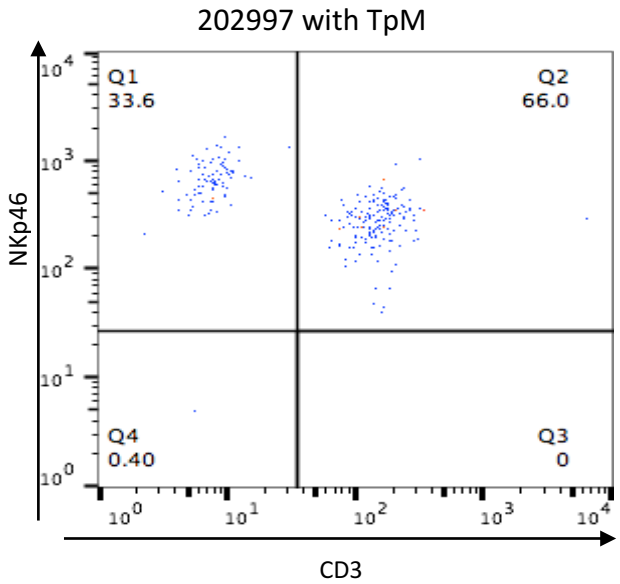

Figure 2.7. FACs analysis result of the final cell line (7 days after 4th stimulation) for animal 202997

2.3.4 Generation of TpM-specific NKp46+ CD3+ cell lines from naive animals

To allow a comparison of the TCR repertoires of TpM-stimulated NKp46+CD3+ populations from naïve and immunized animals, TpM-stimulated NKp46+ CD3+ cell lines were generated from naïve animals (animals 106180 and 106222). The total cell number and FACs analysis results for these two cell lines are shown in Table 2.7 and Table 2.8. For animal 106180, the total cell number increased more than 30-fold after the first TpM stimulation and maintained a stable growth in the subsequent stimulations (Table 2.7). The cell line of animal 106222 exhibited a similar growth trend, and after the first stimulation, the cell number increased more than 50-fold in 7 days (Table 2.8). Similar to the immunized animals, the frequency of NKp46+ CD3+ cells in both naïve cell lines decreased dramatically after the first stimulation and the slowly increased in the subsequent stimulations (Figure 2.11). A total of 1.0×10^6 cells were collected for the 106180 cell line with NKp46+ CD3+ cells constituting >98% of the population (Table 2.7; Figure 2.8). To evaluate the evolution of the TCR repertoire following repeated TpM stimulations, 3 harvests of the cell line from animal 106222 were collected – 7 days after the 2^{nd}, 3^{rd} and 5^{th} stimulations. At each of these points the frequency of contaminating NKp46-CD3+ T-cells was < 2% (Table 2.8; Figure 2.9).

In summary, a total of 7 TpM-stimulated NKp46+ CD3+ T cell lines were generated in this study, which included 3 cell lines from *T. parva* immunized animals (202990, 202997 and 302977), one cell line from naïve animal 106180, and three cell lines from naïve animal 106222 (collected after different numbers of *in vitro* stimulations). mRNA was prepared from these cell lines and stored at -80^{o}C until prepared for NGS analysis.

Animal: 106180						
Procedure	Cell Type	Total Cells number	Fold change of total cell number	Frequency of NKp46+ CD3+ cells	Number of NKp46+ CD3+ cells	Fold change of NKp46+ CD3+ cells
Dynabeads sorting	NKp46+ cells	4.0×10^6				
Cell number after 2 days Dynabeads sorting	NKp46+ cells	8.8×10^5				
Cell number from FACs sorting	NKp46+CD3+ cells	2.27×10^4		95% NKo46+ CD3+ cells	2.1×10^4	
7 days after FACs sorting (7 days after First TpM stimulation)	NKp46+ CD3+ cells	7.0×10^5	30.8-fold increase	35.10% NKp46+ CD3+ cells; (62.71% NKp46+ CD3-cells;2.17% NKp46-CD3+ cells)	2.4×10^5	11.4-fold increase
7 days after Second TpM stimulation	NKp46+ CD3+ cells	2.2×10^6	3.1-fold increase	46.8% NKp46+ CD3+ cells (50.8% NKp46+ CD3-cells;2.23% NKp46-CD3+ cells)	1×10^6	4.1-fold increase
7 days after Third TpM stimulation	NKp46+ CD3+ cells	4.8×10^6	2.1-fold increase	79.1% NKp46+ CD3+ cells (16.6% NKp46+ CD3-cells; 3.29% NKp46-CD3+ cells)	3.8×10^6	3.8-fold increase
FACs sorting (re-purification)	NKp46+CD3+ cells	3.17×10^5			3.0×10^5	
7 days after FACs sorting (7 days after Fourth TpM stimulation)	NKp46+ CD3+ cells	1.0×10^6	3.1-fold increase	98.5% NKp46+ CD3+ cells (0.16% NKp46+ CD3-cells; 1.26% NKp46-CD3+ cells)	9.8×10^5	3.2-fold increase

Table 2.7 The cell number of total cells and NKp46+ CD3+ cells, and fold change of total cells and NKp46+ CD3+ cells of animal 106180.

Animal: 106222						
Procedure	Cell Type	Total cells number	Fold change of total cell cumber	Frequency of NKp46+ CD3+ cells	Number of NKp46+ CD3+ cells	Fold change of NKp46+ CD3+ cells
Dynabeads sorting	NKp46+cells	2.8×10^7				
Cell number after 2 days Dynabeads sorting	NKp46+cells	1.4×10^7				
Cell number from FACs sorting	NKp46+CD3+ cells	1.38×10^5		95% NKp46+ CD3+ cells	1.31×10^5	
7 days after FACs sorting (7 days after First TpM stimulation)	NKp46+ CD3+ cells	7.0×10^6	50.7-fold increase	37.4%NKp46+ CD3+ cells (54.5% NKp46+ CD3-cells; 2.94% NKp46-CD3+ cells)	2.61×10^6	20-fold increase
7 days after Second TpM stimulation (Half cells were collected for NGS)	NKp46+ CD3+ cells	1.5×10^7 Half cells were collected → 7.0×10^6	2.14-fold increase	57.5% NKp46+ CD3+ cells (41.0% NKp46+ CD3-cells;0.12% NKp46-CD3+ cells)	8.62×10^6 →4.0×10^6	3.3-fold increase
7 days after Third TpM stimulation (Half cells were collected for NGS)	NKp46+ CD3+ cells	1.4×10^7 Half cells were collected → 7.0×10^6	2.0-fold increase	58.9% NKp46+ CD3+ cells (40.9% NKp46+ CD3- cells;0.024% NKp46-CD3+ cells)	8.2×10^6 →4.1×10^6	2.0-fold increase
7 days after Fourth TpM stimulation	NKp46+ CD3+ cells	1.0×10^7	1.42-fold increase	87.4% NKp46+ CD3+ cells (14.1% NKp46+ CD3-cells;0.28% NKp46-CD3+ cells)	8.7×10^6	2.1-fold increase
FACs sorting (re-purification)	NKp46+ CD3+ cells	2.35×10^6		95% NKp46+ CD3+ cells	2.2×10^6	
7 days after FACs sorting (7 days after the Fifth TpM stimulation)	NKp46+ CD3+ cells	3.78×10^6	1.6-fold increase	99.4% NKp46+ CD3+ cells (0.33% NKp46+ CD3-cells; 0.11% NKp46-CD3+ cells)	3.7×10^6	1.7-fold increase

Table 2.8 The cell number of total cells and NKp46+ CD3+ cells and fold change of total cells and NKp46+ CD3+ cells of animal 106222.

106180 with TpM

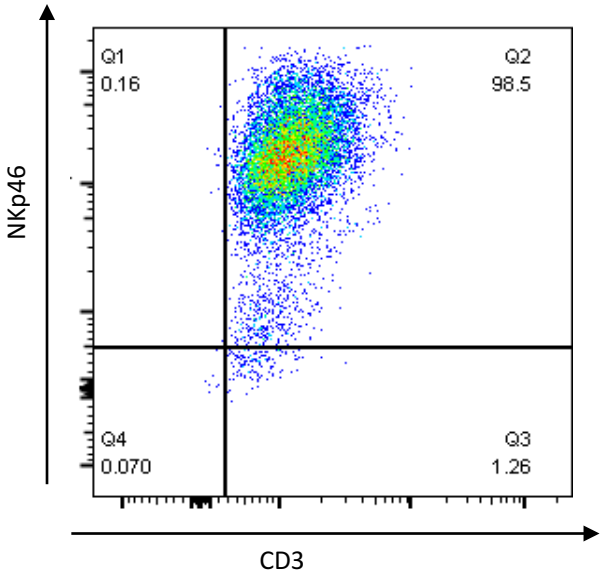

Figure 2.8. FACs analysis result of the final cell line (7 days after 4th stimulation) for animal 106180

106222 with TpM

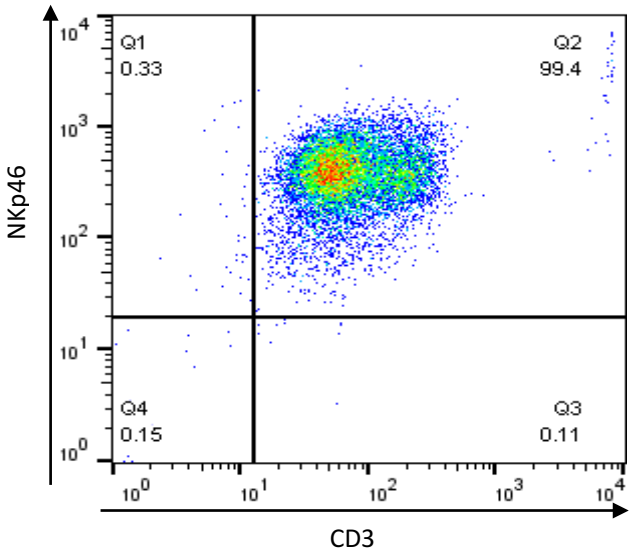

Figure 2.9. FACs analysis result of the final cell line (7 days after 5th stimulation) for animal 106222

2.4. Discussion

The work in this chapter aimed to generate NKp46+ CD3+ cell lines by stimulation with either a specific stimulant (TpM) or a non-specific stimulant in order to allow subsequent investigation of the TCR repertoire of NKp46+ CD3+ cells. The results are based on *in vitro* studies and provide information on the total cell number and frequency of NKp46+ CD3+ cells after each stimulation in order to evaluate the proliferation of cell lines. TpM specific stimulated NKp46+ CD3+ cell lines were generated from both naïve and immune animals, but, despite several attempts, it was not possible to successfully generate non-specific stimulated NKp46+ CD3+ cell lines.

The frequency of NKp46+ CD3+ cells in PBMC varies from 0.14-0.26% with no apparent difference between *T. parva* naïve and immune animals. Based on the cell isolation protocol from a previous study (Connelley, Longhi, et al. 2014), the Dynabeads sorting method was used to isolate the NKp46+ cells. This lead to NKp46+ cell recovery rates of 43-93% and purities of 83-87% The wide range of recovery rate may have been caused by i) loss during centrifugation, ii) miscalculation, and iii) clumping and consequent loss of cells when isolations were not carried out at low temperatures (on ice). An attempt was made to increase the recovery rate by doubling of the numbers of magnetic beads, but this was not successful. In future studies it may be worth investigating increasing the antibody concentration and the incubation time. The NKp46+ CD3+ cells were subsequently isolated from the purified NKp46+ cells by FACs sorting which permits sorting based on multiple parameters. FACs sorting is characterised by the high purity of the sorted cells (>95%) but also relatively low yield. To increase the NKp46+ CD3+ cell yield, the MACs sorting isolation method was also examined in this study, but the results indicate that the purity of the isolated cell lines was relatively low (data not shown). Therefore, FACS sorting was chosen as the preferred method to obtain pure NKp46+ CD3+ cell lines.

IL-2 and Con A were investigated as non-specific stimulants for NKp46+ CD3+ cells in this study, but non-specific stimulated cell lines were not generated successfully. The primary function attributed to IL-2 is the capacity of enhance *in vitro* T cell proliferation and differentiation. Thus IL-2 is regarded as a general cell growth factor and was added to all TpM specific and non-specific stimulated cell lines. Meanwhile, it was also regarded as an autonomous non-specific stimulant. The results indicate that the NKp46+ CD3+ cells

stimulated only with IL-2 were dying off following cell culture and repeated IL-2 non-specific stimulation (the total cell number and frequency of NKp46+ CD3+ cells showed consecutive drops). Thus IL-2 was not an effective non-specific stimulant. Due to its ability to trigger T cell activation by directly interacting with T cell receptor, Con A was also hypothesized as non-specific stimulant in this study. However, the results indicate that Con A stimulation was not sufficient to maintain the purified NKp46+ CD3+ cells *in vitro*. A previous study demonstrated that NKp46+ CD3+ cells can be activated by the CD3 signally pathway (Connelley, Longhi, et al. 2014), thus we hypothesis that the failure to maintain purified NKp46+ CD3+ lines may be due to overgrowth by conventional T-cells or some form of defective signalling between the TCR and CD3 molecules. In a recent study, Con A was also used in an attempt to trigger the proliferation of porcine CD3+ NKp46+ cells but, similar to our findings, proliferation was not detected (Mair et al. 2016). In further studies, non-specific stimulation of NKp46+ CD3+ cell lines could be attempted by maintainance with NK cell growth factors, such as IL-12, IL-15, IL-18, and IL-21 or alternatively by cross-linking of either NKp46 +/- CD3 through cross-linking via well-bound antibodies.

Compared with the IL-2 non-specific stimulated cell lines, a good cell proliferation was observed in the parallel cultured TpM-stimulated cell lines (Table 2.2; Figure 2.1). The frequency of NKp46+ CD3+ cells was analysed 7 days after the second TpM stimulation in animal 702988 and was found to be 91.3% (Figure 2.1). In contrast, frequencies of 5.53% NKp46+ CD3+ cells and 92.1% NKp46- CD3+ cells were found in animal 302977 (Figure 2.1). The marked proliferation of NKp46- CD3+ cells may have been caused by recall of contaminating conventional CD8+ *T. parva* specific memory T-cells in this immunized animal.

TpM specific stimulated cell lines were generated successfully from both naïve and immune animals. However, compared with the immune cattle, the cell lines were much easier to generate from naïve cattle. The fold changes of total cell number are show in Figure 2.10, which indicates that after the first stimulation, 30.8 and 50.7-fold increases were observed in naïve animals 106180 and 106222 respectively, but only 2.3- 3-fold increases occurred in the three immune animals. After FACs sorting, the purity of NKp46+ CD3+ cell lines can reach more than 95%, however, it decreased dramatically (from more than 95% to 35-42%) after the first TpM stimulation in both naïve and immunized cell lines (Figure 2.12). This is mainly caused by early proliferation of NKp46+ CD3- cell contaminants. In order to present

the proliferation of NKp46+ CD3+ cells in a visible way, the number of NKp46+ CD3+ cells was calculated based on the total cell number and the frequency of NKp46+ CD3+ cells, and the fold changes of the number of NKp46+ CD3+ cells is shown in Figure 2.12. The results demonstrated that after the first stimulation, the NKp46+ CD3+ cells increased more than 11-fold in naïve animals but only around 1-fold increase in immune animals. Following subsequent stimulations, the results indicate that the number and frequency of NKp46+ CD3+ cells were growing steadily in both naïve and immune animals (Figure 2.11, Figure 2.12).

Consequently, after the first TpM stimulation, the substantial proliferation of the naïve NKp46+ CD3+ cells suggests that NKp46+ CD3+ cells may not form a long-term maintained memory population that enables a stronger recall in vitro. Further studies that track NKp46+ CD3+ cell responses from the same individual when naïve and then immune would be of interest to further study this.

Chapter 3. NGS analysis of TRB repertoire expressed by NKp46+CD3+ cells

3.1 Introduction

In a previous study panels of Vα and Vβ subgroup-specific primers were used to analyse the TCR repertoire of bovine NKp46+CD3+ cells (Connelley et al. 2008). The results from this study indicated the expression of a broad TCR repertoire, however such low resolution analysis of TCR repertoires cannot describe the clonality of the NKp46+CD3+ responding populations or identify if there are preferential usage of particular V-J combinations or selection for particular CDR3 lengths or motifs. Similar, in the absence of sequence data it is not possible to identify if there are 'public' TCRs that are characteristic for this population. To achieve a high resolution analysis of the TCR repertoire of NKp46+CD3+ populations it was decided to employ a NGS approach.

In this chapter are presented results generated by NGS sequencing of the TRB chains of the TpM-stimulated NKp46+ CD3+ cell lines generated in the previous chapter. The objectives of this chapter are to use the high resolution TCR sequence data to examine; 1) the evolution of the clonality of NKp46+ CD3+ cells following repeated TpM stimulations, 2) the degree of clonality observed in the TpM-stimulated NKp46+CD3+ cell lines, 3) to examine if there is any evidence of conserved TRB chain sequences expressed by TpM-specific NKp46+CD3+ populations derived from different animals and 4) examine if there is any overlap between the TCR repertoires expressed by a TpM-stimulated NKp46+CD3+ population and a conventional TpM-specific CD8+ T-cell population derived from the same animal. Such analysis will help to define if there is evidence of TCR bias that would be consistent with a role for TCR in mediated NKp46+ CD3+ cell recognition of *T. parva* infected cells.

3.2 Material and methods

3.2.1 Molecular techniques

3.2.1.1 Isolation of mRNA

Purification of mRNA was carried out using the Dynabeads® mRNA DIRECT™ Purification Kit (Life technologies—61011) according to the manufacturer's instructions. 300ul Lysis/Binding buffer was added per 1×10^6 cells and the DNA sheared by passing the lysate through a 21-gauge needle attached to a 2.5ml syringe. Lysed cells were then stored at -80°C until the rest of the mRNA isolation procedure was undertaken. For this 50ul aliquots of Dynabeads Oligo (dT)/1×10^6 cells were transferred to a RNAase-free 1.5ml micro-centrifuge tube and placed in DynaMag2 1.5ml tube magnet holder (Life technologies 12321D) for 30s and the cleared supernatant aspirated off. The tube was then removed from the magnet and 50ul of Lysis/Binding buffer added to the beads, and the wash repeated. The cell lysate was then added to the beads and mixed thoroughly by repeat pipetting to ensure complete re-suspension of beads in cell lysate. The bead/cell lysate mixture was then incubated with continuous rotation for 5 minutes at room temperature to allow hybridisation of the polyA of mRNA to the oligo (dT) on the beads. The mixture was then placed in the magnet for 2 minutes and the supernatant aspirated off. The beads were then washed twice with 600ul/$\times10^6$ cells of Washing buffer A and followed by another two washes with Washing buffer B (300ul/$\times10^6$ cells). Following these washed 5ul elution buffer/$\times10^6$ cells was added to the beads and incubate at 65-80^{o}C for 2 minutes; immediately following this the tube was placed in the magnet and the supernatant (containing mRNA) was transferred to a fresh microcentrifuge tube. The mRNA was then quantified by Nanodrop.

3.2.1.2 Quality and conservation of mRNA

The purity and concentration of mRNA were assessed by spectrophotometry (Nanodrop) with readings taken at 260 nm and 280 nm and the mRNA concentration calculated and the 260/280 ratio recorded. mRNA was stored at -80°C until used.

3.2.1.3 SMART-based TRB chain amplification

This was performed as a 2-round PCR amplification. In the first round Phusion High-Fidelity PCR reactions with a final volume of 300µl were performed. These reactions were composed of: 60 µl Phusion HF Buffer (1x), 9µl DMSO (3%), 6 µl dNTP (200 µM), 15 µl Long UPM primer (0.5µM); CTA ATA CGA CTC ACT ATA GGG CAA GCA GTG GTA TCA ACG CAG AGT, and 15 µl TRBC II primer (0.5uM); GTCCGCGAGATCTCTGCTTC, cDNA 12µl, molecular water 180µl and Phusion polymerase 3µl. The final reaction mixture was aliquoted into 6 tubes each with 50 µl. The optimized cycling conditions were: heated lid 110°C, manual hot start at 98°C for 2 min, a first temperature step at 98°C for 30s, 20 cycles of (98°C for 10s, 65°C for 30s, 72°C for 60s) and a final extension period at 72°C for 10 min.

After purification of the first round PCR product (see below), a second PCR reaction - using UPM.3 (0.5 µM) and TRBCivS (0.5 µM) primers (Table 3.1) with multiple sample identifier tags (allowing multiplexing of samples sent for sequencing) and the additional components required for direct sequencing of PCR products on the MiSeq Illumina platform. These reactions mixture are made in 600 µl final volume, with the Phusion High-Fidelity PCR Kit, containing: 120 µl Phusion Buffer (1x), 18 µl DMSO (3%), 12 µl dNTP (200 µM), 30 µl for each primer (Table 3.1), purified first round PCR products 60 µl, molecular water 360 µl and Phusion polymerase 6 µl. The final reaction mixture was distributed in PCR reaction tubes (50 µl/tube). The cycling conditions were: heated lid 110°C, manual hot start at 98°C for 2 min, a first temperature step at 98°C for 30s, 10 cycles of (98°C for 10s, 65°C for 30s, 72°C for 60s) and a final extension period at 72°C for 10 min. Following this PCR, the products were purified, subjected to agarose gel electrophoresis, gel extracted to obtain the band of the anticipated size, and re-purified as described below.

TRBCivs reverse Primers						
	REV1-501	REV2-502	REV3-503	REV4-504	REV5-505	REV6-506
Illumine adaptor	AAT GAT ACG GCG ACC ACC GAG ATC TAC AC					
Multiple tag	ATCGTACG	ACTATCTG	TAGCGAGT	CTGCGTGT	TCATCGAG	CGTGAGTG
Filler	TAT GGT AAT T CA					
Gene-specific	GAC SYG GCT CAG ATC ATC					
TRB forward Primers						
	FOR1-701	FOR2-702	FOR3-703	FOR4-704	FOR5-705	FOR6-706
Illumine adaptor	CAA GCA GAA GAC GGC ATA CGA GAT					
Multiple tag	AACTCTCG	ACTATGTC	AGTAGCGT	CAGTGAGT	CGTACTCA	CTACGCAG
Filler	GTG ACT GGA GTT CAG ACG TGT GCT CTT CCG ATC T					
Gene-specific	CTA ATA CGA CTC ACT ATA GGG CAA GCA G					

Table 2.1 illumina adaptor and Multiple sample tags present in the second round PCR primers

3.2.2 Agarose gel electrophoresis

Agarose gel electrophoresis was conducted with 1.5% agarose/TAE gels (Bioline, London, UK). An intercalating agent of DNA (GelRed, Biotium, California, USA) was used to enable visualisation under UV light. Gels included a lane with a 1Kb Plus DNA Ladder (Thermofisher) to enable band size determination. Electrophoresis was conducted at 110 V for 50 min with TAE Buffer 1x as running buffer.

3.2.3 Purification of PCR products

The purification of PCR products after the first round and the second round PCR of NGS protocol were performed with QIAquick PCR Purification Kit (Qiagen, Manchester, UK) according to the manufacturer protocol except for the DNA elution step. The samples were eluted in water; 60 µl for the first round PCR and 100 µl for the second round PCR. The purification of the DNA fragments after excision from the electrophoresis gel were carried out with the QIAquick Gel Extraction Kit (Qiagen, Manchester, UK) following the manufacturer's instructions. The final PCR product purification prior to NGS sequencing was conducted using AMPure XP Beads (Beckman Coulter, High Wycombe, UK) according to the manufacturer's instructions. In brief, an equal volume of beads and PCR products were thoroughly mixed and incubated for 15 min at room temperature. The samples were placed on a magnetic stand until the beads cleared from the supernatant. The supernatant was discarded and the beads washed twice with 200 µl of freshly prepared 75% ethanol. After the last wash, the samples were dried for 5 min at room temperature. The tubes were removed from the magnetic stand and the beads thoroughly re-suspended in 30 µl of molecular-grade, nuclease-free water. After 2 min incubation at room temperature, the tubes were placed on the magnetic stand, the water aspirated and transferred to a fresh tube.

3.2.4. NGS, bioinformatics pipelines and VDJ analysis

Samples for NGS analysis were submitted to Edinburgh Genomics for sequencing on an Illuminia Miseq platform. Samples were required to pass quality controls (Qubit DNA quantification, Agilent bioanalyzer for size determination) prior to sequencing. NGS sequence data was analyzed using the MiTCR bioinformatics pipeline which had been modified by Dr. Andy Law (Roslin Institute) to accept a bovine TRB database (constructed by Dr. Connelley, Roslin Institute). Non-functional TRB sequences were removed from the datasets prior to

subsequent analysis using algorithms that are part of the VDJ tools software package (done with the assistance of Deepali Vasoya - Roslin Institute).

3.3 Results

3.3.1 Preparation of PCR product for NGS

From previous chapter, a total 7 NKp46+ CD3+ cell lines (302977, 202990, 202997, 106180, 106222 2nd stimulation, 106222 3rd stimulation, and 106222 5th stimulation) were generated and prepared for PCR analysis. With the exception of the NKp46+ CD3+ cell line from animal 302977, all cell lines were successfully amplified by the SMART-based PCR. The forward and reverse primers used in the second round PCR for each cell line show in Table 3.2. The final PCR products were purified by 1.5% TAE agarose gel and DNA bands of ~700bp were extracted and purified, gel cutting results are shown in Figure 3.1.

Animal	TRB Forwards primer sequencing	TRBCivS primer sequencing
106222 NKp46+ CD3+ cells 2nd stimulation	CGTACTCA	ACTATCTG
106222 NKp46+ CD3+ cells 3rd stimulation	AGTAGCGT	TCATCGAG
106222 NKp46+ CD3+ cells 5th stimulation	AACTCTCG	TAGCGAGT
106180 NKp46+ CD3+ cells	ACTATGTC	CGTGAGTG
202997 NKp46+ CD3+ cells	CTACGCAG	CTGCGTGT
202990 NKp46+ CD3+ cells	AGTAGCGT	ACTATCTG

Table 3.2 Forward and reverse primers were used in the second round PCR of different NKp46+ CD3+ cell lines

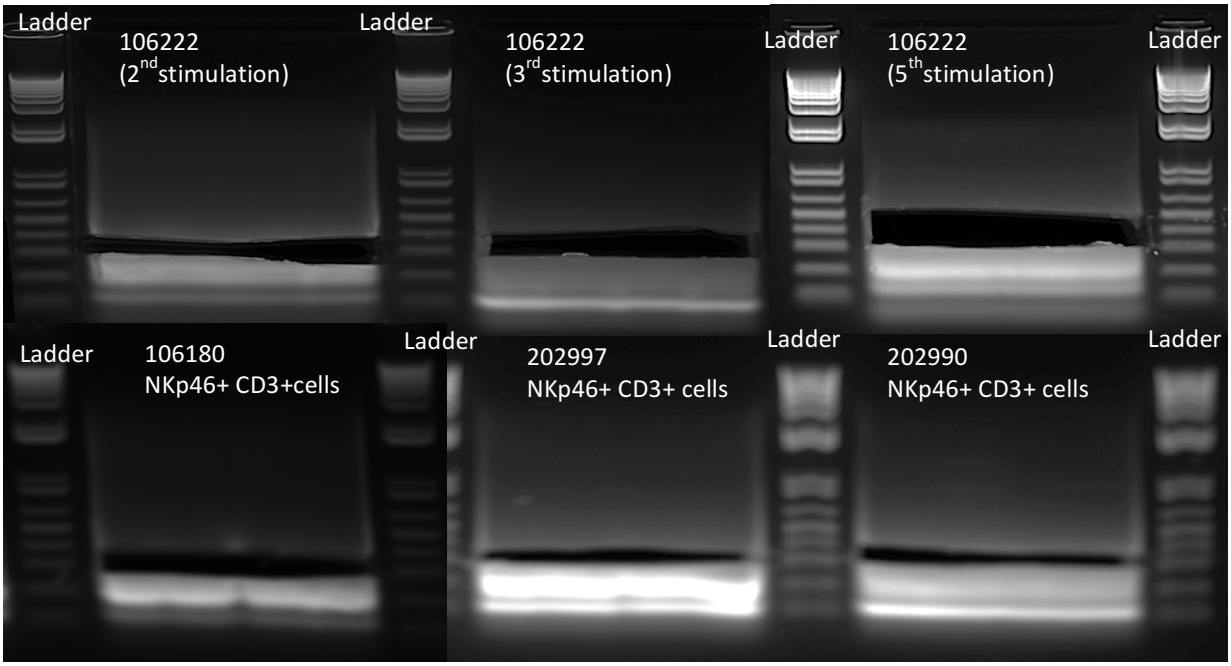

Figure 3.1. Gel cutting image of semi-nested cDNA products (the DNA bands were extracted around 700bp)

The quality of the final purified PCR products were assessed by spectrophotometry (Nanodrop - Table 3.3), and the cDNA size were examined through running agarose gel electrophoresis with different volumes (10ul. 5ul, and 2.5ul) (Figure 3.2). These purified PCR products passed the quality control (QC) with size of 660pb and ready for NGS.

	106222 2nd stimulation	106222 3rd stimulation	106222 5th stimulation	106180 NKp46+ CD3+ cells	202990 NKp46+ CD3+ cells	202997 NKp46+ CD3+ cells
Abs	0.446	0.463	0.246	0.6	0.567	0.319
A260 10mm path	0.896	0.93	0.485	1.251	1.234	0.609
A280 10mm path	0.485	0.529	0.271	0.678	0.664	0.33
260/280	1.85	1.76	1.79	1.85	1.86	1.85
260/230	2.01	2.01	2.01	2.09	2.18	1.91
ng/ul	44.8	46.5	24.3	62.6	61.7	30.4

Table 3.3 Nanodrop results of the final PCR products

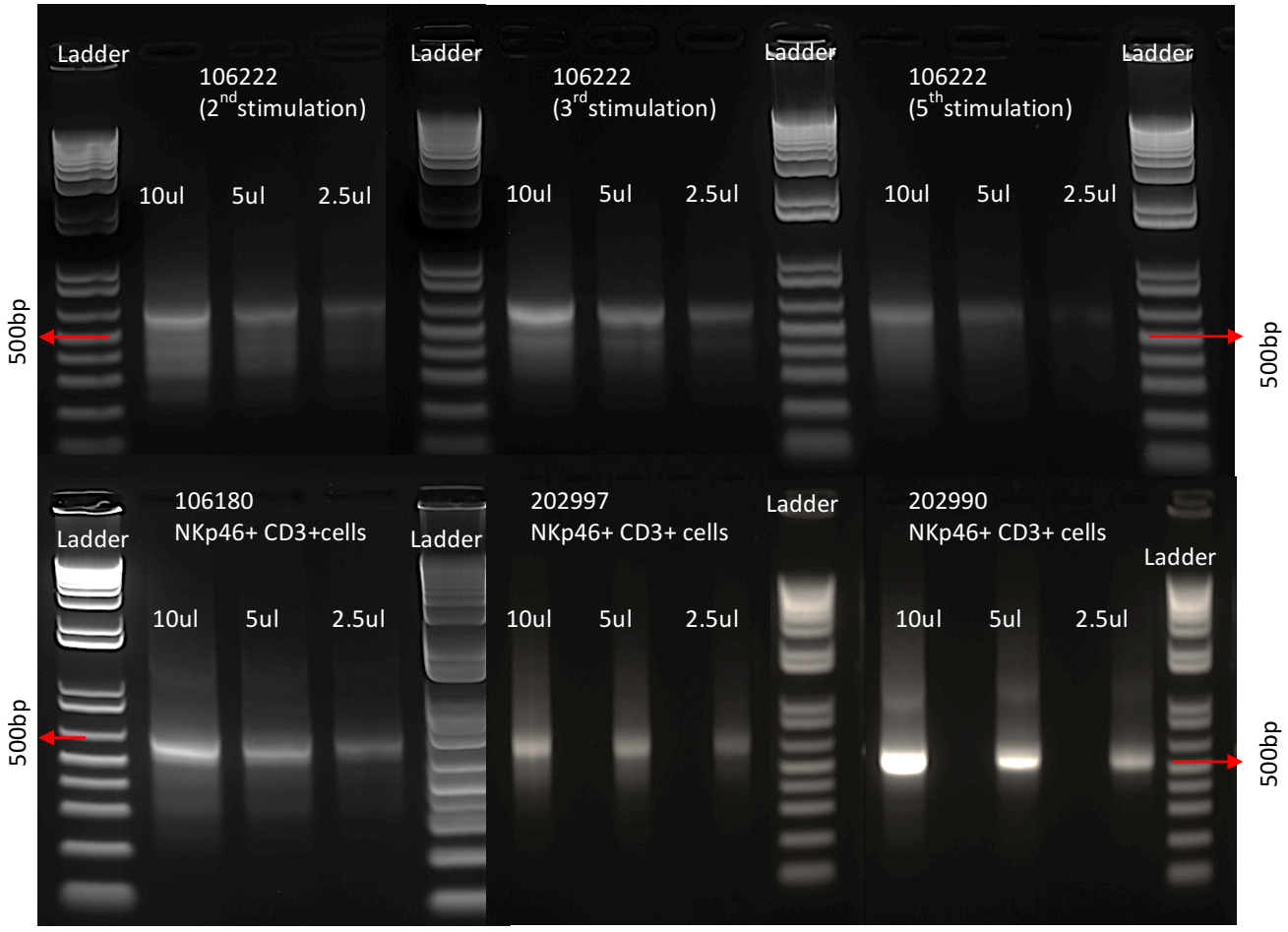

Figure 3.2. Running agarose gel electrophoresis with 10ul, 5 ul, and 2.5 ul volumes of final purified PCR products

3.3.2 NGS analysis of the expressed TRB repertoires

The purified PCR products of the TpM specific stimulation NKp46+ CD3+ cell lines were sequenced in 2 separate MiSeq runs and the data analyzed using a modified MiTCR (Bolotin et al. 2013) bioinformatics pipeline.

3.3.2.1 Evolution of the TRB repertoire during repeated TpM stimulations

The TRB repertoires of NKp46+ CD3+ cell lines from animal 106222 following the 2nd, 3rd, and 5th stimulation with TpM *in vitro* were analysed to evaluate the evolution of the TRB repertoire during repeated TpM stimulations. The top 50 most frequent CDR3 sequences are shown in Table 3.4 (106222 2nd stimulation), Table 3.5 (106222 3rd stimulation), and Table 3.6 (106222 5th stimulation). The evolution of TRB repertoire was assessed by i) changes of TRB diversity and ii) identification of dominant clonotype expansion. Rarefaction analysis (Figure 3.3) shows that the TRB diversity of the 2nd stimulation cell line is much higher than that observed in the 3rd stimulation, and the 5th stimulation is slightly lower than the 3rd stimulation, which indicates that the TRB repertoire narrowed following repeated TpM stimulation, with a substantial decline observed between the 2nd and 3rd stimulations.

A 'virtual spectratype' analysis (Figure 3.4) shows that for the cell lines following the 2nd and 3rd stimulation cell lines there is a 'normal' (Gaussian) distribution of the CDR3 length and generally few high frequency clonotypes. In contrast, in the 5th stimulation cell line there is a skewed distribution of CDR3 length, largely attributable to the expansion of the single dominant clonotype. Repertoire overlap analysis (Figure 3.5) of the clonotypes expressed in the different stimulated NKp46+ CD3+ cell lines shows a high levels of repertoire overlap between cell lines, with the frequency of most individual clonotypes changing slightly between the 2nd, 3rd and 5th stimulations but a substantial increase of a the clonotype TRBV28-1-CASSDPRTAGAVQLYF- TRBJ2-2 observed in the 5th stimulated cell lines (increase from 0.3% in 2nd stimulation and 0.5% in 3rd stimulation to 42.7% in 5th stimulation). This data indicates clonal selection and expansion in *T. parva* stimulated NKp46+ CD3+ cells.

Representation of the frequency of TRBV and TRBJ gene usage are shown in Figure 3.6, it indicates that a broad selection of both TRBV and TRBJ genes are used in the NKp46+CD3+ cell lines. In the 2nd and 3rd stimulation cell lines there appears to be preferential usage of

TRBJ 3-2, 3-7, and 3-4, and TRBV 20-13, 9-9, and 7-1. As would be expected in the 5th stimulation the TRBJ2-2 and TRBV28-1 gene segments are dominant although the same gene segments preferentially using the in the 2nd and 3rd stimulation cell lines are also present at high frequency.

Together this data shows that during repeated TpM stimulations *in vitro* the TRB repertoire narrowed in terms of clonotype diversity but maintained a broad usage of both TRBV and TRBJ genes and generally a range of CDR3 lengths. The expansion of a single dominant clonotype in the 5th stimulation skewed the spectratype and apparent TRBV and TRBJ usage.

106222 2nd stimulation					
#count	freq	cdr3aa	v	d	j
38732	7.46%	CASSPLTSGGLNTQPLYF	TRBV7-1	TRBD3	TRBJ3-2
25334	4.88%	CASSQDGQHRSYEQYF	TRBV9-9	TRBD1	TRBJ3-7
25200	4.86%	CASSQADTLGTQYF	TRBV9-9	TRBD1	TRBJ3-4
23177	4.47%	CGTLDWASTDTQYF	TRBV20-03	TRBD2	TRBJ3-4
22484	4.33%	CGARPGGNAVQLYF	TRBV20-10	TRBD3	TRBJ2-2
16293	3.14%	CSASCFGGGHEQYF	TRBV20-13	TRBD3	TRBJ3-7
15639	3.01%	CSASGHLNTQPLYF	TRBV20-13	TRBD2	TRBJ3-2
13563	2.61%	CSAAPGTQPLYF	TRBV20-13	TRBD3	TRBJ3-2
12975	2.50%	CASSRTRAATDDYHF	TRBV4-5	TRBD1	TRBJ1-2
12354	2.38%	CASSQEMRDPSYEQYF	TRBV9-1	TRBD1	TRBJ3-7
11549	2.23%	CASVTSGQEIQYF	TRBV28-1	TRBD3	TRBJ3-5
10551	2.03%	CATRGQGVYNNPLYF	TRBV6-11	TRBD2	TRBJ3-3
8796	1.70%	CAGGQQLFAGAALTF	TRBV27-1	TRBD1	TRBJ3-6
6958	1.34%	CASSRGMGEGSIDTQYF	TRBV12-2	TRBD1	TRBJ3-4
6729	1.30%	CASSYYAAGYDYHF	TRBV6-18	TRBD1	TRBJ1-2
6641	1.28%	CSAPDFGSGELHF	TRBV20-13	TRBD3	TRBJ3-1
6217	1.20%	CASSQVERTYEQYF	TRBV9-9	TRBD3	TRBJ3-7
5726	1.10%	CASSLAGHGELHF	TRBV10-3	TRBD1	TRBJ3-1
5542	1.07%	CASSKDWGLGDYEQYF	TRBV12-2	TRBD2	TRBJ3-7
5067	0.98%	CSAADFGGCTDTQYF	TRBV20-08	TRBD3	TRBJ3-4
4732	0.91%	CSDWRGHTQYF	TRBV20-13	TRBD2	TRBJ3-4
4594	0.89%	CGASTQESTQYF	TRBV20-03	TRBD1	TRBJ2-3
4553	0.88%	CASSPRGADTQPLYF	TRBV3-1	TRBD3	TRBJ3-2
4488	0.86%	CSARRWGGKTSNNPLYF	TRBV20-08	TRBD3	TRBJ3-3
4083	0.79%	CSAISHNPLYF	TRBV20-13	TRBD3	TRBJ3-3
3793	0.73%	CASSLRLRGTDTQYF	TRBV10-3	TRBD3	TRBJ3-4
3758	0.72%	CASSRSGAYRNNPLYF	TRBV4-3	TRBD3	TRBJ3-3
3712	0.72%	CASASQLGSLYF	TRBV26-2	TRBD2	TRBJ3-3
3524	0.68%	CTCRLDSSYEQYF	TRBVX-1	TRBD1	TRBJ3-7
3071	0.59%	CASSQVWVHTQPLYF	TRBV9-25	TRBD2	TRBJ3-2
2763	0.53%	CASSYDRGISNNPLYF	TRBV10-3	TRBD3	TRBJ3-3
2583	0.50%	CASTTGLKQLYF	TRBV6-4	TRBD2	TRBJ2-2
2566	0.49%	CASSQEPTSNSYEQYF	TRBV9-9	TRBD3	TRBJ3-7
2428	0.47%	CGASLGGGADTQYF	TRBV20-02	TRBD3	TRBJ3-4
2404	0.46%	CASSRSRFGNDPLYF	TRBV4-1	TRBD3	TRBJ3-3
2372	0.46%	CSGGDLSTDTQYF	TRBV19-02	TRBD1	TRBJ3-4
2201	0.42%	CTSSPMNTQPLYF	TRBV6-40	TRBD2	TRBJ3-2
2160	0.42%	CSARRKVPQPLYF	TRBV20-13	TRBD1	TRBJ3-2
2131	0.41%	CASRPSYQMNAVQLYF	TRBV21-8	TRBD1	TRBJ2-2
2103	0.41%	CGATGPRYTDTQYF	TRBV20-02	TRBD1	TRBJ3-4
2088	0.40%	CTCSASGTALDEQYF	TRBVX-1	TRBD1	TRBJ3-7
1924	0.37%	CSASGGVAQPLYF	TRBV20-13	TRBD3	TRBJ3-2
1908	0.37%	CSAGATAAMDYHF	TRBV29-1	TRBD1	TRBJ1-2
1869	0.36%	CASSDWGVLSWPLYF	TRBV10-3	TRBD2	TRBJ3-3
1726	0.33%	CASSHPTFYDYHF	TRBV21-9	TRBD2	TRBJ1-2
1717	0.33%	CAGRQTGTGSSKQYF	TRBV9-30	TRBD2	TRBJ3-7
1681	0.32%	CASRRPRGEQYF	TRBV10-3	TRBD3	TRBJ3-7
1671	0.32%	CASSDPRTAGAVQLYF	TRBV28-1	TRBD1	TRBJ2-2
1633	0.31%	CSARGLGGFEQYF	TRBV20-08	TRBD2	TRBJ3-7
1566	0.30%	CASSRDGGDYHF	TRBV4-6	TRBD2	TRBJ1-2

Table 3.4 Top 50 most frequent CDR3 sequencing of animal 106222 2nd stimulation NKp46+ CD3+ cell line

106222 3rd stimulation					
#count	freq	cdr3aa	v	d	j
28733	11.99%	CASSPLTSGGLNTQPLYF	TRBV7-1	TRBD3	TRBJ3-2
12733	5.31%	CGTLDWASTDTQYF	TRBV20-03	TRBD2	TRBJ3-4
12297	5.13%	CASSIDFGEIYEQYF	TRBV27-1	TRBD3	TRBJ3-7
10716	4.47%	CASVTSGQEIQYF	TRBV28-1	TRBD3	TRBJ3-5
10396	4.34%	CASSQADTLGTQYF	TRBV9-9	TRBD1	TRBJ3-4
8446	3.52%	CTCRLDSSYEQYF	TRBVX-1	TRBD1	TRBJ3-7
8022	3.35%	CSAGRTSDLPLYF	TRBV29-1	TRBD3	TRBJ3-3
7178	2.99%	CSASCFGGGHEQYF	TRBV20-13	TRBD3	TRBJ3-7
6408	2.67%	CASSQEMRDPSYEQYF	TRBV9-1	TRBD1	TRBJ3-7
6231	2.60%	CATRGQGVYNNPLYF	TRBV6-11	TRBD2	TRBJ3-3
6121	2.55%	CASSYYAAGYDYHF	TRBV6-18	TRBD1	TRBJ1-2
4676	1.95%	CASSRGMGEGSIDTQYF	TRBV12-2	TRBD1	TRBJ3-4
4181	1.74%	CASSPTSDRNPLYF	TRBV7-1	TRBD2	TRBJ3-3
4118	1.72%	CASSQDGQHRSYEQYF	TRBV9-9	TRBD1	TRBJ3-7
3985	1.66%	CASSQVERTYEQYF	TRBV9-9	TRBD3	TRBJ3-7
3412	1.42%	CASASNVGWVHEEQHF	TRBV26-2	TRBD2	TRBJ2-1
3236	1.35%	CASASQLGSLYF	TRBV26-2	TRBD2	TRBJ3-3
3213	1.34%	CASSYSTEREAVQLYF	TRBV6-9	TRBD1	TRBJ2-2
3073	1.28%	CASRPSYQMNAVQLYF	TRBV21-8	TRBD1	TRBJ2-2
2656	1.11%	CASSRDRRQSTQYF	TRBV15-2	TRBD1	TRBJ2-3
2607	1.09%	CSASGHLNTQPLYF	TRBV20-13	TRBD2	TRBJ3-2
2576	1.07%	CASSRTRAATDDYHF	TRBV4-5	TRBD1	TRBJ1-2
2463	1.03%	CGARPGGNAVQLYF	TRBV20-10	TRBD3	TRBJ2-2
2021	0.84%	CGASTQESTQYF	TRBV20-03	TRBD1	TRBJ2-3
1864	0.78%	CSAGATAAMDYHF	TRBV29-1	TRBD1	TRBJ1-2
1768	0.74%	CSGGSSLGTQYF	TRBV19-02	TRBD1	TRBJ2-3
1666	0.69%	CASSYYSYEQYF	TRBV6-18	TRBD2	TRBJ3-7
1631	0.68%	CASSWTIRPPSGKTYEQYF	TRBV6-18	TRBD3	TRBJ3-7
1475	0.62%	CASSINPGGMILSDPLYF	TRBV15-2	TRBD2	TRBJ3-3
1412	0.59%	CTSSPMNTQPLYF	TRBV6-40	TRBD2	TRBJ3-2
1405	0.59%	CASSLAGHGELHF	TRBV10-3	TRBD1	TRBJ3-1
1233	0.51%	CASSDPRTAGAVQLYF	TRBV28-1	TRBD1	TRBJ2-2
1224	0.51%	CASSPTGGWETLYF	TRBV21-8	TRBD2	TRBJ2-4
1210	0.50%	CSAAPGTQPLYF	TRBV20-13	TRBD3	TRBJ3-2
1134	0.47%	CSARRWGGKTSNNPLYF	TRBV20-08	TRBD3	TRBJ3-3
1082	0.45%	CASSQEPTSNSYEQYF	TRBV9-9	TRBD3	TRBJ3-7
1022	0.43%	CASSLERIREEQHF	TRBV6-9	TRBD3	TRBJ2-1
1011	0.42%	CASSSCWIGCTQYF	TRBV14-1	TRBD1	TRBJ2-3
989	0.41%	CSAISHNPLYF	TRBV20-13	TRBD3	TRBJ3-3
987	0.41%	CASSQVWVHTQPLYF	TRBV9-25	TRBD2	TRBJ3-2
981	0.41%	CASSKDWGLGDYEQYF	TRBV12-2	TRBD2	TRBJ3-7
978	0.41%	CASSHPTFYDYHF	TRBV21-9	TRBD2	TRBJ1-2
936	0.39%	CASTTGLKQLYF	TRBV6-4	TRBD2	TRBJ2-2
921	0.38%	CAGRQTGTGSSKQYF	TRBV9-30	TRBD2	TRBJ3-7
861	0.36%	CAASRDPRVNTQPLYF	TRBV19-04	TRBD1	TRBJ3-2
816	0.34%	CASSKVGTLISNDPLYF	TRBV12-2	TRBD1	TRBJ3-3
789	0.33%	CASRQDWGVGGEEQHF	TRBV6-18	TRBD2	TRBJ2-1
751	0.31%	SSPLTSGGLNTQPLYF	TRBV6-19	TRBD3	TRBJ3-2
739	0.31%	CASSPRGADTQPLYF	TRBV3-1	TRBD3	TRBJ3-2
724	0.30%	CASNVGGSNYDYHF	TRBV9-33	TRBD1	TRBJ1-2

Table 3.5 Top 50 most frequent CDR3 sequencing of animal 106222 3rd stimulation NKp46+ CD3+ cell line

106222 5th stimulation					
#count	freq	cdr3aa	v	d	j
83736	42.73%	CASSDPRTAGAVQLYF	TRBV28-1	TRBD1	TRBJ2-2
9117	4.65%	CASSPLTSGGLNTQPLYF	TRBV7-1	TRBD3	TRBJ3-2
5053	2.58%	CASSQDGQHRSYEQYF	TRBV9-9	TRBD1	TRBJ3-7
4819	2.46%	CASSQADTLGTQYF	TRBV9-9	TRBD1	TRBJ3-4
4786	2.44%	CSGTTQPLYF	TRBV20-13	TRBD1	TRBJ3-2
3791	1.93%	CGTLDWASTDTQYF	TRBV20-03	TRBD2	TRBJ3-4
3277	1.67%	SSDPRTAGAVQLYF	TRBV6-19	TRBD1	TRBJ2-2
2838	1.45%	CGARPGGNAVQLYF	TRBV20-10	TRBD3	TRBJ2-2
2824	1.44%	CASSRGMGEGSIDTQYF	TRBV12-2	TRBD1	TRBJ3-4
2378	1.21%	CASSQEMRDPSYEQYF	TRBV9-1	TRBD1	TRBJ3-7
2187	1.12%	CSASCFGGGHEQYF	TRBV20-13	TRBD3	TRBJ3-7
2159	1.10%	CASSRTRAATDDYHF	TRBV4-5	TRBD1	TRBJ1-2
1843	0.94%	CASVTSGQEIQYF	TRBV28-1	TRBD3	TRBJ3-5
1764	0.90%	CSASGHLNTQPLYF	TRBV20-13	TRBD2	TRBJ3-2
1452	0.74%	CASSQVERTYEQYF	TRBV9-9	TRBD3	TRBJ3-7
1446	0.74%	CASSIDFGEIYEQYF	TRBV27-1	TRBD3	TRBJ3-7
1433	0.73%	CASRRDTQPLYF	TRBV6-13	TRBD3	TRBJ3-2
1348	0.69%	CASSLGIQGAQDTQYF	TRBV9-6	TRBD3	TRBJ3-4
1338	0.68%	CAGGQQLFAGAALTF	TRBV27-1	TRBD1	TRBJ3-6
1220	0.62%	CSAAPGTQPLYF	TRBV20-13	TRBD3	TRBJ3-2
963	0.49%	CASASQLGSLYF	TRBV26-2	TRBD2	TRBJ3-3
938	0.48%	CATRGQGVYNNPLYF	TRBV6-11	TRBD2	TRBJ3-3
910	0.46%	CASRPSYQMNAVQLYF	TRBV21-8	TRBD1	TRBJ2-2
908	0.46%	CASSKDWGLGDYEQYF	TRBV12-2	TRBD2	TRBJ3-7
883	0.45%	CASSQVWVHTQPLYF	TRBV9-25	TRBD2	TRBJ3-2
861	0.44%	CSDWRGHTQYF	TRBV20-13	TRBD2	TRBJ3-4
841	0.43%	CASSYYAAGYDYHF	TRBV6-18	TRBD1	TRBJ1-2
812	0.41%	CASSRSGAYRNNPLYF	TRBV4-3	TRBD3	TRBJ3-3
810	0.41%	CASSPRGADTQPLYF	TRBV3-1	TRBD3	TRBJ3-2
773	0.39%	CASSRSRFGNDPLYF	TRBV4-1	TRBD3	TRBJ3-3
719	0.37%	CTCRLDSSYEQYF	TRBVX-1	TRBD1	TRBJ3-7
715	0.36%	CSARRWGGKTSNNPLYF	TRBV20-08	TRBD3	TRBJ3-3
707	0.36%	CSGGLGIEQYF	TRBV20-08	TRBD2	TRBJ3-7
663	0.34%	CASSHPTFYDYHF	TRBV21-9	TRBD2	TRBJ1-2
625	0.32%	CSAPDFGSGELHF	TRBV20-13	TRBD3	TRBJ3-1
596	0.30%	CASSLAGHGELHF	TRBV10-3	TRBD1	TRBJ3-1
584	0.30%	CASASNVGWVHEEQHF	TRBV26-2	TRBD2	TRBJ2-1
534	0.27%	CASSQEPTSNSYEQYF	TRBV9-9	TRBD3	TRBJ3-7
534	0.27%	CSAGRTSDLPLYF	TRBV29-1	TRBD3	TRBJ3-3
527	0.27%	CGASTQESTQYF	TRBV20-03	TRBD1	TRBJ2-3
497	0.25%	CSAISHNPLYF	TRBV20-13	TRBD3	TRBJ3-3
483	0.25%	CASSRDGGDYHF	TRBV4-6	TRBD2	TRBJ1-2
474	0.24%	CASSLGTASEQYF	TRBV4-6	TRBD1	TRBJ3-7
463	0.24%	CASSLRLRGTDTQYF	TRBV10-3	TRBD3	TRBJ3-4
455	0.23%	CSAADFGGCTDTQYF	TRBV20-08	TRBD3	TRBJ3-4
451	0.23%	CASSRDRRQSTQYF	TRBV15-2	TRBD1	TRBJ2-3
402	0.21%	CASTTGLKQLYF	TRBV6-4	TRBD2	TRBJ2-2
384	0.20%	CSASGGVAQPLYF	TRBV20-13	TRBD3	TRBJ3-2
382	0.19%	CASSQGSGGAYEQYF	TRBV9-26	TRBD3	TRBJ3-7
377	0.19%	CASRLRGNDPLYF	TRBV6-7	TRBD3	TRBJ3-3

Table 3.6 Top 50 most frequent CDR3 sequencing of animal 106222 5th stimulation NKp46+ CD3+ cell line

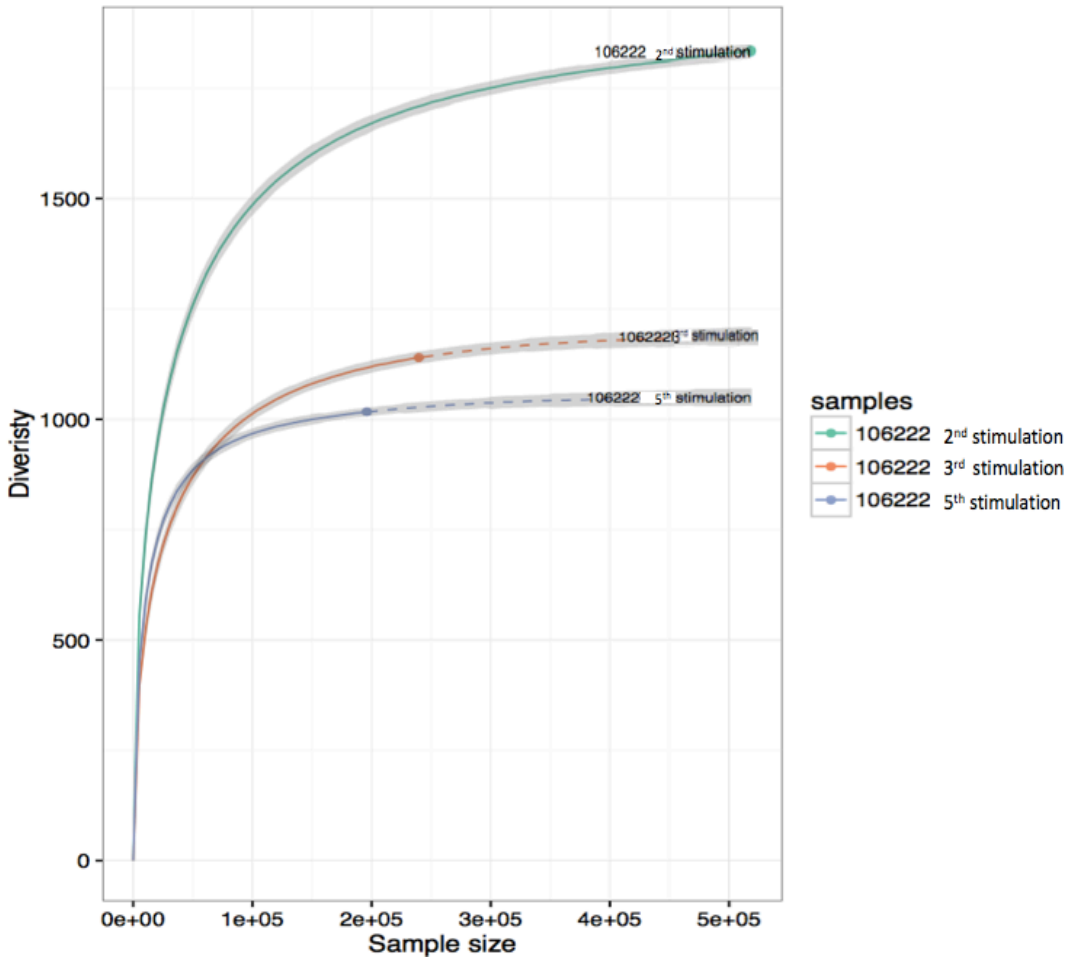

Figure 3.3. Rarefaction analysis of TRB repertoire from the animal 106222 2nd, 3rd, and 5th stimulations. The number of unique clonotypes in a sub-sample (diversity) plotted against its size (Sample size). Solid and dashed lines are diversity estimates computed by interpolating and extrapolating using a multinomial model respectively.

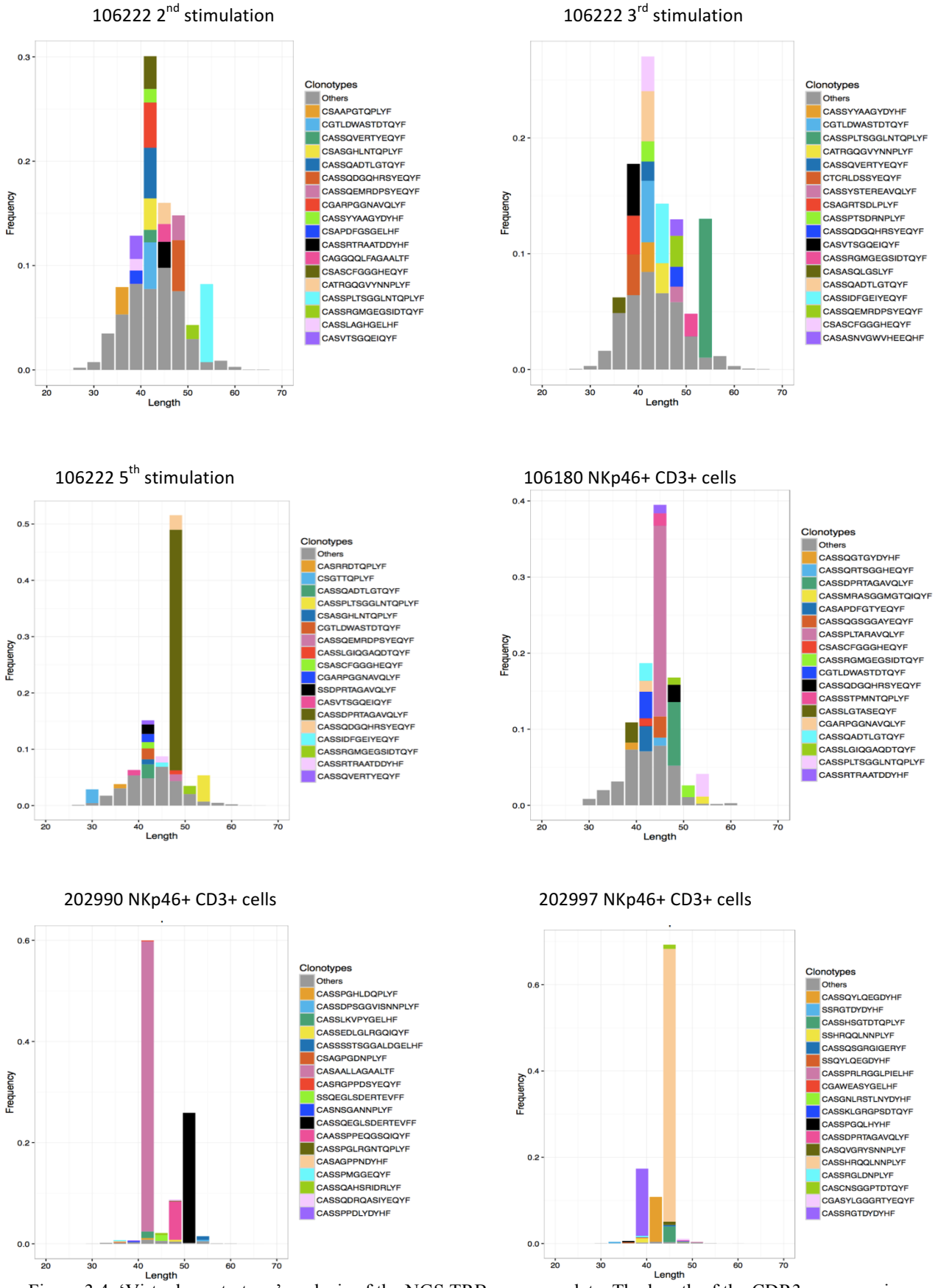

Figure 3.4. 'Virtual spectratype' analysis of the NGS TRB sequence data. The length of the CDR3 sequence is plotted against the read frequency for each sample. The most frequent clones are shown as distinct coloured blocks as indicated in the key

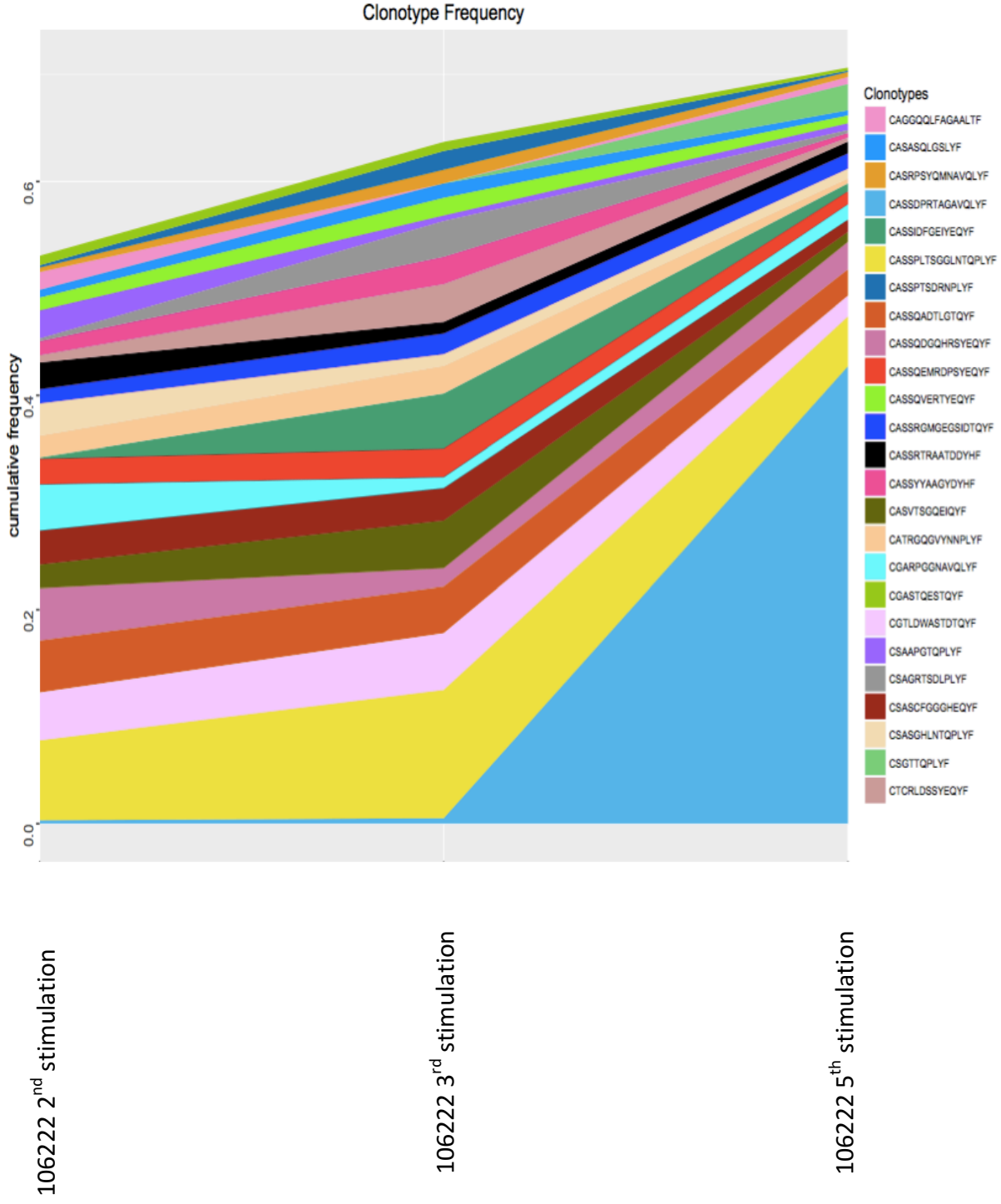

Figure 3.5. Repertoire overlap analysis of the clonotypes present in NKp46+ CD3+ cell lines of animal 106222 2nd, 3rd and 5th stimulations.

106222 2nd stimulation

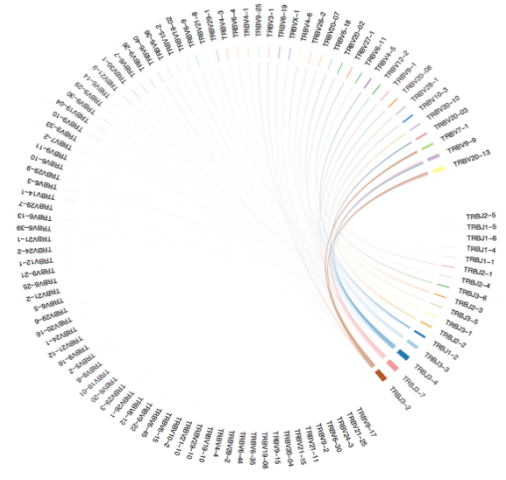

106222 3rd stimulation

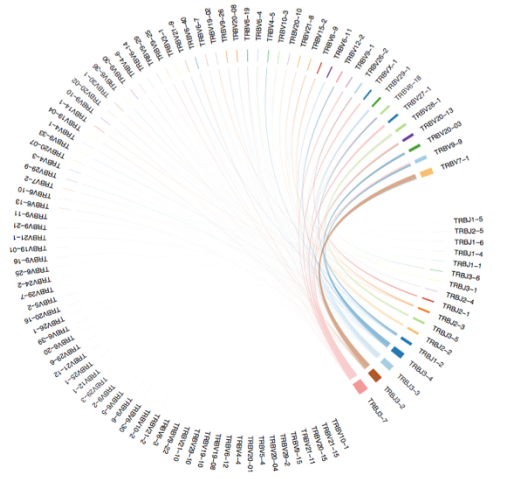

106222 5th stimulation

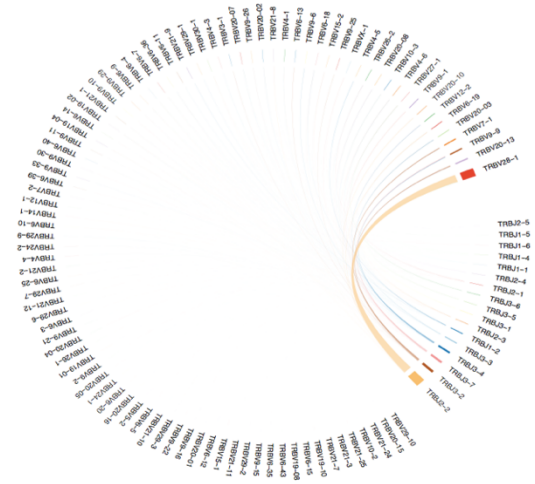

106180 NKp46+ CD3+ cells

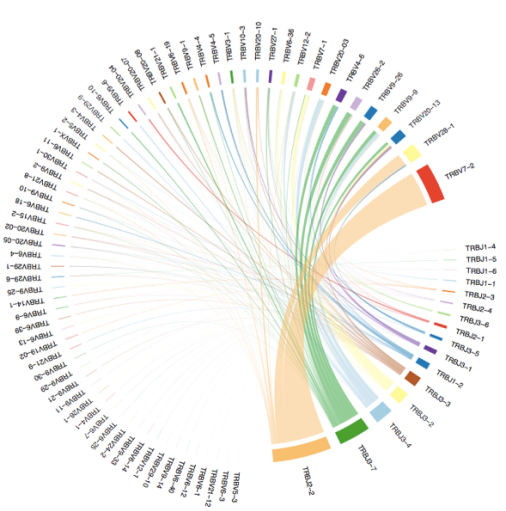

202990 NKp46+ CD3+ cells

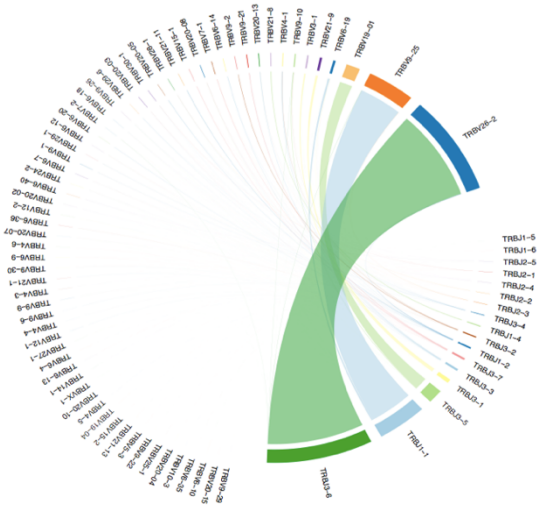

202997 NKp46+ CD3+ cells

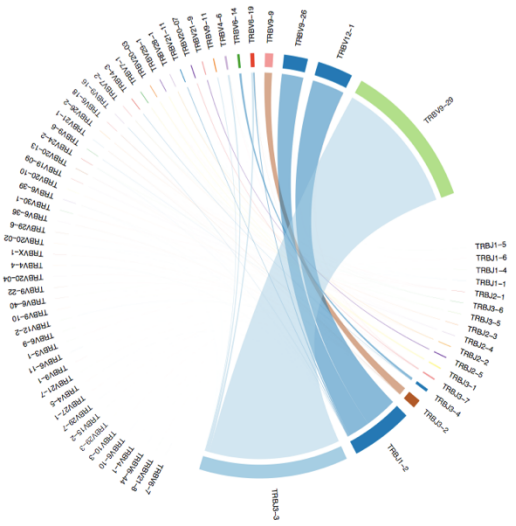

Figure 3.6. Representation of the frequency of TRBV and TRBJ usage in the six samples analysed by NGS

3.3.2.2 Comparison of the TRB repertoire of NKp46+ CD3+ cell lines between different animals

In this section, the TRB repertoires of NKp46+ CD3+ cell lines from animals 106180, 106222 (5^{th} stimulation), 202990 and 202997 were compared to address the study objective of determining the commonalties of TRB repertoire between different animals. The top 50 most frequent CDR3 sequences of animal 106180, 202990 and 202997 are shown in Table 3.7, Table 3.8 and Table 3.9 respectively.

Rarefaction analysis (Figure 3.7) of NKp46+ CD3+ cell lines indicates that the animal 106222 (5^{th} stimulation – total of 1017 unique clonotypes identified) expressed the most diverse TRB repertoire, followed by animal 202990, 106180, and 202997 (total 1017, 509, 229 and 223 unique clonotypes were identified respectively). Virtual spectratype analysis (Figure 3.4) shows a skewed distribution of CDR3 length and a single dominant clonotype expansion in all NKp46+ CD3+ cell lines.

Comparison of the TRB repertoire overlap between the NKp46+CD3+ cell lines derived from the 2 naïve animals 106180 and 106222 (Figure 3.8) shows high levels of repertoire overlap (clonotypes accounting for 65% and 85% of reads in 106180 and 106222 respectively). Some of these clonotypes were expressed with high frequency in both naïve animals, such as CASSDPRTAGAVQLYF (42.7% in 106222 and 8.3% in 106180), CASSPLTSGGLNTQPLYF (4.6% in 106222 and 2.9% in 106180), CASSQDGQHRSYEQYF (2.5% in 106222 and 2.2% in 106180), CASSQADTLGTQYF (2.4% in 106222 and 2.3% in 106180), and CGTLDWASTDTQYF (1.9% in 106222 and 3.5% in 106180). With regards to TRBV and TRBJ gene usage both cell lines exhibited a broad repertoire of usage, but notably for both TRBV and TRBJ the 4 most commonly used genes were the same, with the exception of the closely related TRBV7-1 in 106180 and TRBV7-2 in 106222 (Figure 3.6). Comparison of the spectratypes indicated that despite the similarity in the TRB clonotypes and gene usage between the cell lines the most dominant CDR3 lengths differed between the two lines.

In contrast, there was no overlap of distinct characteristics of TRB chains (i.e. no TRBV and TRBJ gene segments or CDR3 size/motif) was observed either between two immunized animals (202990 and 202997) or between naïve and immunized animals (data not shown).

106180 NKp46+ CD3+ cell line					
#count	freq	cdr3aa	v	d	j
2562	25.07%	CASSPLTARAVQLYF	TRBV7-2	TRBD1	TRBJ2-2
853	8.35%	CASSDPRTAGAVQLYF	TRBV28-1	TRBD1	TRBJ2-2
357	3.49%	CGTLDWASTDTQYF	TRBV20-03	TRBD2	TRBJ3-4
338	3.31%	CASAPDFGTYEQYF	TRBV26-2	TRBD3	TRBJ3-7
305	2.98%	CASSPLTSGGLNTQPLYF	TRBV7-1	TRBD3	TRBJ3-2
284	2.78%	CASSQGSGGAYEQYF	TRBV9-26	TRBD3	TRBJ3-7
271	2.65%	CASSLGTASEQYF	TRBV4-6	TRBD1	TRBJ3-7
235	2.30%	CASSQADTLGTQYF	TRBV9-9	TRBD1	TRBJ3-4
233	2.28%	CASSQDGQHRSYEQYF	TRBV9-9	TRBD1	TRBJ3-7
167	1.63%	CASSSTPMNTQPLYF	TRBV6-36	TRBD3	TRBJ3-2
157	1.54%	CASSRGMGEGSIDTQYF	TRBV12-2	TRBD1	TRBJ3-4
148	1.45%	CGARPGGNAVQLYF	TRBV20-10	TRBD3	TRBJ2-2
113	1.11%	CASSRTRAATDDYHF	TRBV4-5	TRBD1	TRBJ1-2
108	1.06%	CASSQRTSGGHEQYF	TRBV21-1	TRBD3	TRBJ3-7
105	1.03%	CSASCFGGGHEQYF	TRBV20-13	TRBD3	TRBJ3-7
96	0.94%	CASSLGIQGAQDTQYF	TRBV9-6	TRBD3	TRBJ3-4
95	0.93%	CASSMRASGGMGTQIQYF	TRBV4-6	TRBD3	TRBJ3-5
93	0.91%	CASSQGTGYDYHF	TRBV4-4	TRBD2	TRBJ1-2
93	0.91%	CSAPDFGSGELHF	TRBV20-13	TRBD3	TRBJ3-1
83	0.81%	CSASLGLNYEQYF	TRBV20-13	TRBD2	TRBJ3-7
83	0.81%	CSAISHNPLYF	TRBV20-13	TRBD3	TRBJ3-3
79	0.77%	CSAQHGGSYEEQHF	TRBV20-04	TRBD2	TRBJ2-1
76	0.74%	CASSLAGHGELHF	TRBV10-3	TRBD1	TRBJ3-1
75	0.73%	CASSQEMRDPSYEQYF	TRBV9-1	TRBD1	TRBJ3-7
73	0.71%	CASVTSGQEIQYF	TRBV28-1	TRBD3	TRBJ3-5
72	0.71%	CSASGHLNTQPLYF	TRBV20-13	TRBD2	TRBJ3-2
67	0.66%	CSAGFSGTDTQYF	TRBV29-9	TRBD1	TRBJ3-4
63	0.62%	CASSSIRGVAGAALTF	TRBV9-26	TRBD3	TRBJ3-6
63	0.62%	CASSIDFGEIYEQYF	TRBV27-1	TRBD3	TRBJ3-7
63	0.62%	CASSPRGADTQPLYF	TRBV3-1	TRBD3	TRBJ3-2
59	0.58%	CASSRSGAYRNNPLYF	TRBV4-3	TRBD3	TRBJ3-3
54	0.53%	CATRGQGVYNNPLYF	TRBV6-11	TRBD2	TRBJ3-3
53	0.52%	CAGGQQLFAGAALTF	TRBV27-1	TRBD1	TRBJ3-6
53	0.52%	CASSPAGGIYGELHF	TRBV9-26	TRBD2	TRBJ3-1
47	0.46%	CASSYYAAGYDYHF	TRBV6-18	TRBD1	TRBJ1-2
44	0.43%	CASSSRLRLADTQYF	TRBV6-36	TRBD3	TRBJ3-4
40	0.39%	SSPLTARAVQLYF	TRBV6-19	TRBD1	TRBJ2-2
39	0.38%	CASSYDRGISNNPLYF	TRBV10-3	TRBD3	TRBJ3-3
39	0.38%	CASSSEWGGGINEQYF	TRBV4-4	TRBD2	TRBJ3-7
39	0.38%	CASSRDGGDYHF	TRBV4-6	TRBD2	TRBJ1-2
37	0.36%	CSARRWGGKTSNNPLYF	TRBV20-08	TRBD3	TRBJ3-3
37	0.36%	CASRPSYQMNAVQLYF	TRBV21-8	TRBD1	TRBJ2-2
37	0.36%	CSAVEQAGVSYEQYF	TRBV20-08	TRBD1	TRBJ3-7
37	0.36%	CSGTTQPLYF	TRBV20-13	TRBD1	TRBJ3-2
36	0.35%	CTCRLDSSYEQYF	TRBVX-1	TRBD1	TRBJ3-7
34	0.33%	SSDPRTAGAVQLYF	TRBV6-19	TRBD1	TRBJ2-2
34	0.33%	CSDWRGHTQYF	TRBV20-13	TRBD2	TRBJ3-4
33	0.32%	CASSPRDTYEQYF	TRBV9-26	TRBD1	TRBJ3-7
33	0.32%	CSAAPGTQPLYF	TRBV20-13	TRBD3	TRBJ3-2
33	0.32%	CGAREWVGQYF	TRBV20-07	TRBD2	TRBJ3-4

Table 3.7 Top 50 most frequent CDR3 sequencing of animal 106180 NKp46+ CD3+ cell line

202990 NKp46+ CD3+ cell line					
#count	freq	cdr3aa	v	d	j
593891	57.37%	CASAALLAGAALTF	TRBV26-2	TRBD1	TRBJ3-6
266184	25.71%	CASSQEGLSDERTEVFF	TRBV9-25	TRBD2	TRBJ1-1
78448	7.58%	CAASSPPEQGSQIQYF	TRBV19-01	TRBD2	TRBJ3-5
13258	1.28%	CASSLKVPYGELHF	TRBV21-9	TRBD3	TRBJ3-1
11823	1.14%	SSQEGLSDERTEVFF	TRBV6-19	TRBD2	TRBJ1-1
7440	0.72%	CASSSSTSGGALDGELHF	TRBV3-1	TRBD3	TRBJ3-1
4307	0.42%	CASSQAHSRIDRLYF	TRBV21-8	TRBD1	TRBJ1-4
3800	0.37%	CASSEDLGLRGQIQYF	TRBV9-10	TRBD3	TRBJ3-5
3351	0.32%	CASSPGHLDQPLYF	TRBV9-2	TRBD1	TRBJ3-2
2904	0.28%	CASSDPSGGVISNNPLYF	TRBV4-1	TRBD3	TRBJ3-3
2825	0.27%	CASSQDRQASIYEQYF	TRBV9-21	TRBD1	TRBJ3-7
2296	0.22%	CASNSGANNPLYF	TRBV6-14	TRBD3	TRBJ3-3
2060	0.20%	CASAGPPNDYHF	TRBV26-2	TRBD2	TRBJ1-2
1874	0.18%	CASSPMGGEQYF	TRBV7-1	TRBD2	TRBJ3-7
1655	0.16%	CASRGPPDSYEQYF	TRBV15-1	TRBD1	TRBJ3-7
1469	0.14%	CASSPPDLYDYHF	TRBV21-11	TRBD3	TRBJ1-2
1387	0.13%	CSAGPGDNPLYF	TRBV20-13	TRBD3	TRBJ3-3
1331	0.13%	CASSPGLRGNTQPLYF	TRBV4-1	TRBD3	TRBJ3-2
1231	0.12%	CSARCSGGDWPLYF	TRBV20-13	TRBD3	TRBJ3-3
1107	0.11%	CASSQDLLDFGAGAALTF	TRBV9-25	TRBD3	TRBJ3-6
1028	0.10%	CSAAGDYDYHF	TRBV20-05	TRBD3	TRBJ1-2
859	0.08%	CSARIRTAQRWPSYEQYF	TRBV20-08	TRBD1	TRBJ3-7
836	0.08%	CSAVRGGRHNPLYF	TRBV20-08	TRBD3	TRBJ3-3
795	0.08%	CASSDPRTAGAVQLYF	TRBV28-1	TRBD1	TRBJ2-2
785	0.08%	CASSEDPWALFAGAALTF	TRBV9-10	TRBD1	TRBJ3-6
736	0.07%	SSSSTSGGALDGELHF	TRBV6-19	TRBD3	TRBJ3-1
711	0.07%	CASSSWRDTQPLYF	TRBV9-10	TRBD3	TRBJ3-2
698	0.07%	CASSLGGRESTQYF	TRBV9-25	TRBD2	TRBJ2-3
636	0.06%	CASSYSEPEECDYHF	TRBV6-20	TRBD2	TRBJ1-2
601	0.06%	CAWSSHMPPGLGGDPLYF	TRBV30-1	TRBD2	TRBJ3-3
570	0.06%	CASSSGTDYDYHF	TRBV4-1	TRBD1	TRBJ1-2
564	0.05%	CSAREVRGEDGELHF	TRBV20-08	TRBD3	TRBJ3-1
516	0.05%	CASSPPGHWGFAGAALTF	TRBV7-2	TRBD2	TRBJ3-6
447	0.04%	CSAGEYTGTDTQYF	TRBV29-1	TRBD1	TRBJ3-4
425	0.04%	CSAGGPIIGDYHF	TRBV29-6	TRBD1	TRBJ1-2
405	0.04%	CASSQDFGESGSSTDTQYF	TRBV9-1	TRBD3	TRBJ3-4
397	0.04%	CASSSTPMNTQPLYF	TRBV6-36	TRBD3	TRBJ3-2
396	0.04%	CGASQPYHEQYF	TRBV20-03	TRBD1	TRBJ3-7
383	0.04%	CGATDFGLSNNPLYF	TRBV20-03	TRBD3	TRBJ3-3
381	0.04%	CASTGDFAGAALTF	TRBV26-2	TRBD2	TRBJ3-6
373	0.04%	CASSVRTLTNDRLYF	TRBV3-1	TRBD1	TRBJ1-4
369	0.04%	CAWSFRTTDEEQHF	TRBV30-1	TRBD2	TRBJ2-1
361	0.03%	CSARKVAGSGVSVINNPLYF	TRBV20-13	TRBD3	TRBJ3-3
352	0.03%	CASAPLRGDRPLYF	TRBV26-2	TRBD3	TRBJ3-3
344	0.03%	CASSRYYSNSYEQYF	TRBV15-1	TRBD3	TRBJ3-7
323	0.03%	CASSEPKGGLSTDTQYF	TRBV28-1	TRBD3	TRBJ3-4
312	0.03%	SSLKVPYGELHF	TRBV6-19	TRBD3	TRBJ3-1
309	0.03%	CASSQREIQYF	TRBV9-26	TRBD1	TRBJ3-5
301	0.03%	CASSYNSRSYDYHF	TRBV6-14	TRBD1	TRBJ1-2
282	0.03%	CASSQDRVGLYDYHF	TRBV9-26	TRBD2	TRBJ1-2

Table 3.8 Top 50 most frequent CDR3 sequencing of animal 202990 NKp46+ CD3+ cell line

202997 NKp46+ CD3+ cell line					
#count	freq	cdr3aa	v	d	j
434053	63.22%	CASSHRQQLNNPLYF	TRBV9-29	TRBD1	TRBJ3-3
106831	15.56%	CASSRGTDYDYHF	TRBV12-1	TRBD2	TRBJ1-2
71326	10.39%	CASSQYLQEGDYHF	TRBV9-26	TRBD1	TRBJ1-2
24679	3.59%	CASSHSGTDTQPLYF	TRBV9-9	TRBD2	TRBJ3-2
7034	1.02%	SSHRQQLNNPLYF	TRBV6-19	TRBD1	TRBJ3-3
6702	0.98%	CASCNSGGPTDTQYF	TRBV6-14	TRBD3	TRBJ3-4
5365	0.78%	CASQVGRYSNNPLYF	TRBV4-6	TRBD2	TRBJ3-3
2547	0.37%	CASSRGLDNPLYF	TRBV9-11	TRBD3	TRBJ3-3
2516	0.37%	CASSQSGRGIGERYF	TRBV21-9	TRBD2	TRBJ2-5
2361	0.34%	CGASYLGGGRTYEQYF	TRBV20-07	TRBD2	TRBJ3-7
2337	0.34%	SSRGTDYDYHF	TRBV6-19	TRBD2	TRBJ1-2
2024	0.29%	CASSPGQLHYHF	TRBV21-11	TRBD1	TRBJ1-2
1366	0.20%	SSQYLQEGDYHF	TRBV6-19	TRBD1	TRBJ1-2
1229	0.18%	CASSDPRTAGAVQLYF	TRBV28-1	TRBD1	TRBJ2-2
1072	0.16%	CASSPRLRGGLPIELHF	TRBV7-1	TRBD3	TRBJ3-1
1050	0.15%	CASSKLGRGPSDTQYF	TRBV4-3	TRBD2	TRBJ3-4
1007	0.15%	CGAWEASYGELHF	TRBV20-03	TRBD2	TRBJ3-1
798	0.12%	CASGNLRSTLNYDYHF	TRBV9-16	TRBD1	TRBJ1-2
721	0.11%	CSAGLRGLYGELHF	TRBV29-1	TRBD3	TRBJ3-1
591	0.09%	CSVAGQDYYGELHF	TRBV29-1	TRBD1	TRBJ3-1
512	0.07%	CASSDAGRGHSYEQYF	TRBV12-1	TRBD3	TRBJ3-7
508	0.07%	CASSNFGGALRTQPLYF	TRBV6-18	TRBD3	TRBJ3-2
455	0.07%	CASSPLTARAVQLYF	TRBV7-2	TRBD1	TRBJ2-2
421	0.06%	CASSLGIQGAQDTQYF	TRBV9-6	TRBD3	TRBJ3-4
374	0.05%	CASSRRGRDTRTDTQYF	TRBV6-14	TRBD1	TRBJ3-4
315	0.05%	SSHSGTDTQPLYF	TRBV6-19	TRBD2	TRBJ3-2
279	0.04%	CAASISWGDLSETLYF	TRBV19-09	TRBD2	TRBJ2-4
259	0.04%	CASSQGATTQPLYF	TRBV21-1	TRBD1	TRBJ3-2
259	0.04%	CAGWTSSQIQYF	TRBV24-2	TRBD1	TRBJ3-5
252	0.04%	CGARPGGNAVQLYF	TRBV20-10	TRBD3	TRBJ2-2
246	0.04%	CASSLGTASEQYF	TRBV4-6	TRBD1	TRBJ3-7
217	0.03%	CASASTGLLIDTQYF	TRBV26-2	TRBD1	TRBJ2-3
217	0.03%	CASSYPDGNSYEQYF	TRBV6-18	TRBD3	TRBJ3-7
208	0.03%	CASSPAGTARETLYF	TRBV7-2	TRBD1	TRBJ2-4
190	0.03%	CASTSTQDYHF	TRBV24-2	TRBD2	TRBJ1-2
171	0.02%	CASSSTPMNTQPLYF	TRBV6-36	TRBD3	TRBJ3-2
170	0.02%	CASSPTVRVSGAALTF	TRBV7-2	TRBD1	TRBJ3-6
169	0.02%	CSARGHSRASETLYF	TRBV20-13	TRBD1	TRBJ2-4
169	0.02%	CASTLGANYDYHF	TRBV9-26	TRBD3	TRBJ1-2
129	0.02%	CASSDWGVVVFAGAALTF	TRBV28-1	TRBD2	TRBJ3-6
112	0.02%	CSGTTQPLYF	TRBV20-13	TRBD1	TRBJ3-2
111	0.02%	CGLQEGNGELHF	TRBV20-03	TRBD1	TRBJ3-1
111	0.02%	CSASVYEQYF	TRBV20-04	TRBD1	TRBJ3-7
106	0.02%	CASSQGSGGAYEQYF	TRBV9-26	TRBD3	TRBJ3-7
105	0.02%	CASSQVEGTYGELHF	TRBV9-26	TRBD3	TRBJ3-1
104	0.02%	SSLGTAWGYHF	TRBV6-19	TRBD1	TRBJ1-2
102	0.01%	CGASNGDSLLMNTEVFF	TRBV20-02	TRBD1	TRBJ1-1
102	0.01%	CASSGTESNNPLYF	TRBV6-39	TRBD1	TRBJ3-3
100	0.01%	CASSQRTSGAIRGELHF	TRBV21-1	TRBD3	TRBJ3-1
99	0.01%	CASSRGMGEGSIDTQYF	TRBV12-2	TRBD1	TRBJ3-4

Table 3.9 Top 50 most frequent CDR3 sequencing of animal 202997 NKp46+ CD3+ cell line

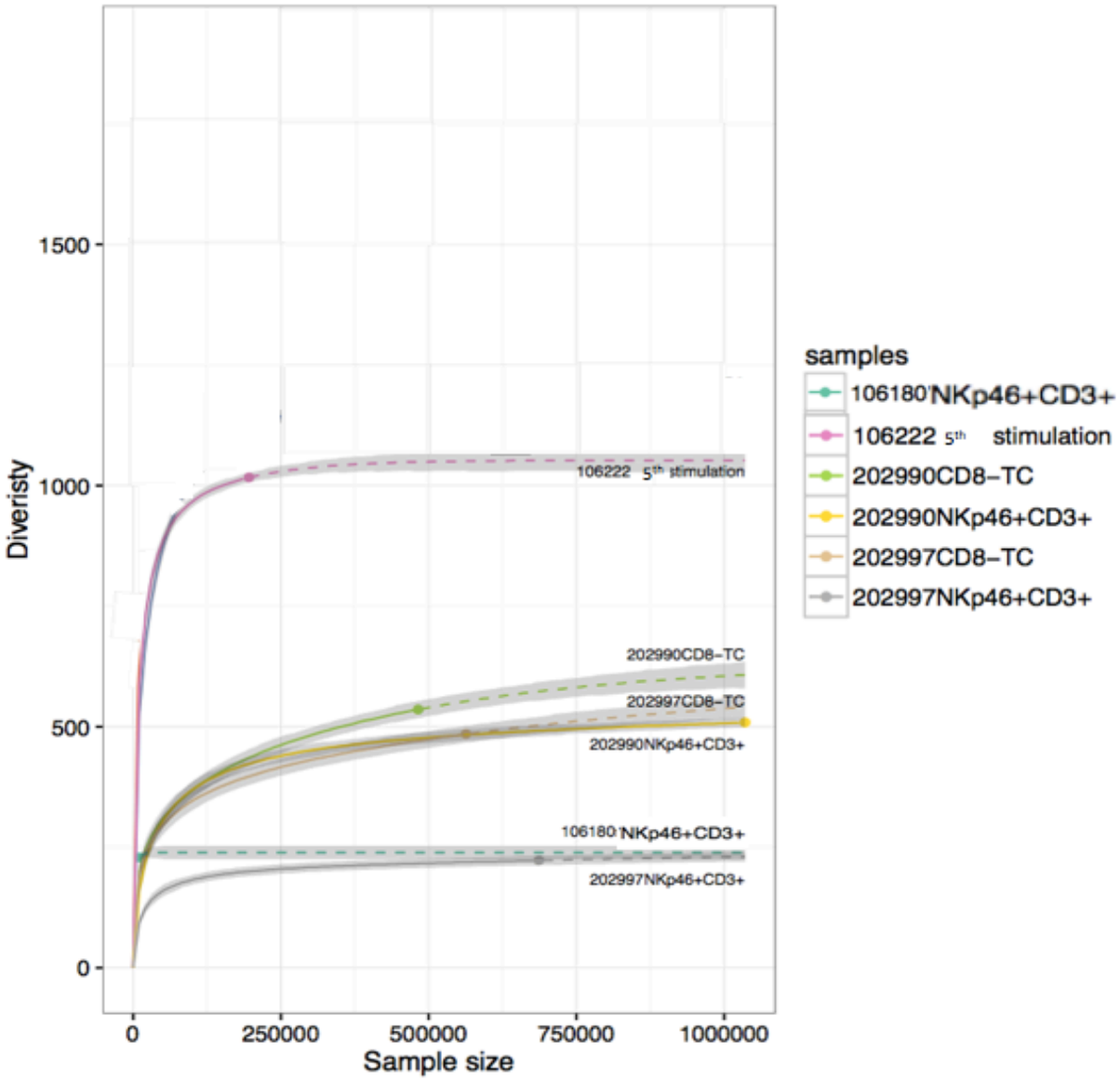

Figure 3.7 Rarefaction analysis of TRB repertoire from the animal 106222 (5th stimulations), 106180 NKp46+ CD3+ cells, 202990 NKp46+ CD3+ cells, 202990 CD8+, 202997 NKp46+ CD3+ cells, 202997 CD8+ cells.

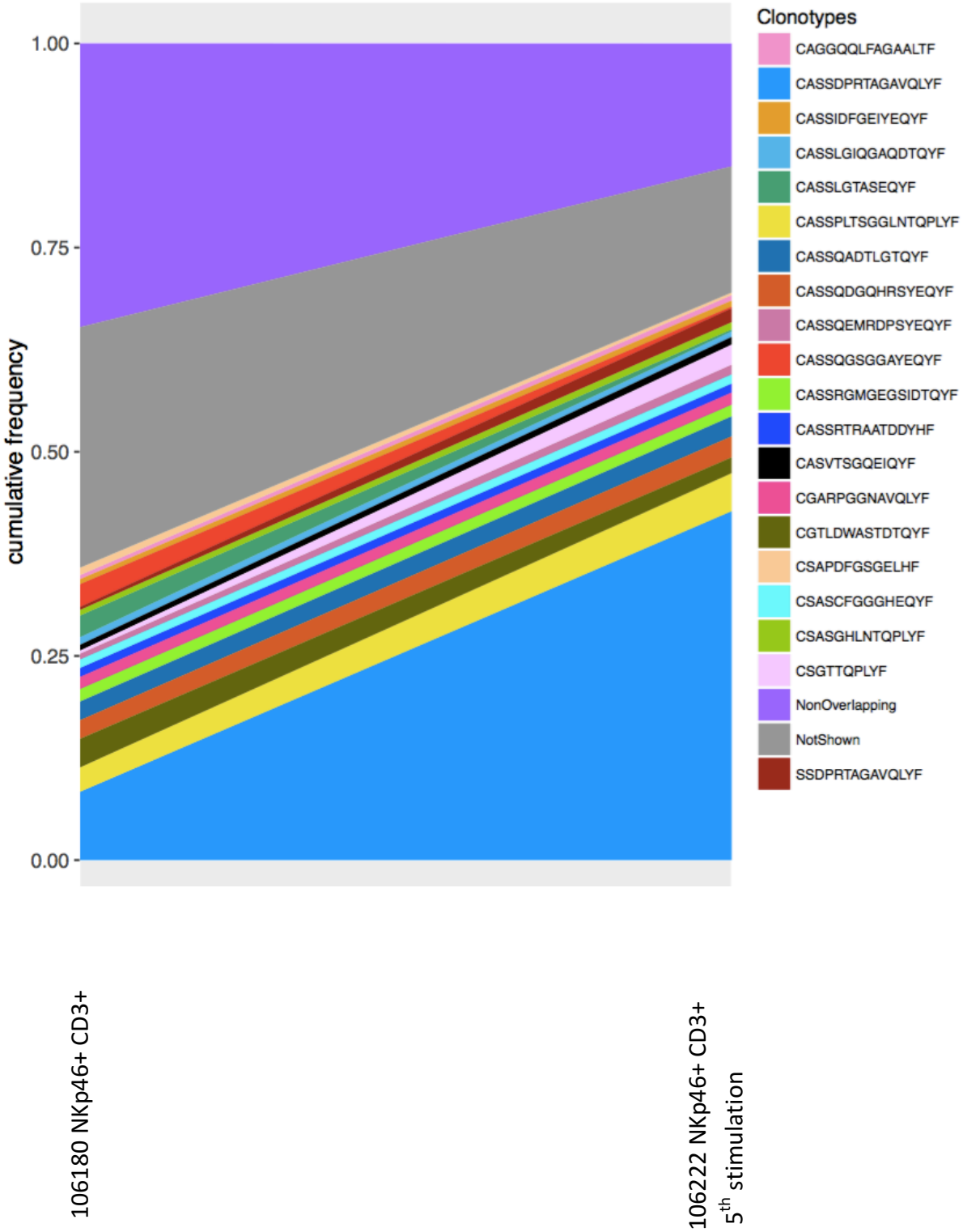

Figure 3.8. Repertoire overlap analysis of the clonotypes present in NKp46+ CD3+ cell lines of animal 106222 (5^{th} stimulation) and animal 106180.

3.3.2.3. Comparison between TRB repertoires of autologous NKp46+ CD3+ T cells and CD8+ T cells

Comparison of the TRB repertoires expressed by autologous TpM-specific NKp46+ CD3+ T cells and CD8+ T cells was performed to identify if NKp46+CD3+ T cells used any of the TRB used by conventional T cells, which could provide evidence of recognition of the same peptide-MHC ligands. The top 50 most frequent CDR3 sequences of 202990 and 202997 conventional (NKp46-CD3+) CD8+ cell lines are shown in Table 3.10, and Table 3.11 (data from Dr. Timothy Connelley). Rarefaction analysis (Figure 3.7) indicates that the TRB diversity of the conventional CD8+ T cell lines was higher than that of the NKp46+ CD3+ cell lines, which may be in part a reflection of the smaller number of cells harvested for the NKp46+ CD3+ cell lines. Virtual spectratype analysis of the conventional CD8+ T cell lines (Figure 3.8) shows a skewed distribution of CDR3 length with expansion of a number of dominant clonotypes. There was evidence of preferential usage of particular TRBV and TRBJ genes (Figure 3.9) in both conventional CD8+ T-cell lines but these didn't correspond to those observed in the matching NKp46+CD3+ cell lines. Repertoire overlap analysis showed no conserved TRB sequences indicating that NKp46+CD3+ and conventional NKp46-CD3+CD8+ T-cell lines are distinct and thus there is no evidence support recognition by the two TpM-specific populations of the same ligand.

202990 CD8+ T cell line					
#count	freq	cdr3aa	v	d	j
124745	25.87%	CASSQSGAQGEEQHF	TRBV9-2	TRBD1	TRBJ2-1
77136	15.99%	CASSYRDSHSQPLYF	TRBV9-25	TRBD1	TRBJ3-2
68793	14.26%	CASSLGQPNDYHF	TRBV6-4	TRBD1	TRBJ1-2
35275	7.31%	CASAESIVPNTQPLYF	TRBV26-2	TRBD1	TRBJ3-2
23038	4.78%	CASSPTSDRSDTQYF	TRBV3-1	TRBD3	TRBJ3-4
20182	4.18%	CSAGDRTSGASLYF	TRBV29-6	TRBD3	TRBJ3-3
16188	3.36%	CASAESPGGGRAQIQYF	TRBV26-1	TRBD2	TRBJ3-5
9385	1.95%	CASSDTAGQGELHF	TRBV9-30	TRBD1	TRBJ3-1
9363	1.94%	CSARLGGGINNPLYF	TRBV20-13	TRBD2	TRBJ3-3
7241	1.50%	CASSYQFGGAGEQYF	TRBV9-30	TRBD3	TRBJ3-7
6595	1.37%	CASSVRTASYEQYF	TRBV9-30	TRBD1	TRBJ3-7
5678	1.18%	CASSARQQGYAVQLYF	TRBV28-1	TRBD1	TRBJ2-2
4126	0.86%	CASLPYNPLYF	TRBV4-1	TRBD3	TRBJ3-3
3278	0.68%	CASSEDSTQIQYF	TRBV9-22	TRBD2	TRBJ3-5
3033	0.63%	CASSQ*RAYTQPLYF	TRBV9-25	TRBD1	TRBJ3-2
2972	0.62%	CASSRSGTAEDDYHF	TRBV9-2	TRBD1	TRBJ1-2
2897	0.60%	CASSQSQIQYF	TRBV14-1	TRBD3	TRBJ3-5
2780	0.58%	CASSLNSDSYEQYF	TRBV21-11	TRBD1	TRBJ3-7
2354	0.49%	CGALIRGGYEQYF	TRBV20-02	TRBD3	TRBJ3-7
2244	0.47%	SSLGQPNDYHF	TRBV6-19	TRBD1	TRBJ1-2
1929	0.40%	CASSRDQIAAYFAGAALTF	TRBV4-1	TRBD1	TRBJ3-6
1828	0.38%	CASSQDSDQIQYF	TRBV9-22	TRBD1	TRBJ3-5
1759	0.36%	CASSVDWGETLYF	TRBV9-30	TRBD2	TRBJ2-4
1594	0.33%	CGALGRNSYEQYF	TRBV20-07	TRBD3	TRBJ3-7
1525	0.32%	CSALPTAGYAIQYF	TRBV29-1	TRBD1	TRBJ3-5
1475	0.31%	CASSQDVGGSLETLYF	TRBV9-25	TRBD2	TRBJ2-4
1473	0.31%	CASSEGIAAETLYF	TRBV9-10	TRBD1	TRBJ2-4
1425	0.30%	CASGSGSERYF	TRBV25-1	TRBD2	TRBJ2-5
1421	0.29%	CSAKGGGGINNPLYF	TRBV20-13	TRBD2	TRBJ3-3
1399	0.29%	CASSQFPGNYDYHF	TRBV21-11	TRBD1	TRBJ1-2
1399	0.29%	CGALGRGGYEQYF	TRBV20-02	TRBD3	TRBJ3-7
1378	0.29%	SSQSGAQGEEQHF	TRBV6-19	TRBD1	TRBJ2-1
1367	0.28%	CASSSSQIQYF	TRBV14-1	TRBD1	TRBJ3-5
1170	0.24%	CGARDTAMSDYHF	TRBV20-02	TRBD1	TRBJ1-2
1096	0.23%	CASGDSTKQYF	TRBV12-1	TRBD1	TRBJ3-7
1040	0.22%	CASELGGLSQSTQYF	TRBV9-1	TRBD2	TRBJ2-3
979	0.20%	CGALLRGGYEQYF	TRBV20-02	TRBD3	TRBJ3-7
974	0.20%	CAASTPGQTIQAQNF	TRBV19-04	TRBD1	TRBJ1-5
895	0.19%	CAIRDSSYGELHF	TRBV25-1	TRBD1	TRBJ3-1
878	0.18%	CASSLTSSGGAYDNPLYF	TRBV9-1	TRBD3	TRBJ3-3
861	0.18%	CASSQGGGWAQPLYF	TRBV9-1	TRBD2	TRBJ3-2
844	0.18%	CGALRGNDRLYF	TRBV20-03	TRBD3	TRBJ1-4
829	0.17%	CASSSSISGDRLYF	TRBV9-25	TRBD1	TRBJ1-4
696	0.14%	CASSDIRGERAGRKQEQYF	TRBV9-30	TRBD3	TRBJ3-7
693	0.14%	CASSQEAGANPEVFF	TRBV9-25	TRBD3	TRBJ1-1
651	0.13%	CASSRTENNPLYF	TRBV21-1	TRBD1	TRBJ3-3
589	0.12%	CASTGTASYEQYF	TRBV6-18	TRBD1	TRBJ3-7
578	0.12%	SSYRDSHSQPLYF	TRBV6-19	TRBD1	TRBJ3-2
556	0.12%	CGLQEGNGELHF	TRBV20-03	TRBD1	TRBJ3-1
540	0.11%	CASSEARTPINNPLYF	TRBV9-30	TRBD2	TRBJ3-3

Table 3.10 Top 50 most frequent CDR3 sequencing of animal 202990 CD8+ T cell line

202997 CD8+ T cell line					
#count	freq	cdr3aa	v	d	j
130959	23.25%	CASSMRASGGMGTQIQYF	TRBV4-6	TRBD3	TRBJ3-5
51374	9.12%	CASSQRTSGGHEQYF	TRBV21-1	TRBD3	TRBJ3-7
41308	7.33%	CAWSLGLGAVQLYF	TRBV30-1	TRBD2	TRBJ2-2
37900	6.73%	CASSQRTAGTGGYEQYF	TRBV21-1	TRBD2	TRBJ3-7
33176	5.89%	CTSSYAPTAGNGDRLYF	TRBV6-40	TRBD1	TRBJ1-4
30902	5.49%	CASTDLGRRGMDGELHF	TRBV6-9	TRBD3	TRBJ3-1
29919	5.31%	CSAARRSGGSNNPLYF	TRBV29-6	TRBD3	TRBJ3-3
17554	3.12%	CASSQRTSGAIRGELHF	TRBV21-1	TRBD3	TRBJ3-1
17366	3.08%	CASSVQGSSRARLGNSPLHF	TRBV9-10	TRBD1	TRBJ1-6
15309	2.72%	CASSQRGAKDTQYF	TRBV21-1	TRBD3	TRBJ3-4
9959	1.77%	CASSPSYGAGEQYF	TRBV3-1	TRBD3	TRBJ3-7
9894	1.76%	CASSLGIQGAQDTQYF	TRBV9-6	TRBD3	TRBJ3-4
7660	1.36%	CASSREIDEQYF	TRBV15-2	TRBD1	TRBJ3-7
7336	1.30%	CASSSGSRGNPLYF	TRBV6-36	TRBD1	TRBJ3-3
6804	1.21%	CASSLGQRDYHF	TRBV9-9	TRBD2	TRBJ1-2
6771	1.20%	CASSYGRLGVLMEEQHF	TRBV10-3	TRBD2	TRBJ2-1
6659	1.18%	CASSSRGSHSQSTQYF	TRBV21-1	TRBD3	TRBJ2-3
6471	1.15%	CASSRRDSGAYEQYF	TRBV21-1	TRBD1	TRBJ3-7
4942	0.88%	CASSLSGGEDTQYF	TRBV9-6	TRBD3	TRBJ3-4
4596	0.82%	CASSSNEGSYEQYF	TRBV3-1	TRBD1	TRBJ3-7
4245	0.75%	CSGGTRDTNDRLYF	TRBV19-02	TRBD1	TRBJ1-4
3263	0.58%	CASSHGLASETLYF	TRBV9-11	TRBD2	TRBJ2-4
2868	0.51%	CASGGRSSYEEQHF	TRBV24-2	TRBD1	TRBJ2-1
2785	0.49%	CSAGRGRNNPLYF	TRBV29-3	TRBD2	TRBJ3-3
2680	0.48%	CASSQGIHPQTQPLYF	TRBV9-6	TRBD1	TRBJ3-2
2509	0.45%	SSMRASGGMGTQIQYF	TRBV6-19	TRBD3	TRBJ3-5
2454	0.44%	CTCSKDRGSQIQYF	TRBVX-1	TRBD1	TRBJ3-5
2387	0.42%	CASSYSGQPGTEVFF	TRBV6-9	TRBD1	TRBJ1-1
2380	0.42%	CASSQRTSGGGEQYF	TRBV21-1	TRBD3	TRBJ3-7
2187	0.39%	CAWSLSRGDEQYF	TRBV30-1	TRBD2	TRBJ3-7
2175	0.39%	CASNIGGAGEQYF	TRBV24-2	TRBD1	TRBJ3-7
2038	0.36%	CASGRG*QAYHF	TRBV9-11	TRBD1	TRBJ1-2
1915	0.34%	CASSVASNAVQLYF	TRBV3-1	TRBD1	TRBJ2-2
1879	0.33%	CASSLNAVQLYF	TRBV6-9	TRBD1	TRBJ2-2
1832	0.33%	CASSREDSSDDRLYF	TRBV15-2	TRBD1	TRBJ1-4
1644	0.29%	CASSDGLATDNNPLYF	TRBV9-29	TRBD1	TRBJ3-3
1611	0.29%	CASSWGVGQSTQYF	TRBV9-25	TRBD2	TRBJ2-3
1436	0.25%	CASDWGGEQHF	TRBV15-2	TRBD2	TRBJ2-1
1408	0.25%	CGAPDPKGVSYDYHF	TRBV20-03	TRBD2	TRBJ1-2
1304	0.23%	CATGDSARTQPLYF	TRBV10-3	TRBD1	TRBJ3-2
1263	0.22%	CASSDGLPGDYHF	TRBV9-33	TRBD2	TRBJ1-2
1112	0.20%	CASSQDSGRNWGEGETLYF	TRBV9-1	TRBD2	TRBJ2-4
1086	0.19%	CASSEMAAYYTQPLYF	TRBV9-11	TRBD1	TRBJ3-2
1056	0.19%	CASSRAGRGDYHF	TRBV15-2	TRBD3	TRBJ1-2
1052	0.19%	CASSREGRLGGDEETLYF	TRBV15-2	TRBD2	TRBJ2-4
1038	0.18%	CASSLEAQDYHF	TRBV6-4	TRBD1	TRBJ1-2
1029	0.18%	CASSPRGARDTQYF	TRBV21-1	TRBD3	TRBJ3-4
997	0.18%	CASSQDMARNWDFGAGNNPLYF	TRBV9-1	TRBD3	TRBJ3-3
966	0.17%	CASSQGGGGDGELHF	TRBV9-6	TRBD2	TRBJ3-1
939	0.17%	CASSPLRGAGNNPLYF	TRBV10-3	TRBD3	TRBJ3-3

Table 3.11 Top 50 most frequent CDR3 sequencing of animal 202997 CD8+ cell line

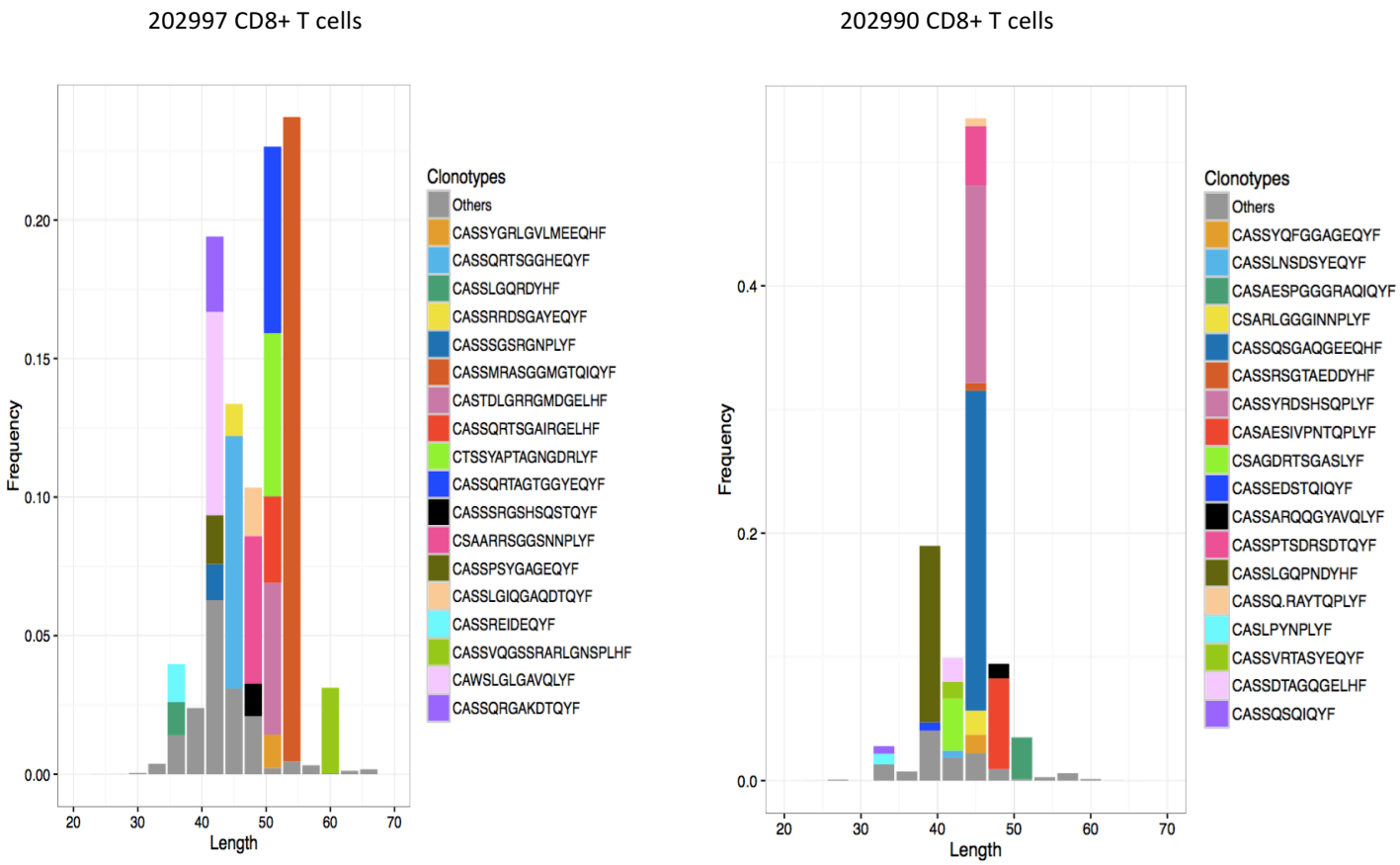

Figure 3.9. 'Virtual spectratype' analysis of the NGS TRB sequence data of 202997 CD8+ T cells and 202990 CD8+ T cells. The length of the CDR3 sequence is plotted against the read frequency for each sample. The most frequent clones are shown as distinct coloured blocks as indicated in the key

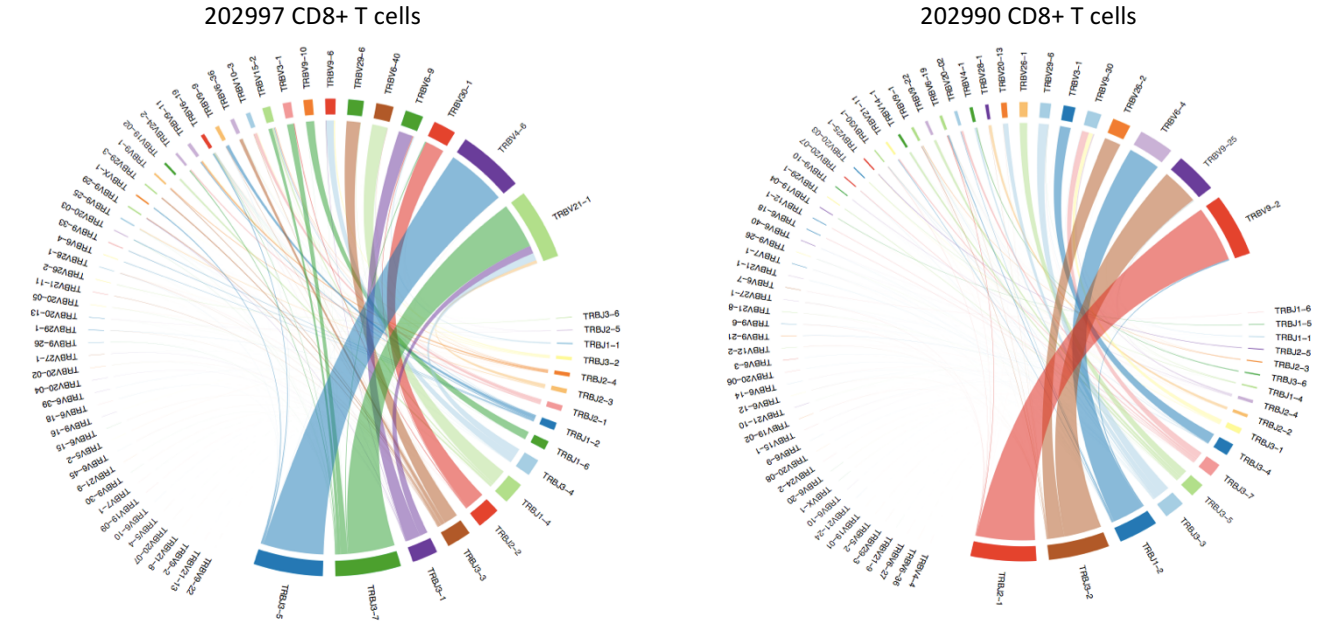

Figure 3.10. Representation of the frequency of TRBV and TRBJ usage CD8+ T cell lines of animal 202997 and 202990 analysed by NGS

3.4. Discussion

The work in this chapter describes the results from NGS analysis of TpM-specific stimulated NKp46+ CD3+ cell lines to provide higher resolution data on the expressed TRB repertoire.

The rarefaction analysis data for the 106222 2nd, 3rd, and 5th stimulated cell lines from animal 106222 demonstrated that the clonal diversity of *T. parva*-specific NKp46+ CD3+ cell lines narrowed during repeated TpM stimulations. As expected repertoire overlap analysis indicated that most of the clonotypes identified at the 3 time points were the same and that there was a progressive decrease in the number of reads coming from clonotypes not present at the other time points. A notable feature of these cell lines was the abrupt expansion of a single clonotype (TRBV28-1-CASSDPRTAGAVQLYF- TRBJ2-2) in the 5th stimulation that caused a dramatic skew in the virtual spectratype analysis and an apparent preference for that TRBV and TRBJ combination that was not present in the 2nd and 3rd stimulations. The reason for the remarkable expansion of this single clonotype is as yet unknown but may suggest a strong selection following sustained *in vitro* culture. Together the data is consistent with maintenance of a fairly stable but narrowing TRB repertoire in NKp46+CD3+ cells during multiple TpM-stimulations *in vitro*.

In naïve animals 106180 and 106222, there was a significant overlap in the clonotypes (accounting for 65% and 85% of reads respectively), with many clonotypes expressed at high frequency in both animals. In contrast the TRB repertoires from the 2 *T. parva*-immunised animals were discrete with no clonotypic overlap with each other or the 2 naïve animals. Notably 106222 and 106180 were both BoLA-A14+ whereas 202997 and 202990 were not, however further data would be needed to verify if clonal selection was associated with MHCI-haplotype. Further data from more *T. parva*-naïve animals would also be required to evaluate in more detail if the degree of conservation of the TRB repertoire of NKp46+CD3+ cells was consistent. In all *T. parva*-specific NKp46+ CD3+ cell lines the most frequent TRB clonotypes accounted for 25-63% of total reads suggesting a clonal dominance and therefore selection. However, there was no clear pattern of consistent preference for TRBV, TRBJ or CDR3 sequence in the most dominant clonotypes making it difficult to make conclusions about preferred TRB sequences.

Compare between the TCR repertoires of TpM specific NKp46+ CD3+ cells and CD8+ T cells from both 202997 and 202990 revealed no common TRB sequences. This is consistent

with the NKp46+CD3+ and conventional CD8+ T cell populations recognising distinct ligands. This suggests that the NKp46+CD3+ cells may, as expected not be specific to peptide-MHCI complexes but instead other, as yet to be determined restricting elements.

Chapter 4 Final conclusions

During this study, the *T. parva*-specific stimulated NKp46+ CD3+ cells were maintained and generated *in vitro* from naïve and immunized cattle. In a previous study, the *T. parva* stimulated NKp46+ CD3+ cell lines were only generated from naïve animals (Connelley et al. 2014) and it had been hypothesised that NKp46+ CD3+ cells may have the capacity to form a memory population (Connelley – personal communication), and consequently that establishing *T. parva*-specific NKp46+CD3+ cell lines from immunised animals *in vitro* would be easier. However, in this study proliferation of *T. parva*-responsive NKp46+CD3+ cell lines was greater in naïve than in immunised animals, suggesting that if a memory population is formed the ability to recall it by *in vitro* stimulation is limited.

The aim of this study was to analyze the TCR repertoire of TpM-stimulated NKp46+CD3+ populations to look for evidence of TCR selection that would indicate a role for TCR in mediating recognition of TpM. From a previous study (Connelley et al. 2014), panels of Vα and Vβ subgroup-specific primers suggested that NKp46+ CD3+ cells expressed a highly diverse TCR repertoire. To better determine this, a novel NGS high resolution approach for analysing bovine TRB repertoires has been applied to study *T. parva*-specific NKp46+CD3+ cell lines in this project. To identify the evolution of TCR repertoire following repeated *T. parva* stimulations, we analysed NKp46+ CD3+ cell lines from animal 106222 after the 2nd, 3rd, and 5th stimulations, which provided evidence that following repeated *T. parva* stimulations the clonal diversity in the population was generally stable but did narrow. A remarkably high level of conservation between the TRB repertoires was observed between the 2 naïve animals in the study - 106180 and 10622 – but the repertoires of the 2 *T. parva* immunised animals were unique with no overlap with each other or the naïve animals. Whilst the high level of overlap between 106180 and 106222 provides evidence strongly suggestive of TRB involvement in the recognition of *T. parva* the lack of data of TRB repertoires in non-*T. parva* stimulated populations prevents firm conclusion being drawn. Unfortunately, the attempts to generate such lines in this study were unsuccessful and future work attempting other methods to generate non-specific lines (e.g. through cross-linking NKp46 or CD3 via well bound anti-NK46/CD3 antibodies) is warranted. Also necessary is the generation of data from further animals to verify the consistency of this TRB repertoire across animals of more diverse MHC haplotypes.

Of further interest is the fact that NKp46+CD3+ cell lines were more difficult to expand *in vitro* from immunised than naïve animals. This was contradictory to the starting expectation. When combined with the fact that the NKp46+CD3+ cell lines from the immunised animals were 'private' (i.e. unique to the individual animal) there is a possibility that *in vivo* exposure to the parasite is causing some substantial modification of the TRB repertoire of the NKp46+CD3+ - possibly suggestive of clonal deletion. Such an effect has obvious biological implications and needs further consideration – ideally experiments that track the NKp46+CD3+ responses longitudinally in individuals prior to and after an immunisation with *T. parva*. In any subsequent studies integration of analysis of the TRA chain repertoire would also be advantageous.

In summary in this study a high resolution description of the TRB repertoire of bovine NKp46+CD3+ cell lines has been achieved. The data obtained suggests that in naïve animals there may be a highly conserved TRB repertoire used by T. parva-specific populations that is distinct from conventional CD8 T-cells. To fully appreciate the significance of the data further studies looking NKp46+CD3+ cell lines from more animals and selected under different conditions are needed.

References

Ambrosino, E. et al., 2007. Cross-regulation between type I and type II NKT cells in regulating tumor immunity: a new immunoregulatory axis. *Journal of immunology (Baltimore, Md. : 1950)*, 179(8), pp.5126–5136.

Arstila, T.P. et al., 1999. A direct estimate of the human alphabeta T cell receptor diversity. *Science (New York, N.Y.)*, 286(5441), pp.958–961.

Barker, P.E. et al., 1984. Chromosomal location of human T-cell receptor gene Ti beta. *Science*, 226(4672), pp.348–349.

Bendelac, A., Savage, P.B. & Teyton, L., 2007. The biology of NKT cells. *Annual Review of Immunology*, 25, pp.297–336.

Bernardin, F. et al., 2004. Number of CD4+ and CD8+ T-cell CDR3 clonotypes expanding during acute infection of macaques with simian immunodeficiency virus. *Virology*, 322(1), pp.105–117.

Bolotin, D.A. et al., 2013. MiTCR: software for T-cell receptor sequencing data analysis. *Nat Meth*, 10(9), pp.813–814.

Bolotin, D.A. et al., 2012. Next generation sequencing for TCR repertoire profiling: Platform-specific features and correction algorithms. *European Journal of Immunology*, 42(11), pp.3073–3083.

Borg, N. a et al., 2005. The CDR3 regions of an immunodominant T cell receptor dictate the 'energetic landscape' of peptide-MHC recognition. *Nature immunology*, 6, pp.171–180.

Bosc, N. & Lefranc, M.P., 2000. The mouse (Mus musculus) T cell receptor beta variable (TRBV), diversity (TRBD) and joining (TRBJ) genes. *Experimental and clinical immunogenetics*, 17(4), pp.216–28.

Bouneaud, C., Kourilsky, P. & Bousso, P., 2000. Impact of Negative Selection on the T Cell Repertoire Reactive to a Self-Peptide. *Immunity*, 13(6), pp.829–840.

Le Bourhis, L. et al., 2010. Antimicrobial activity of mucosal-associated invariant T cells.

Nature immunology, 11(8), pp.701–708.

Bousso, P. et al., 1998. Individual variations in the murine T cell response to a specific peptide reflect variability in naive repertoires. *Immunity*, 9(2), pp.169–178.

Brazin, K.N. et al., 2015. Structural features of the a??TCR mechanotransduction apparatus that promote pMHC discrimination. *Frontiers in Immunology*, 6(SEP).

Brennan, P.J. et al., 2011. Invariant natural killer T cells recognize lipid self antigen induced by microbial danger signals. *Nature immunology*, 12(12), pp.1202–11.

Brigl, M. & Brenner, M.B., 2004. CD1: antigen presentation and T cell function. *Annual review of immunology*, 22, pp.817–90.

Burnet, F.M., 1976. A modification of {J}erne's theory of antibody production using the concept of clonal selection. *The Australian Journal of Science*, 20(3), pp.67–69.

Caccia, N. et al., 1984. The T cell receptor β chain genes are located on chromosome 6 in mice and chromosome 7 in humans. *Cell*, 37(3), pp.1091–1099.

Calabi, F. et al., 1989. Two classes of CD1 genes. *European journal of immunology*, 19(2), pp.285–292.

Casrouge, a et al., 2000. Size estimate of the alpha beta TCR repertoire of naive mouse splenocytes. *Journal of immunology*, 164(11), pp.5782–5787.

Chan, A.C. et al., 2013. Ex-vivo analysis of human Natural Killer T cells demonstrates heterogeneity between tissues and within established CD4+ and CD4- subsets. *Clinical and Experimental Immunology*, 172(1), pp.129–137.

Cohn, M. et al., 2007. Reflections on the clonal-selection theory. *Nature reviews. Immunology*, 7(10), pp.823–30.

Connelley, T. et al., 2008. Dissection of the clonal composition of bovine alphabeta T cell responses using T cell receptor Vbeta subfamily-specific PCR and heteroduplex analysis. *Journal of immunological methods*, 335(1-2), pp.28–40.

Connelley, T. et al., 2009. Genomic analysis reveals extensive gene duplication within the bovine TRB locus. *BMC genomics*, 10, p.192.

Connelley, T. et al., 2011. NKp46 defines ovine cells that have characteristics corresponding to NK cells. *Veterinary Research*, 42(1).

Connelley, T.K., Degnan, K., et al., 2014. Genomic analysis offers insights into the evolution of the bovine TRA/TRD locus. *BMC Genomics*, 15(1), pp.1–17.

Connelley, T.K., Longhi, C., et al., 2014. NKp46+ CD3+ cells: a novel nonconventional T cell subset in cattle exhibiting both NK cell and T cell features. *J. Immunol.*, 192(8), pp.3868–80.

Correia-Neves, M. et al., 2001. The shaping of the T cell repertoire. *Immunity*, 14(1), pp.21–32.

Cose, S.C., Kelly, J.M. & Carbone, F.R., 1995. Characterization of diverse primary herpes simplex virus type 1 gB-specific cytotoxic T-cell response showing a preferential V beta bias. *Journal of Virology*, 69(9), pp.5849–5852.

Dusseaux, M. et al., 2011. Human MAIT cells are xenobiotic resistant, tissue-targeted, CD161hi IL-17 secreting T cells. *Blood*, 117(4), pp.1250–1260.

Ellis, S. a et al., 1999. Variation in the number of expressed MHC genes in different cattle class I haplotypes. *Immunogenetics*, 50(5-6), pp.319–28.

Felio, K. et al., 2009. CD1-restricted adaptive immune responses to Mycobacteria in human group 1 CD1 transgenic mice. *The Journal of experimental medicine*, 206(11), pp.2497–2509.

Folch, G. & Lefranc, M.P., 2000. The human T cell receptor beta variable (TRBV) genes. *Experimental and clinical immunogenetics*, 17(1), pp.42–54.

Fujii, S. et al., 2002. Prolonged IFN-gamma-producing NKT response induced with alpha-galactosylceramide-loaded DCs. *Nature immunology*, 3(9), pp.867–874.

Fuss, I.J. et al., 2014. IL-13Rα2-bearing, type II NKT cells reactive to sulfatide self-antigen populate the mucosa of ulcerative colitis. *Gut*, 63(11), pp.1728–36.

Garboczi, D.N. et al., 1996. Structure of the complex between human T-cell receptor, viral peptide and HLA-A2. *Nature*, 384(6605), pp.134–141.

Garcia, K.C. et al., 1996. An alpha beta T Cell Receptor Structure at 2.5 A and Its Orientation in the TCR-MHC Complex. *Science*, 274(5285), pp.209–219.

Garcia, K.C. & Adams, E.J., 2005. How the T cell receptor sees antigen--a structural view. *Cell*, 122(3), pp.333–6.

Gauss, G.H. & Lieber, M.R., 1996. Mechanistic constraints on diversity in human V(D)J recombination. *Molecular and Cellular Biology*, 16(1), pp.258–269.

Girardi, E. et al., 2012. Type II natural killer T cells use features of both innate-like and conventional T cells to recognize sulfatide self antigens. *Nature immunology*, 13(9), pp.851–6.

Girardi, E. & Zajonc, D.M., 2012. Molecular basis of lipid antigen presentation by CD1d and recognition by natural killer T cells. *Immunological Reviews*, 250(1), pp.167–179.

Glusman, G. et al., 2001. Comparative genomics of the human and mouse T cell receptor loci. *Immunity*, 15, pp.337–349.

Godfrey Poulton, D.I. et al., 2001. CD1d-Restricted NKT Cells: An CD1d-Restricted NKT Cells: An Interstrain Comparison. *J. Immunol*, 167, pp.1164–1173.

Godfrey, D.I. et al., 2010. Antigen recognition by CD1d-restricted NKT T cell receptors. *Seminars in Immunology*, 22(2), pp.61–67.

Godfrey, D.I. et al., 2004. NKT cells: what's in a name? *Nature reviews. Immunology*, 4(3), pp.231–7. Available at: http://dx.doi.org/10.1038/nri1309.

Godfrey, D.I. et al., 2015. The burgeoning family of unconventional T cells. *Nature Immunology*, 16(11), pp.1114–1123.

Harrington, L.E. et al., 2005. Interleukin 17-producing CD4+ effector T cells develop via a lineage distinct from the T helper type 1 and 2 lineages. *Nature immunology*, 6(11), pp.1123–32.

Ignatowicz, L., Kappler, J. & Marrack, P., 1996. The repertoire of T cells shaped by a single MHC/peptide ligand. *Cell*, 84(4), pp.521–529.

Jahng, A. et al., 2004. Prevention of autoimmunity by targeting a distinct, noninvariant

CD1d-reactive T cell population reactive to sulfatide. *The Journal of experimental medicine*, 199(7), pp.947–57.

Kasinrerk, W. et al., 1993. CD1 molecule expression on human monocytes induced by granulocyte-macrophage colony-stimulating factor. *Journal of immunology (Baltimore, Md. : 1950)*, 150(2), pp.579–584.

Kasmar, A., Van Rhijn, I. & Moody, D.B., 2009. The evolved functions of CD1 during infection. *Current Opinion in Immunology*, 21(4), pp.397–403.

Kass, I., Buckle, A.M. & Borg, N.A., 2014. Understanding the structural dynamics of TCR-pMHC interactions. *Trends in Immunology*, 35(12), pp.604–612.

Kawano, T. et al., 1997. CD1d-restricted and TCR-mediated activation of valpha14 NKT cells by glycosylceramides. *Science (New York, N.Y.)*, 278(08282103), pp.1626–1629.

Lanier, L.L., 2005. NK cell recognition. *Annual review of immunology*, 23, pp.225–74.

Lehner, B.P.J. et al., 1995. Human HLA-A0201-restricted Cytotoxic T Lymphocyte Recognition of Influenza A Is Dominated by T Cells Bearing the Vβ17 Gene Segment. *Journal of Experimental Medicine*, 181(January), pp.79–91.

Liao, W., Lin, J.X. & Leonard, W.J., 2011. IL-2 family cytokines: New insights into the complex roles of IL-2 as a broad regulator of T helper cell differentiation. *Current Opinion in Immunology*, 23(5), pp.598–604.

Manning, T.C. et al., 1998. Alanine scanning mutagenesis of an alphabeta T cell receptor: Mapping the energy of antigen recognition. *Immunity*, 8(4), pp.413–425.

Meresse, B. et al., 2006. Reprogramming of CTLs into natural killer-like cells in celiac disease. *The Journal of experimental medicine*, 203(5), pp.1343–55.

Moody, D.B. et al., 2000. CD1c-mediated T-cell recognition of isoprenoid glycolipids in Mycobacterium tuberculosis infection. *Nature*, 404(6780), pp.884–888.

Moody, D.B. et al., 2004. T cell activation by lipopeptide antigens. *Science (New York, N.Y.)*, 303(January), pp.527–531.

Narni-mancinelli, E. et al., 2011. Fate mapping analysis of lymphoid cells expressing the

NKp46 cell surface receptor. *Proc Natl Acad Sci USA*, pp.2–7.

Netea, M.G., 2013. Training innate immunity: The changing concept of immunological memory in innate host defence. *European Journal of Clinical Investigation*, 43(8), pp.881–884.

Nikolich-Žugich, J., Slifka, M.K. & Messaoudi, I., 2004. The many important facets of T-cell repertoire diversity. *Nature Reviews Immunology*, 4(2), pp.123–132.

Olivier, M. et al., 2013. Plasticity of migrating CD1b+and CD1b- lymph dendritic cells in the promotion of Th1, Th2 and Th17 in response to Salmonella and helminth secretions. *PLoS ONE*, 8(11).

Patel, O. et al., 2013. Recognition of vitamin B metabolites by mucosal-associated invariant T cells. *Nature communications*, 4(May), p.2142.

Patel, O. et al., 2011. Vβ2 natural killer T cell antigen receptor-mediated recognition of CD1d-glycolipid antigen. *Proceedings of the National Academy of Sciences of the United States of America*, 108(47), pp.19007–12.

Paul, W.E. & Seder, R.A., 1994. Lymphocyte responses and cytokines. *Cell*, 76(2), pp.241–251.

Quigley, M.F. et al., 2011. Unbiased molecular analysis of T cell receptor expression using template-switch anchored RT-PCR. *Current protocols in immunology / edited by John E. Coligan ... [et al.]*, Chapter 10, p.Unit10.33.

Radley, D.E. et al., 1975. East coast fever: 3. Chemoprophylactic immunization of cattle using oxytetracycline and a combination of theilerial strains. *Veterinary Parasitology*, 1(1), pp.51–60.

Van Rhijn, I. et al., 2013. A conserved human T cell population targets mycobacterial antigens presented by CD1b. *Nature immunology*, 14(7), pp.706–13.

Van Rhijn, I. et al., 2015. Lipid and small-molecule display by CD1 and MR1. *Nature reviews. Immunology*, 15(10), pp.643–54.

Rossjohn, J. et al., 2012. Recognition of CD1d-restricted antigens by natural killer T cells.

Nature reviews. Immunology, 12(12), pp.845–57.

Rowen, L., Koop, B.F. & Hood, L., 1996. The complete 685-kilobase DNA sequence of the human beta T cell receptor locus. *Science (New York, N.Y.)*, 272(5269), pp.1755–1762.

Ru, H. et al., 2015. Molecular Mechanism of V(D)J Recombination from Synaptic RAG1-RAG2 Complex Structures. *Cell*, 163(5), pp.1138–1152.

Rudd, B.D. et al., 2011. Evolution of the antigen-specific CD8+ TCR repertoire across the life span: evidence for clonal homogenization of the old TCR repertoire. *Journal of immunology (Baltimore, Md. : 1950)*, 186(4), pp.2056–64.

Rudolph, M.G., Stanfield, R.L. & Wilson, I. a, 2006. How TCRs bind MHCs, peptides, and coreceptors. *Annual review of immunology*, 24, pp.419–66.

Rufer, N., 2005. Molecular tracking of antigen-specific T-cell clones during immune responses. *Current Opinion in Immunology*, 17(4 SPEC. ISS.), pp.441–447.

Saraiva, M. et al., 2009. Interleukin-10 Production by Th1 Cells Requires Interleukin-12-Induced STAT4 Transcription Factor and ERK MAP Kinase Activation by High Antigen Dose. *Immunity*, 31(2), pp.209–219.

Siddiqui, S., Visvabharathy, L. & Wang, C.R., 2015. Role of Group 1 CD1-Restricted T Cells in Infectious Disease. *Front Immunol*, 6, p.337.

Sieling, P. a et al., 1999. CD1 expression by dendritic cells in human leprosy lesions: correlation with effective host immunity. *Journal of immunology (Baltimore, Md. : 1950)*, 162(3), pp.1851–8.

Sivori, S. et al., 1997. P46, a Novel Natural Killer Cell-Specific Surface Molecule That Mediates Cell Activation. *The Journal of experimental medicine*, 186(7), pp.1129–1136.

Sugita, M. et al., 2000. CD1c molecules broadly survey the endocytic system. *Proceedings of the National Academy of Sciences of the United States of America*, 97(15), pp.8445–50.

Takahashi, T. et al., 1998. Immunologic self-tolerance maintained by CD25+CD4+ naturally anergic and suppressive T cells: induction of autoimmune disease by breaking their anergic/suppressive state. *International immunology*, 10(12), pp.1969–1980.

Teng, M.K. et al., 1998. Identification of a common docking topology with substantial variation among different TCR-peptide-MHC complexes. *Current Biology*, 8(7), pp.409–12.

Terabe, M. et al., 2005. A nonclassical non-Valpha14Jalpha18 CD1d-restricted (type II) NKT cell is sufficient for down-regulation of tumor immunosurveillance. *The Journal of experimental medicine*, 202(12), pp.1627–33.

Tomasello, E. et al., 2012. Mapping of NKp46+ cells in healthy human lymphoid and non-lymphoid tissues. *Frontiers in Immunology*, 3(NOV).

Tonegawa, S., 1983. Somatic generation of antibody diversity. *Nature*, 302(5909), pp.575–581.

Trautmann, L. et al., 2005. Selection of T Cell Clones Expressing High-Affinity Public TCRs within Human Cytomegalovirus-Specific CD8 T Cell Responses. *The Journal of Immunology*, 175(9), pp.6123–6132.

Treiner, E. et al., 2003. Selection of evolutionarily conserved mucosal-associated invariant T cells by MR1. *Nature*, 422(6928), pp.164–9.

Turner, S.J. et al., 2009. Functional implications of T cell receptor diversity. *Current Opinion in Immunology*, 21(3), pp.286–290.

Turner, S.J. et al., 2006. Structural determinants of T-cell receptor bias in immunity. *Nature Reviews Immunology*, 6(12), pp.883–894.

Ussher, J.E., Klenerman, P. & Willberg, C.B., 2014. Mucosal-associated invariant T-cells: New players in anti-bacterial immunity. *Frontiers in Immunology*, 5(OCT).

Walzer, T. et al., 2007. Identification, activation, and selective in vivo ablation of mouse NK cells via NKp46. *Proceedings of the National Academy of Sciences of the United States of America*, 104(9), pp.3384–9.

Warren, R.L. et al., 2011. Exhaustive T-cell repertoire sequencing of human peripheral blood samples reveals signatures of antigen selection and a directly measured repertoire size of at least 1 million clonotypes. *Genome Research*, 21(5), pp.790–797.

Wollenberg, A. et al., 1996. Immunomorphological and Ultrastructural Characterization of Langerhans Cells and a Novel, Inflammatory Dendritic Epidermal Cell (IDEC) Population in Lesional Skin of Atopic Eczema. *Journal of Investigative Dermatology*, 106(3), pp.446–453.

Yakimchuk, K. et al., 2011. Borrelia burgdorferi infection regulates CD1 expression in human cells and tissues via IL1-?? *European Journal of Immunology*, 41(3), pp.694–705.

Young, D.C. et al., 2009. Synthesis of dideoxymycobactin antigens presented by CD1a reveals T cell fine specificity for natural lipopeptide structures. *Journal of Biological Chemistry*, 284(37), pp.25087–25096.

Zhou, D. et al., 2004. Lysosomal glycosphingolipid recognition by NKT cells. *Science*, 306(5702), pp.1786–9.